AFFDL-TR-64-169

LITHIUM SPRAY STRUCTURAL COOLING

Andrew L. Mistretta
Bell Aerosystems Company

Division of Bell Aerospace Corporation - A Textron Company

TECHNICAL REPORT NO. AFFDL-TR-64-169
November 1964

Contract AF 33(657)-8386

AF Flight Dynamics Laboratory
Research and Technology Division
Air Force Systems Command
Wright-Patterson Air Force Base, Ohio

FOREWORD

This report was prepared by the Bell Aerosystems Company, Buffalo, N. Y., under USAF Contract No. AF33(657)-8386. Mr. Andrew L. Mistretta was Technical Director during the testing phase and Mr. John A. Dickson was Technical Director during the fabrication phase. The contract was initiated under Project No. 1368, "Structural Design Concepts", Task No. 136804 "Reentry and Hyperthermantic Structures". The work was administered under the direction of the AF Flight Dynamics Laboratory, Research and Technology Division, with Mr. R. T. Achard acting as Project Engineer.

This report covers work conducted from May 1962 to October 1964.

Sincere appreciation is expressed to Dr. Bruce E. Mathews and Messrs. C. A. Langston and W. Powers of the Induction Heating Project Laboratory of the University of Florida, for their efforts in the design and fabrication of the induction heating work coils and the operation of the induction generators during test. The efforts of the personnel of the MSA Research Corporation in the design, fabrication and operation of the lithium loop during test are gratefully acknowledged, especially Messrs. K. R. Barker, R. C. Andrews and J. R. Betz. Special acknowledgment to Mr. Wilfred H. Dukes and Mr. Frank M. Anthony of the Bell Aerosystems Company for their consultation and guidance during the program. The efforts of C. K. Martina, instrumentation engineer and K. Jemison, instrumentation technician, of the Bell Aerosystems Company are also gratefully acknowledged.

ABSTRACT

The objective of this program was to demonstrate the feasibility of an open cycle lithium spray absorptive cooling system for nose cap applications and to determine maximum heat flux capability of the system.

Test specimens were designed and fabricated. The experimental program which was established demonstrated the feasibility of the lithium spray system. While subjected to a heat flux of 600 BTU/ft^2-sec, equivalent to a radiation equilibrium temperature of about 5800°F, specimen surface temperature did not exceed 2200°F. Instrumentation difficulties precluded tests at higher heat fluxes; therefore, the maximum potential of the system could not be determined experimentally. Approximate analytical estimates indicate a minimum potential capability of 3000 BTU/ft^2-sec.

For the application of the test heat fluxes, the Inductive Heating System of the University of Florida was used.

This technical report has been reviewed and is approved.

Richard F. Hoener

RICHARD F. HOENER
Acting Chief
Structures Division

CONTENTS

CONTENTS (CONT)

ILLUSTRATIONS

ILLUSTRATIONS (CONT)

TABLES

SECTION 1

INTRODUCTION

In the development of airframes for manned reentry vehicles, emphasis has been placed on radiative cooled structural concepts because they represent lighter systems, for the long flight times of interest, than alternate systems based on absorptive cooling. Radiation systems are necessarily restricted, however, in the intensity of heating that can be accommodated, because of material temperature limitations. Beyond the temperature limits for refractory materials attention returns to absorptive systems, particularly for vehicle stagnation areas, where the heating is most severe.

The objective of this program was to demonstrate the feasibility of an open cycle lithium spray absorptive system and to determine the maximum heat flux which the system could tolerate. The experimental program which was established demonstrated that it was feasible to use a lithium spray for structural cooling. While subjected to a heat flux of 600 BTU/ft^2-sec, equivalent to a radiation equilibrium temperature of about 5800°F, specimen temperatures did not exceed 2200°F. Instrumentation difficulties precluded tests at higher heat fluxes; therefore, the maximum potential of the system could not be determined experimentally.

As a goal, a heat flux of 1000 BTU/ft^2-sec was established based upon a superorbital reentry of a vehicle with a 12-inch radius hemispherical nose. Studies leading to a vehicle and flight path selection having a heat flux rate of 1000 BTU/ft^2-sec at the stagnation point are presented in Section 2. Results from this study were used for transient heating cycles conducted on a prototype nose model. A description of a proposed open cycle lithium spray system for a hemispherical nose is also included in Section 2.

Section 3 presents discussions of the test specimens, specimen instrumentation, the lithium loop, operation of the loop during specimen testing, the induction heating facility, and the design of the induction heating work coil. Three types of test specimens were fabricated for three different purposes; first to evaluate spray cooling, next to determine the ability of a wet vapor mixture to pick up heat in forced convection, and finally, to observe the combination of the two cooling effects in a scale model of a prototype nose cooling system. The specimens designed and fabricated to accomplish this evaluation were identified as A, B, and C test specimens.

The experimented program is discussed in Section 4. Problems which arose are identified and reasons for curtailing the test program and eliminating the B specimen testing are given.

Manuscript released by author October 1964 for publication as an RTD Technical Report.

The test results are discussed in Section 5. The potential and advantages of a lithium spray system are discussed in Section 6, as well as the areas of further investigation which are required to produce a flight weight system. The conclusions and recommendations are given in Section 7.

The procedure used to install thermocouples on the test specimens is presented in Appendix I. During the pretest checkout of the lithium loop, the supply tank failed and discussions concerning the fabrication history of the tank and postulations as to the failure are included in Appendix II. Appendix III contains the tabulated test data from the test specimens and the lithium loop.

During this program, the services of two major subcontractors were utilized. Detailed design, fabrication, and operation of the loop during testing was performed by personnel of the MSA Research Corporation of Callery, Pennsylvania. The design of the induction heating work coils and operation of the induction heating generators were performed by personnel of the Induction Heating Project Laboratory at the University of Florida. The test site was at the University of Florida.

SECTION 2

MISSION AND SYSTEM DESCRIPTION

A. MISSION

The conceptual mission toward which this program was directed was a superorbital (35,000 fps at 400,000-ft altitude) reentry, whose trajectory was a single reentry and was compatible to human endurance and future practical applications. For test purposes, a preselected concept vehicle and mission was to be used. Selection of the mission was to be such that a 12-inch radius hemispherical nose of the vehicle would be subjected to a heat flux of 1000 BTU/ft^2-sec at the stagnation point.

This section first discusses the selection of the vehicle and its flight path, and then the heating conditions which were to serve as a basis for the testing of a subscale model.

1. Design Vehicle

Thermal protection for the 12-inch radius hemispherical nose of a vehicle approximately described as having a wing loading (W/S) between 25 and 60 lb/ft^2 and a variable lift coefficient (C_L) for control was specified. A wide range of configurations falls within these specifications: the wing-body types as exemplified by Dyna-Soar, the delta shaped lifting bodies, and the cone or semi-cone bodies such as the Eggers M-1 and M-2. Configurations with low wing loadings, and also with high hypersonic lift-to-drag ratios such as the delta shaped vehicles and the wing-body types, are attractive because they can be flown at high altitudes where heating conditions are less severe and they possess an appreciable maneuvering capability which relaxes midcourse guidance requirements and maximizes landing point selectivity. For any superorbital mission, however, the desire will always be to have a high ratio of weight of active payload to weight of structure plus its thermal protection system because this will provide a high degree of mission efficiency from takeoff to landing. Consequently, wing loadings of payloads (i.e., the reentry vehicles themselves) indicate trends toward high values. A survey of the configurations studied by the Bell Aerosystems Company and other contractors for advanced superorbital missions showed no reasonable reentry configuration which has a W/S of less than about 48 lb/ft^2; the highest value was 76 lb/ft^2. Therefore, the upper value of the range of W/S specified seemed an appropriate design criterion, and 60 lb/ft^2 was chosen as the design value for wing loading.

In addition to the wing loading, maximum values of the aerodynamic parameters lift-to-drag ratio (L/D_{max}) and lift coefficient ($C_{L_{max}}$) or, equivalently, the vehicle drag polar (a curve of lift coefficient versus the drag coefficient) are required to define the conceptual vehicle. Reentry corridor width as well as maneuverability is primarily dependent on the maximum L/D of the vehicle. A survey of recent superorbital studies of lifting configurations for early missions of space probes and lunar

explorations indicated maximum L/D's between 0.4 and 1.0 and maximum C_L's between 0.4 and 0.8. These were largely configurations in which volumetric and structural efficiency were emphasized over aerodynamic performance. Operational requirements that emphasize range and maneuverability in order to provide worldwide landing capability from almost any initial atmospheric reentry conditions may require higher L/D designs. For example, an L/D = 1.5 will provide one earth circumference in range control from escape velocity reentry conditions. In the present case, with the relatively steep -10° reentry angle and maximum C_L pullout specified as design conditions, reentry range and choice of L/D_{max} did not appear critical. In view of the above, $L/D_{max} = 1$ was selected as being both realistic and representative. A maximum $C_L = 0.6$ was chosen as being representative of a vehicle with that L/D.

A further consideration in the choice of both W/S and C_L was that reentry trajectories are dependent on the parameter W/C_LS instead of on the dissociated values of W/S and C_L. A choice of $C_L = 0.6$ with W/A = 60 lb/ft^2 produced a value of $W/C_LS = 100$, and this value is pertinent to a wide variety of vehicles with lower W/A's reentering at low C_L's because of, for example, trim limits. Thus, from the standpoint of nose heating, the chosen configuration is also representative of a vehicle with a wing loading of 40 and a limit lift coefficient of 0.4, which is also a realistic situation.

Figure 1 presents the drag polar which was estimated for the selected conceptual vehicle. Maximum C_L occurs at an angle of attack of 53° and maximum L/D is at an angle of 38°.

In summary, then, the design vehicle has a configuration such that:

W/S	= 60 lb/ft^2
$(L/D)_{max}$	= 1.0
$C_{L_{max}}$	= 0.6
W/C_LS	= 100 lb/ft^2
$C_{L_{max}}$	occurs at an angle of attack of 53°
$(L/D)_{max}$	occurs at an angle of attack of 38°

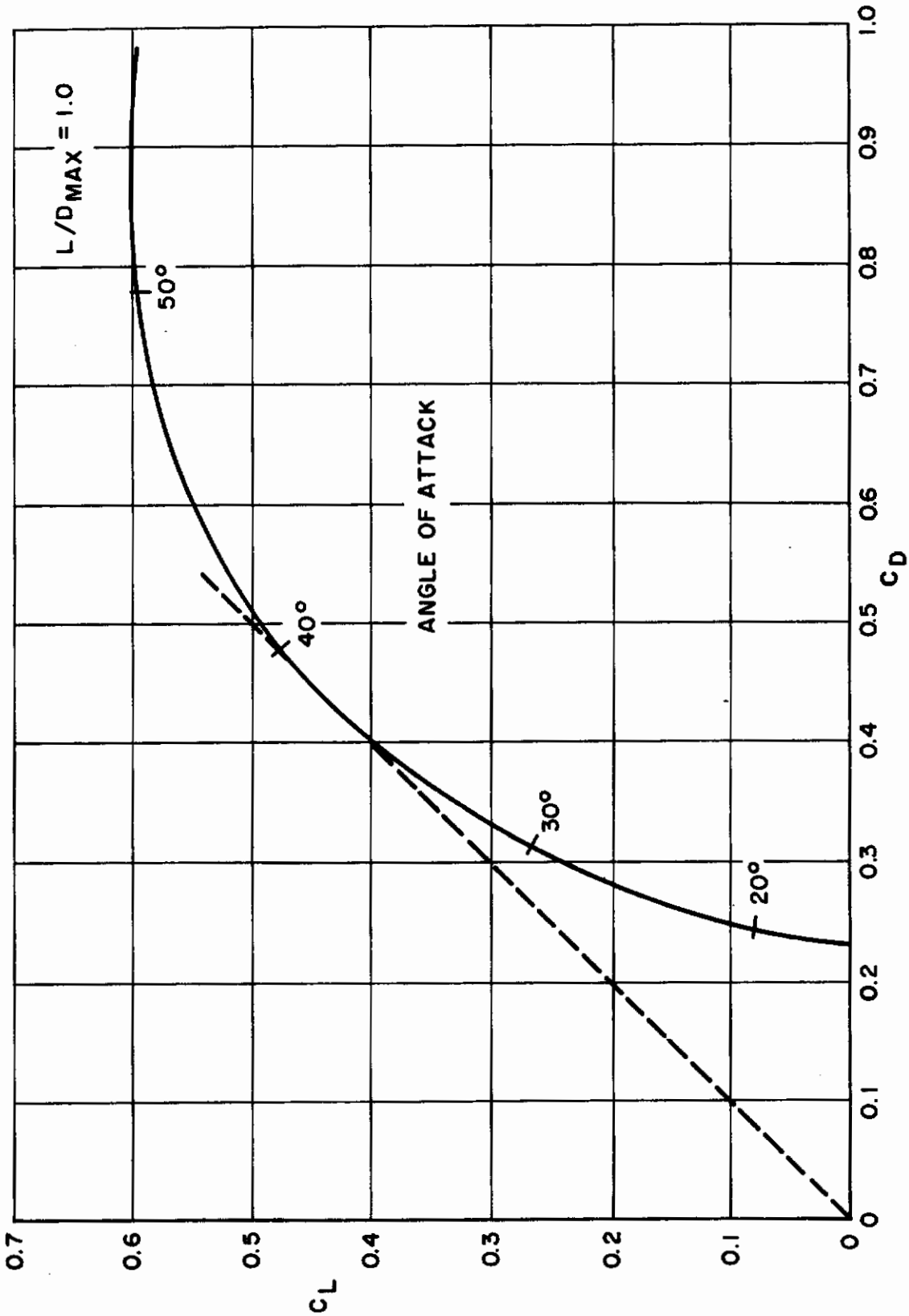

Figure 1. Lift-Drag Polar

2. Flight Path Selection

The selection of a flight path for the design vehicle was based on a study made of the heating conditions which the vehicle would encounter during very steep reentry and also during the shallowest reentry from which the vehicle could remain in the atmosphere (the skip or overshoot boundary). The steep reentry, because of the vehicle's deep penetration of the atmosphere at high velocities, establishes the maximum heating intensity which the nose thermal protection system must handle. The shallow reentry, because of the very long flight times which are possible, may establish the maximum heat load (i.e., the integral of the heating rate with respect to time) which must be dissipated. After the initial pullup, a wide variety of trajectories may be flown to effect transition to equilibrium flight.

A summary of the trajectory studies is shown in Figure 2 as altitude-velocity profiles. For reentry at a flight path angle of -10°, maximum C_L attitude is maintained to perigee or beyond, depending on the control during the transition phase. Perigee occurs 51.8 seconds after reentry at an altitude of 161,500 feet and a velocity of 28,875 ft/sec. Maximum resultant acceleration is 17.5 g, maximum dynamic pressure is 995 lb/ft^2, and the maximum heat flux rate is 900 BTU/ft^2 sec.

Three types of transition control were investigated. From perigee, constant altitude flight was made by maintaining the $C_{L_{max}}$ attitude, and hence, maximum C_D, but modulating the roll angle ϕ cyclically to provide the proper amount of vertical aerodynamic force for level flight without developing any significant lateral displacement. Because of the high decelerations, this type of program produces short range, short flight time, and low total heat load. Range from reentry to a velocity of 4000 ft/sec is 790 nautical miles, time is 310 seconds, and the convective heat load to the stagnation point of the 1-foot radius nose is 41,220 BTU/ft^2.

The second type of transition control was essentially ballistic flight at the C_D for $C_{L_{max}}$, obtained again by maintaining the $C_{L_{max}}$ attitude but flying alternately at roll angles of +90° and -90° to negate lateral displacement. This was initiated about 5 seconds after perigee. For this case, range from reentry to V = 4000 ft/sec is 1640 nautical miles, flight time is 630 seconds and convective heat load to the stagnation point is 56,680 BTU/ft^2.

The third type of transition control is flight at maximum C_L but with the vehicle inverted (ϕ = 180°). The object of this method of control is to obtain the maximum possible range from the steep reentry by allowing the pullup maneuver to continue until the last moment at which the ascent trajectory can be converted to a pullover path which makes a smooth transition into the equilibrium glide. By inverting the vehicle, the pullover can be effected at the maximum positive C_L, which for a nonsymmetrical vehicle would be greater than the maximum negative C_L. Also

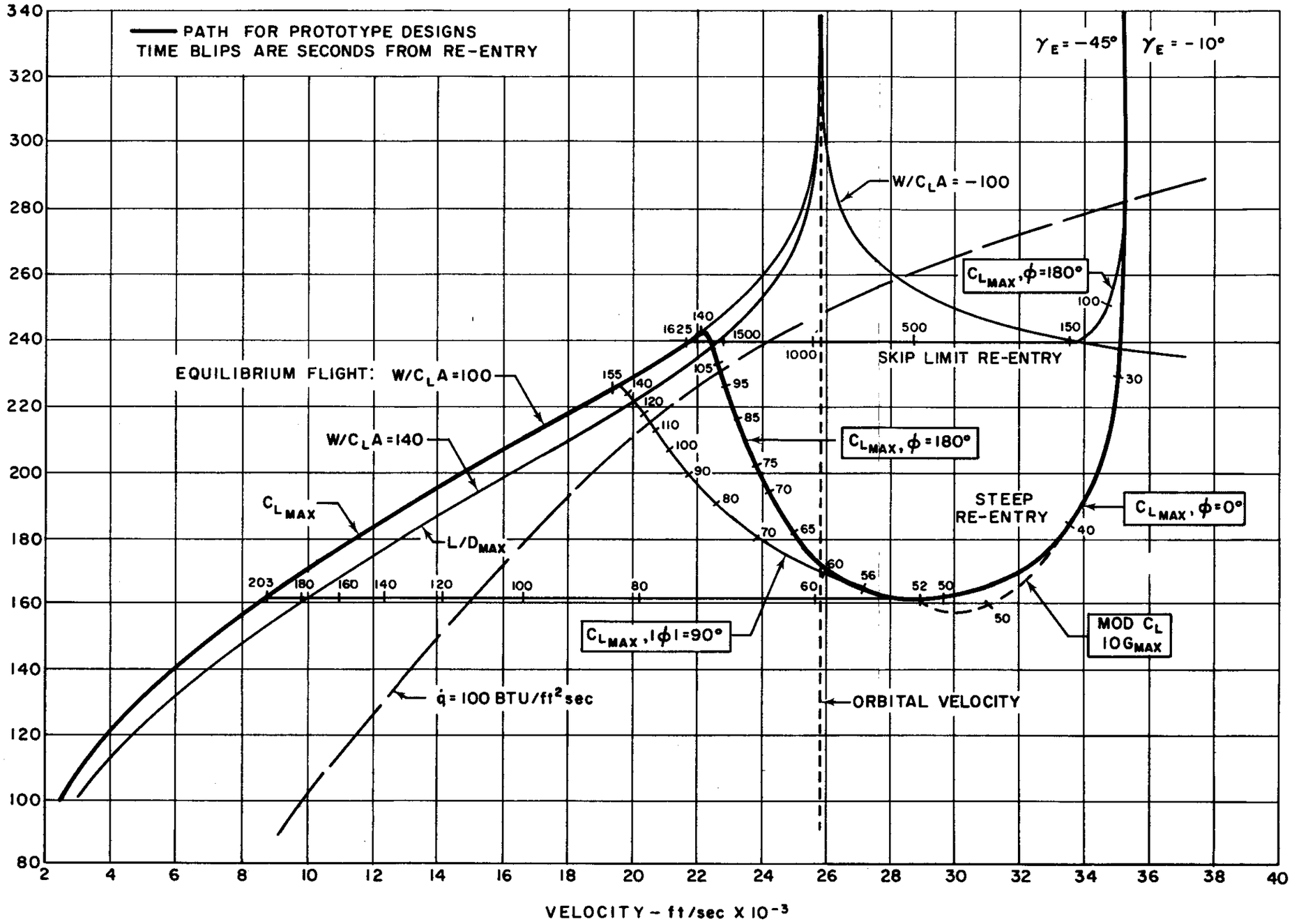

Figure 2. Reentry Profiles

the lower surface continues to be the compression area so that no additional thermal protection is required for those surfaces which are in expansion flow during the initial pullup phase. This transition is initiated about 14 seconds after perigee. If the equilibrium flight is at $C_{L_{max}}$, the range is 2230 nautical miles from reentry to 4000 ft/sec velocity, time is 797 seconds, and the convective heat load to the stagnation point is 65,750 BTU/ft^2. By comparison, if the equilibrium suborbital flight had been made at $(L/D)_{max}$ with $W/C_L S = 140$, the range would be 2910 nautical miles, the time 1074 seconds, and the convective stagnation point heat flux 85,700 BTU/ft^2.

When reentry is made from the skip limit, the aerodynamic lift force must be directed toward earth to oppose the centrifugal force and hold the vehicle in the atmosphere. Reentry is therefore made at $C_{L_{max}}$, $\phi = 180°$ so that the same advantage as described in the preceding paragraph is realized. Perigee occurs on the equilibrium altitude-velocity profile for negative $\frac{W}{C_{L_{max}} S}$. For the selected conceptual vehicle $\left(\frac{W}{C_{L_{max}} S} = 100 \right)$ perigee is reached 138 seconds after reentry at a velocity of 33,610 ft/sec and an altitude of 240,000 feet. Maximum resultant acceleration is 1.2g, maximum dynamic pressure is 70 lb/ft^2 and the maximum convective heat flux rate to the stagnation point of the 1-foot radius nose is 284 BTU/ft^2 sec.

One type of transition control from the skip limit reentry to equilibrium flight was examined. This was level flight from perigee obtained by modulating the angle of attack to produce the necessary lift. At velocities greater than orbital, the vehicle is flown inverted; at velocities less than orbital it is flown right side up. For this path from reentry to a velocity of 4000 ft/sec the flight time is 2244 seconds, the range is 8680 nautical miles, and the convective heat load to the stagnation point is 255,250 BTU/ft^2.

The heat flux for this type of transition from a shallow reentry is excessively high. Considerations of the ground landing areas which the vehicle can attain from reentry suggest that the intent to employ this type of trajectory is not advisable. A vehicle should certainly be capable of effecting a safe landing from any initial reentry condition within its corridor. If, however, the accuracy of the guidance system which is used prior to reentry is considered equal to the reentry corridor tolerance (measured either in flight path angle or altitude), then the maximum range which can be guaranteed from all reentries is the maximum range attainable from the steepest tolerable reentry, while the minimum guaranteed range for all reentries is the minimum range attainable from the shallowest reentry. There is no way to obtain very short ranges from a skip limit reentry which is defined by flying at $C_{L_{max}}$, $\phi = 180°$, because there is no way to develop more lift to force the vehicle down from perigee into the dense atmosphere where energy can be dissipated rapidly

by drag. For this reason, the skip limit boundary to the reentry corridor should be defined for flight at some percentage of the maximum C_L or should simply be set at a reentry angle value slightly steeper than that defined by maximum C_L.

The foregoing discussion led to the selection of a flight path for design and test purposes consisting of:

A steep reentry beginning at an altitude of 400,000 feet with velocity of 35,000 ft/sec.

A flight path angle of -10°.

Pullup phase control with $C_{L_{max}}$ and a roll angle of 0°.

Transition at $C_{L_{max}}$ with a roll angle of 180°.

Equilibrium flight at $C_{L_{max}}$.

A range to 4000 ft/sec of 2230 nautical miles.

A convective heat load to the stagnation point of a 12-inch radius nose of 65,750 BTU/ft^2.

The time histories of significant parameters for the design trajectory are given in Figure 3.

3. Convective Heating

The convective stagnation point heat flux rate ($\dot{q}$) varies with time, as shown in Figure 3, with a peak value of 900 BTU/ft^2 sec at 45 seconds after the start of reentry, and a value approaching zero at 800 seconds after reentry, when the flight velocity has decreased to 4000 feet per second.

The convective aerodynamic heat flux to the stagnation point was determined using an empirical equation of Detra, Kemp, and Riddell (Reference 1), which is an empirical correlation of the method of Fay and Riddell (Reference 2):

$$\dot{q} = 17600 \frac{1}{\sqrt{R}} \left(\frac{\rho}{\rho_o}\right)^{0.5} \left(\frac{V}{V_c}\right)^{3.15} \left(\frac{h_s - h_w}{h_s - h_{w_{500°R}}}\right)$$

$\dot{q}$ = heat flux rate to the stagnation point, BTU/ft^2 sec

R = nose radius, feet

ρ = free stream density

ρ_o = sea level density

V = free stream velocity

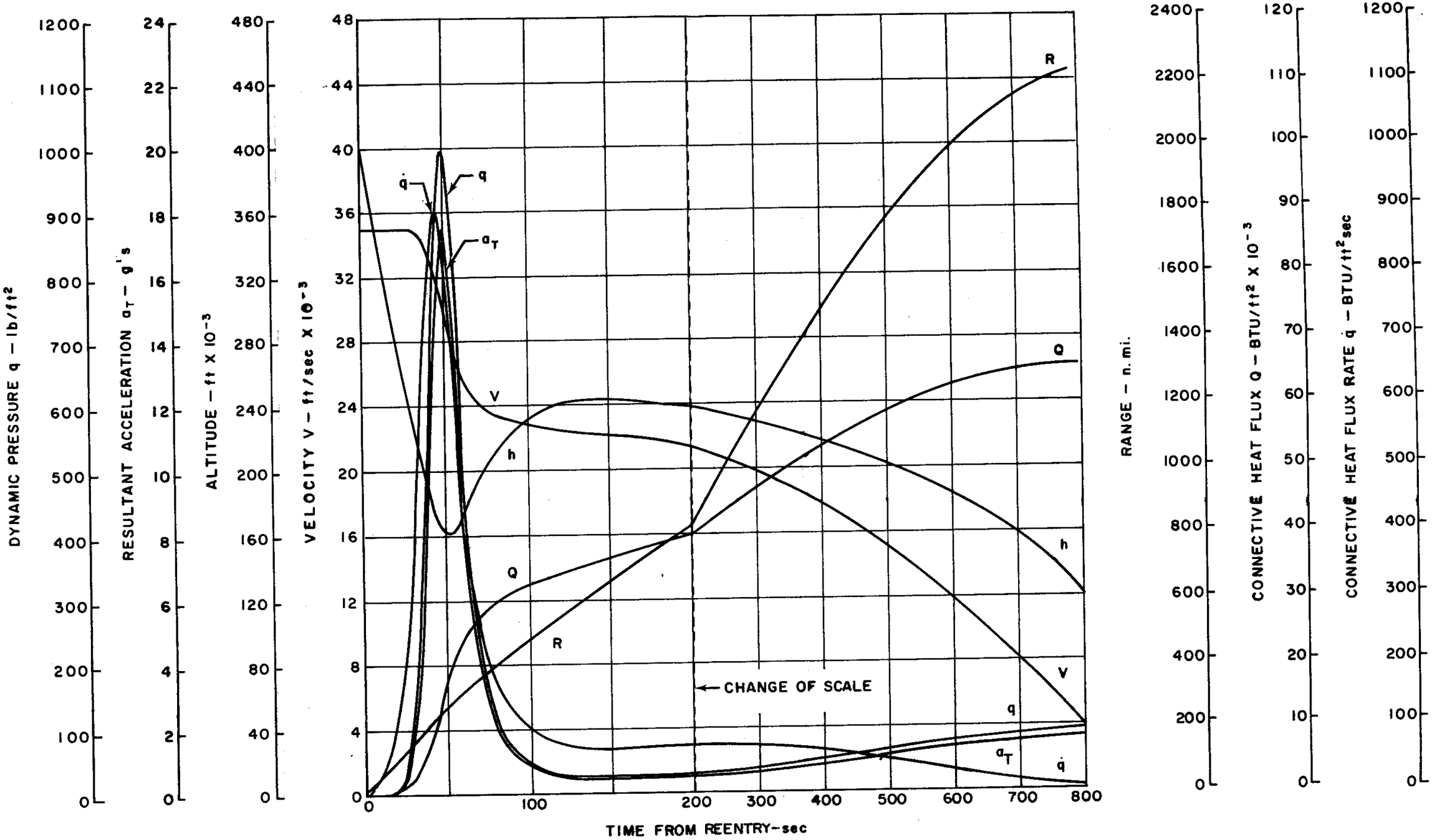

Figure 3. Time History of Significant Parameters for the Design Trajectory

V_c = satellite velocity

h_s = total free stream enthalpy

h_w = enthalpy at the wall

$h_{w_{500°R}}$ = enthalpy at a 500°R wall

The computation is part of the IBM 7090 program which produced all the data in Figure 3.

4. Total Heating

The total heating to the nose includes, in addition to the convective aerodynamic heating, the heating due to gas cap radiation. The gas cap radiation intensity was determined using the work of Kivel (Reference 3) which presents the ratio of equilibrium gas cap radiative-to-convective aerodynamic heating versus altitude and velocity, as a function of the nose radius. The design flight path from Figure 2 was superimposed on the radiative-convective heating ratio curves for a 1-foot radius nose, all versus altitude and velocity, to produce Figure 4. Figure 4 provided the means for computing a time history of equilibrium gas cap radiation heat flux rate, which was combined with the time history of convective aerodynamic heat flux rate from Figure 3 to give the total heating rate variation at the nose stagnation point throughout the flight, as shown in Figure 5. Figure 5 formed the basis for the transient heating cycles which were conducted on the subscale model as is discussed in Section 4.

B. LITHIUM SPRAY SYSTEM

Figure 6 shows a schematic of an open cycle lithium spray system for a hemispherical nose. A full cone jet spray is provided over the central portion of the inner surface of the nose by means of a centrally located spray nozzle. Flow is supplied from an electrically heated tank of liquid lithium by means of a pressurized gas system. Vapor formed when the spray makes contact with the hot surface flows rearward and provides convective cooling for the remainder of the hemisphere not covered by the spray. The vapor is collected at the end of the convective passages, piped to the aft end of the vehicle, and expelled overboard.

The flow rate would initially be the full value, commensurate with peak heating intensity, and would remain constant until after peak heating, whereupon the decreasing supply of pressurized gas permits a gradual decrease in coolant flow (approximating the rate of decrease in demand) thus eliminating temperature sensors and control valves. Being a one pass system, the open cycle spray eliminates the need for recirculating pumps and heat exchangers but does retain the requirement for accurate flow or gross inefficiencies would result.

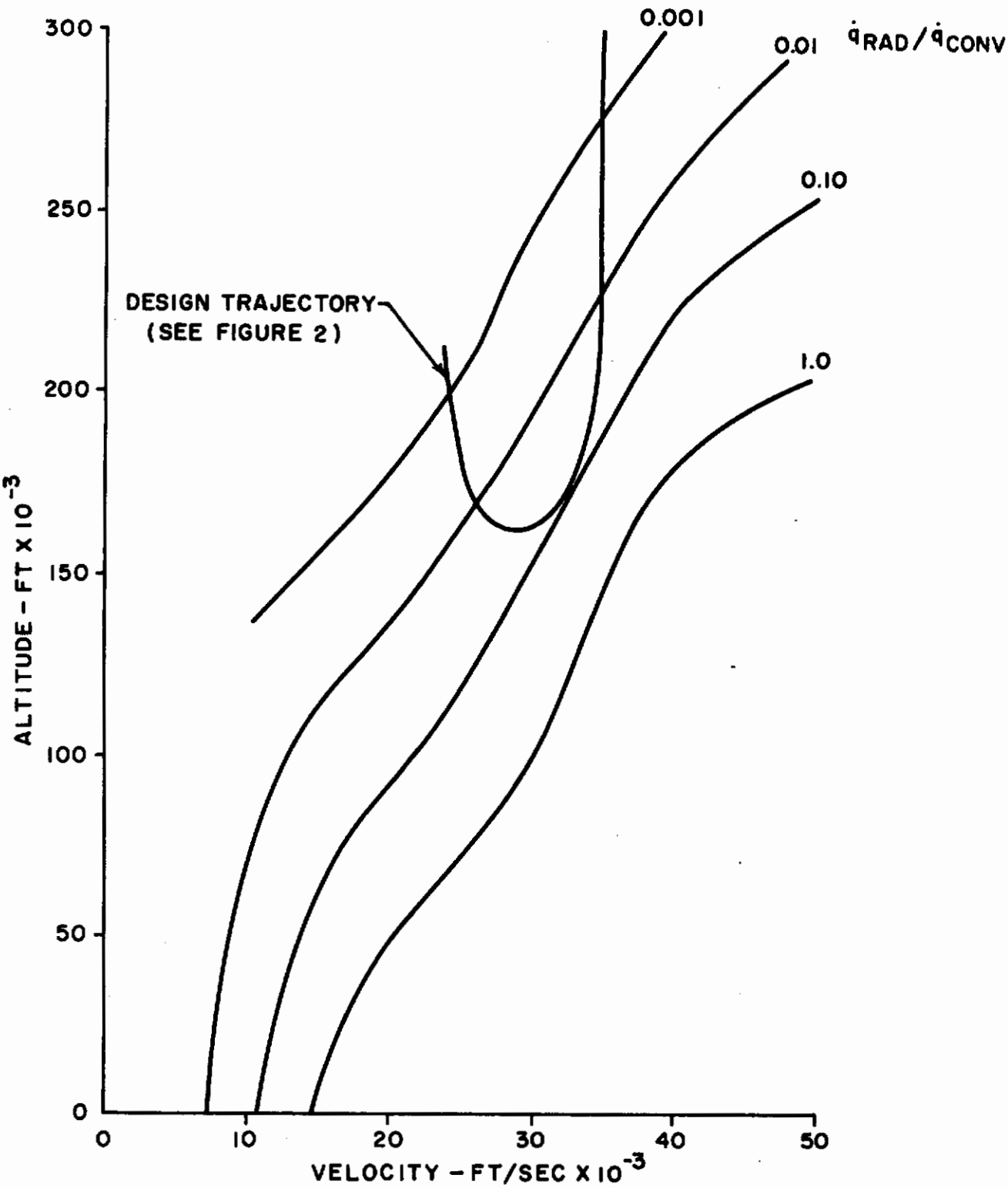

Figure 4. Nose Equilibrium Gas Cap Radiation Intensity

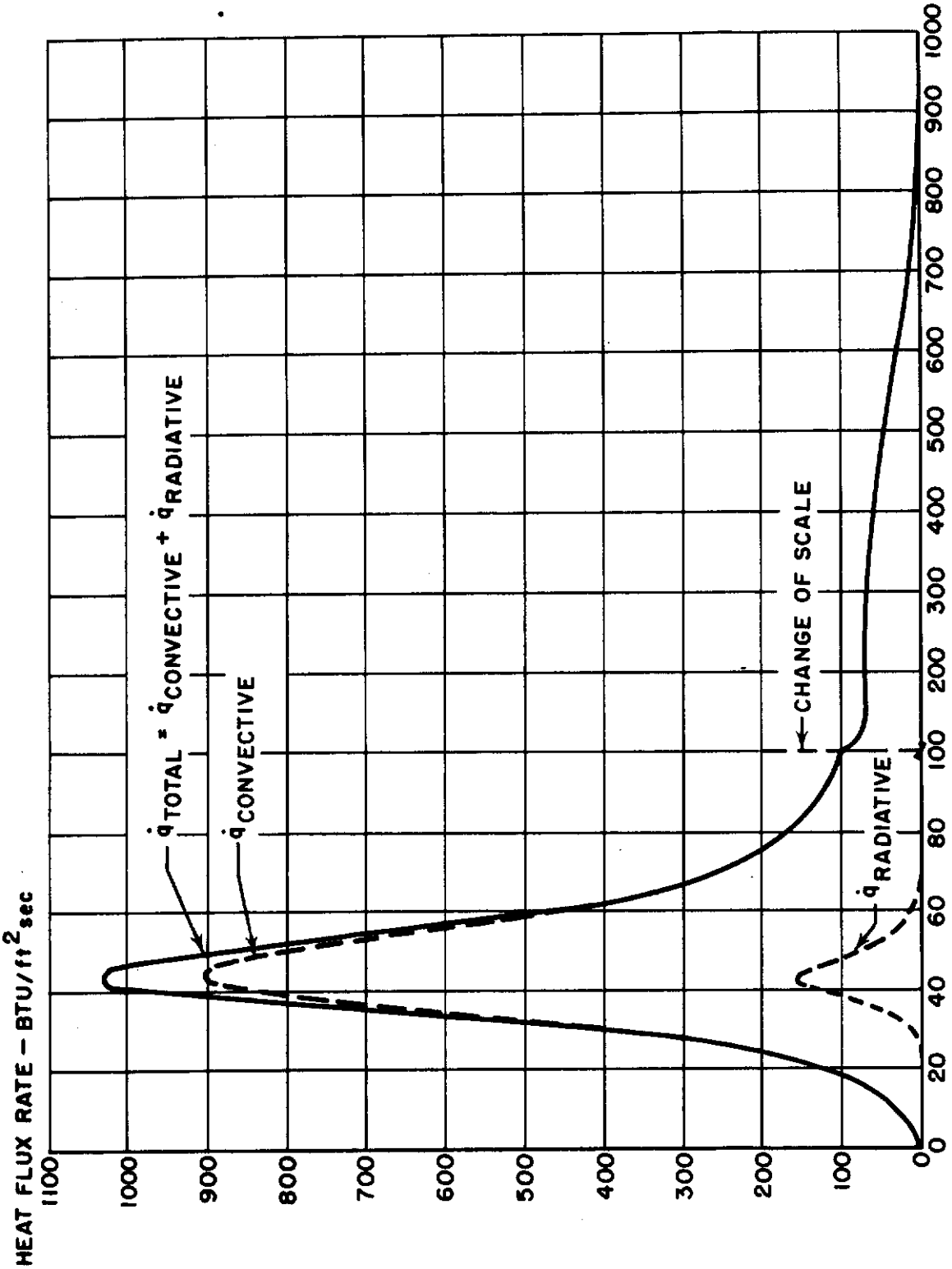

Figure 5. Convective, Gas Cap Radiative, and Total Heat Flux Rates at the Nose Stagnation Point versus Time From Reentry

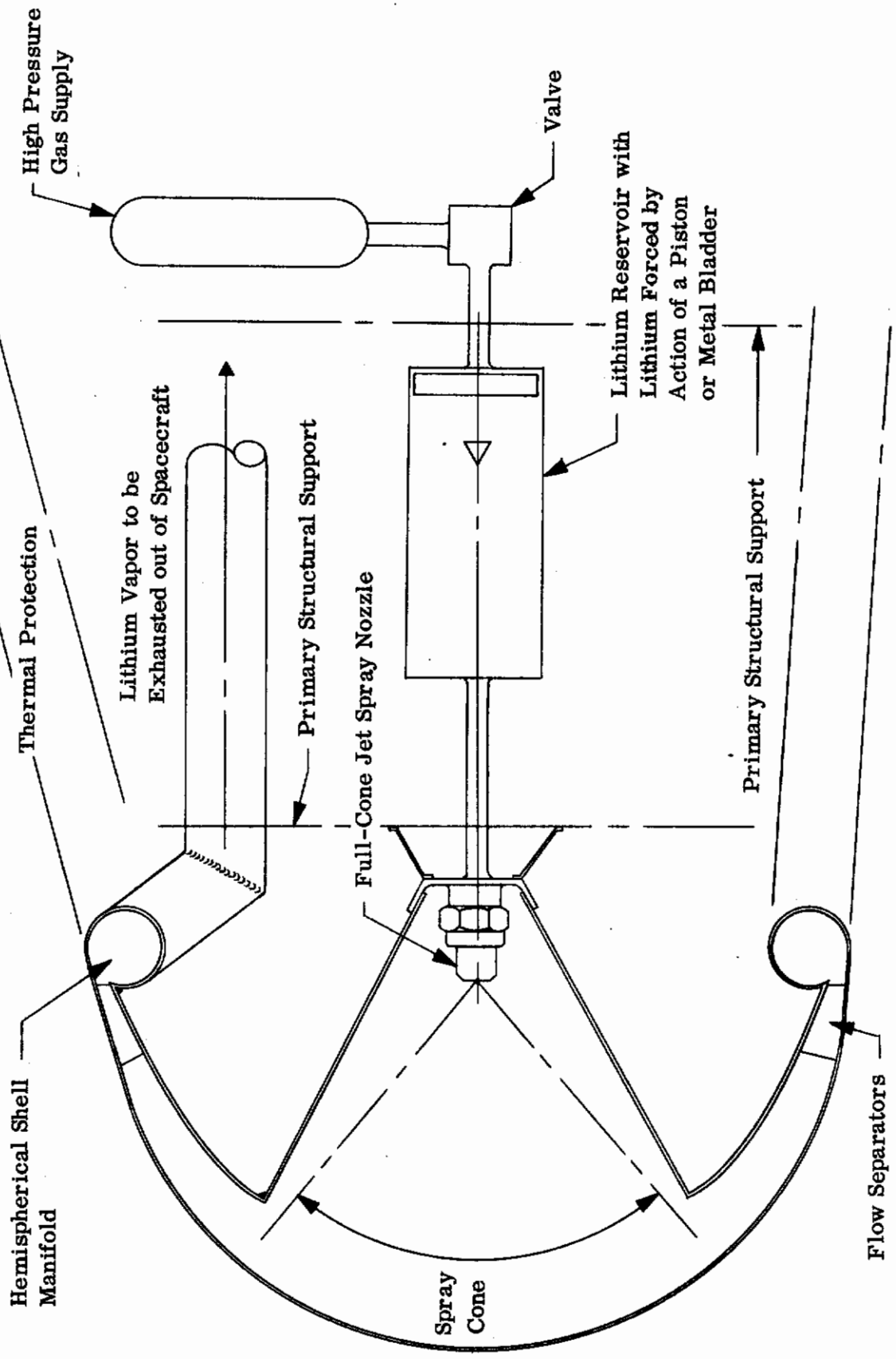

Figure 6. Typical Design for Lithium Spray System

Lithium is selected as the heat transfer fluid due to its large heat of vaporization, approximately 10,000 BTU/lb. A solid at room temperature with a density of 30 lb/ft^3, lithium melts at 360°F. Liquid metal slurries are not considered because of spraying difficulties and, in addition, the heat of vaporization of the common slurries is much lower than lithium and the weight penality of the heating system is more than offset by the larger heat of vaporization of lithium.

The lithium open cycle spray system does not involve a major extension of the present state-of-the-art in material requirements or equipment, but there is a need for answers to some basic questions if the system feasibility is to be determined:

(1) What is the maximum heat flux that can be accommodated by a lithium spray?

(2) What is the heat transfer rate to a flowing liquid-vapor mixture?

To provide answers for these questions, test specimens were fabricated, a test program established and the specimens tested as discussed in the following sections.

SECTION 3

TEST PREPARATION

A. TEST SPECIMENS

1. General

Three types of test specimens were fabricated, identified as A, B and C test specimens. The purpose of the A test specimens was to find the limiting heat flux rate that could be accommodated by spray cooling, and to find the most efficient rate at which lithium could be sprayed against a heated surface and still provide adequate, reliable cooling. The B test specimens were designed to determine the degree to which lithium vapor could be saturated and even super heated, as a supplement to the cooling effect obtained by spray boiling. The C test specimen was a scale model of a prototype hemispherical nose, cooled by spray boiling of liquid lithium, followed by convective cooling by the flowing lithium vapor. The entire hemisphere was to be inductively heated externally, and cooled by lithium striking the central portion of the inner surface in the form of a fine spray, boiling, and flowing toward a toroidal collecting ring as vapor, wiping, and therefore cooling the heated surfaces on the way.

The atmospheric boiling point of lithium is 2430°F, decreasing in temperature as the ambient pressure is reduced. It was desirable to reduce the boiling point during testing as much as practicable in order to reduce the operating temperature of the test specimens and consequently, their material property requirements. The vapor pressure-temperature combination chosen was 0.5 psia and 1700°F; that is, by evacuating the test specimen such that the ambient pressure is 0.5 psia, it would be possible to boil lithium at about 1700°F, a substantial temperature reduction from its atmospheric boiling point. With a temperature drop of approximately 500°F for a heat flux rate of 1000 BTU/ft^2-sec through the specimen wall, the external surface temperature would be 2200°F for the A and C test specimens. Based primarily on strength, but also with consideration for liquid metal corrosion and mass transfer, availability and fabrication properties, the 1% zirconium alloy of columbium was selected. All of the external surfaces of the A anc C specimens were protected with an oxidation resistant coating with an Al-Sn base which was applied by the Syclor Division of General Telephone and Electronics Laboratories. The external surface temperature of the B test specimens was limited to 2000°F and Haynes 25 was selected based primarily on cost. The Haynes 25 did not require an oxidation resistant coating.

The test loop, which supplied the liquid lithium to the test specimens and received the exhaust vapor, is a large assembly and the cost of making the loop in columbium would have been prohibitive. Consequently, the loop material is Haynes 25 and it became necessary to connect, in an absolutely leak tight manner, the Haynes 25 loop and the columbium A and C test specimens. In addition, it was necessary to connect each specimen to the lithium loop at the test site at the University of Florida,

where only standard welding equipment was available. Therefore, the columbium test specimens were designed to include columbium-to-Haynes 25 transition joints at both their inlet and outlet lines, so that each in turn could be attached to the loop through Haynes 25 welds. Attempts to electron beam weld the two materials were unsuccessful due to the boiling point of the Haynes 25 being below the melting point of the columbium. The use of intermediate materials for joining was also unsuccessful. The problem was finally resolved by using Conoseal joints, manufactured by the Marman Division of Aeroquip Corporation. The joint is composed of a Haynes 25 and columbium coupling and the seal between the two is made through a Haynes 25 gasket, which is plastically deformed by two large Haynes 25 flanges which are bolted together.

2. A Test Specimens

The A test specimen is shown in detail in Figure 7, a reduction of the engineering drawing. Two A specimens were fabricated, differing only in that the surface on which the lithium impinged, which is the central portion of the internal surface of the 6.00 inch spherical radius disc, is smooth for one and knurled for the other. Spinning was used to a large extent in forming of the basic parts and welding in an argon-purged evacuated dry box for joining of the parts.

Before the specimen was shipped out to be coated, one of the Haynes 25 flanges of the Conoseal joint was slipped on the -15 exhaust tube and the columbium coupling was welded to the exhaust tube. After coating, a stainless steel spray nozzle was mounted on a columbium adaptor and the adaptor was welded to the -5 weld assembly of Figure 8. Figure 8 includes a layout of the complete A specimen, showing the nozzle, adaptor and Conoseal joints. A photograph of the A specimen is shown in Figure 9; the large bolted flanges which are visible are part of the Conoseal joints.

3. B Test Specimens

Two B specimens were fabricated (Figure 10); one had a completely open flow section, while the flow section of the second specimen contained five spacers that would act as fins and provide more heated surface from which the flowing vapor would remove heat. The test specimens were to be heated from the top surface only, and the spacers could act as conduction paths to the lower surface of the flow passage. The B specimens were fabricated entirely from Haynes 25 material and assembled by heliarc welding.

4. C Test Specimen

The C specimen was a scale model of a prototype 4.0 inch diameter hemispherical nose and a complete description is given in Figure 11, a reduced layout of the C specimen. Figure 12 is a photograph of some of the detailed parts. The same method of fabrication and coating as was used in the A specimens was followed. The entire assembly is shown in Figures 8 and 13.

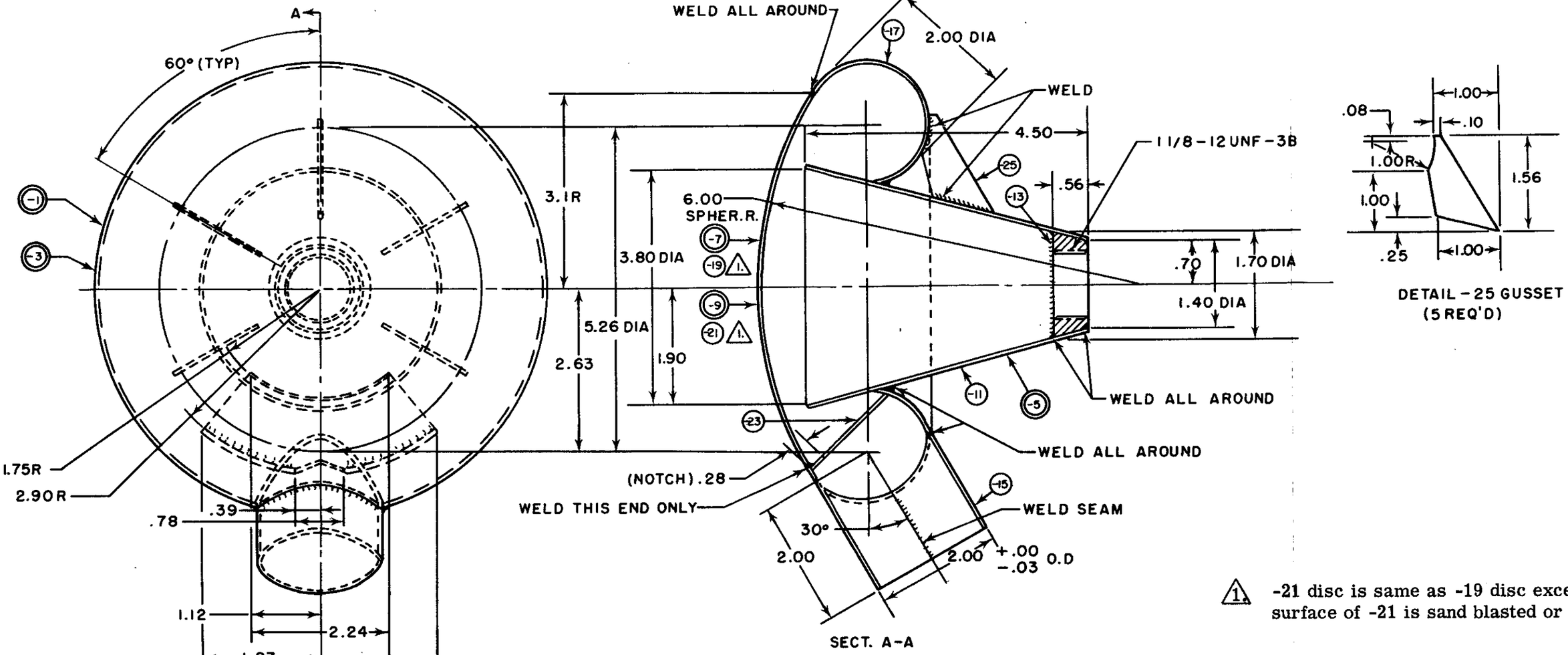

BAC DWG NO. 7149-987001

QUANTITY REQD					CODE IDENT	PART OR IDENTIFYING NO.	NOMENCLATURE OR DESCRIPTION	MATERIAL OR NOTE	SPECIFICATION	DIA	THK	W	LG
-9	-7	-5	-3	-1									
		5				-25	GUSSET	COLUMBIUM - 1% ZIRCONIUM			.060	1.5	1.7
1	1					-23	BAFFLE	COLUMBIUM - 1% ZIRCONIUM			.060	2.8	4.4
1						-21	DISC	COLUMBIUM - 1% ZIRCONIUM			.060	7.8	7.8
	1					-19	DISC	COLUMBIUM - 1% ZIRCONIUM			.060	7.8	7.8
		1				-17	TORUS	COLUMBIUM - 1% ZIRCONIUM			.060	9.4	18.8
		1				-15	TUBE	COLUMBIUM - 1% ZIRCONIUM			.060	2.4	7.4
		1				-13	INSERT	COLUMBIUM - 1% ZIRCONIUM		2.0			0.8
		1				-11	CONE	COLUMBIUM - 1% ZIRCONIUM			.060	6.0	12.0
			1			-9	DISC ASSY						
				1		-7	DISC ASSY						
			1	1		-5	WELD ASSY						
						-3	TEST SPECIMEN						
						7149-987001-1	TEST SPECIMEN						

LIST OF MATERIALS OR PARTS LIST

⚠1. -21 disc is same as -19 disc except inside surface of -21 is sand blasted or equivalent.

Figure 7. A Test Specimen Drawing

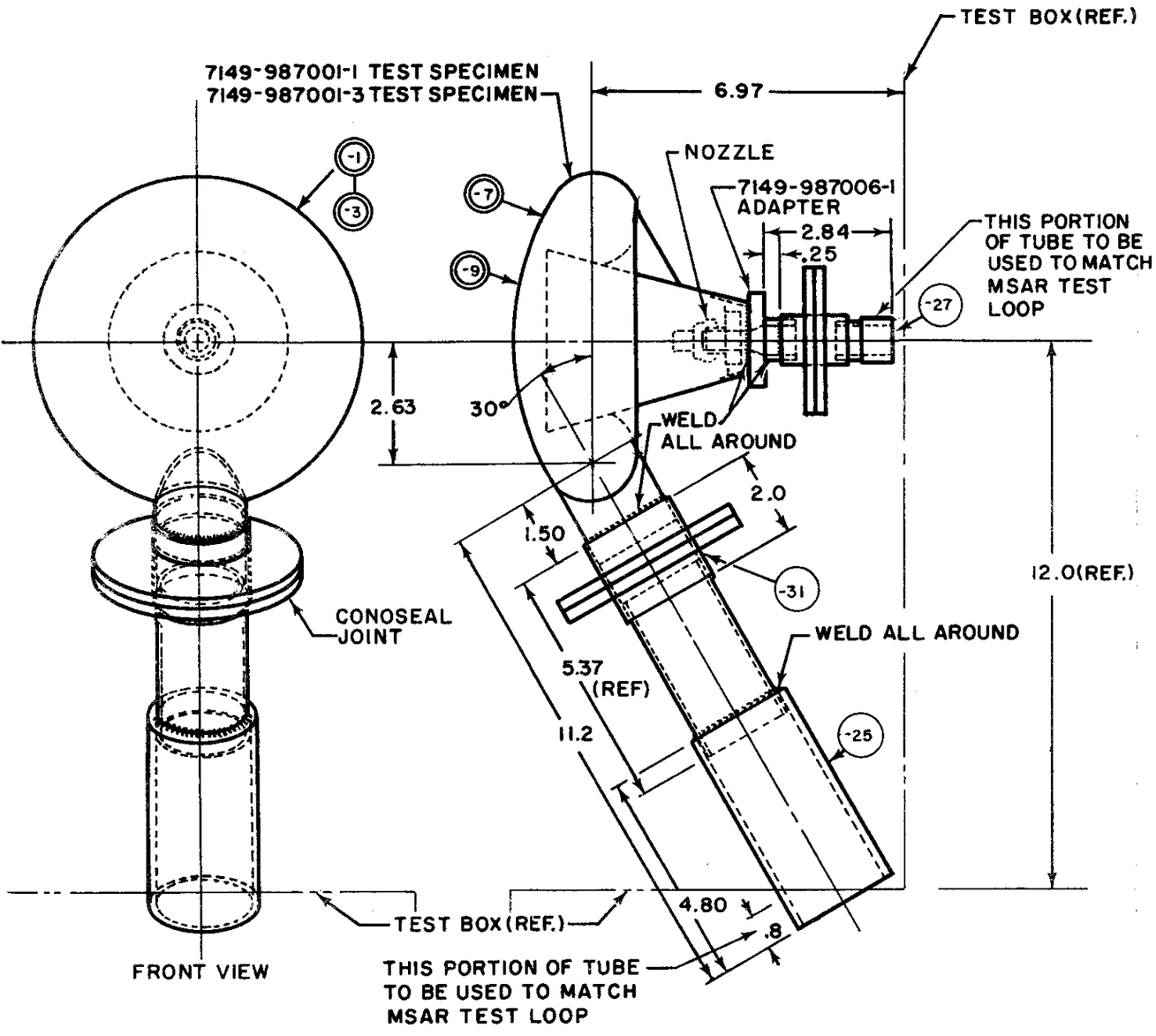

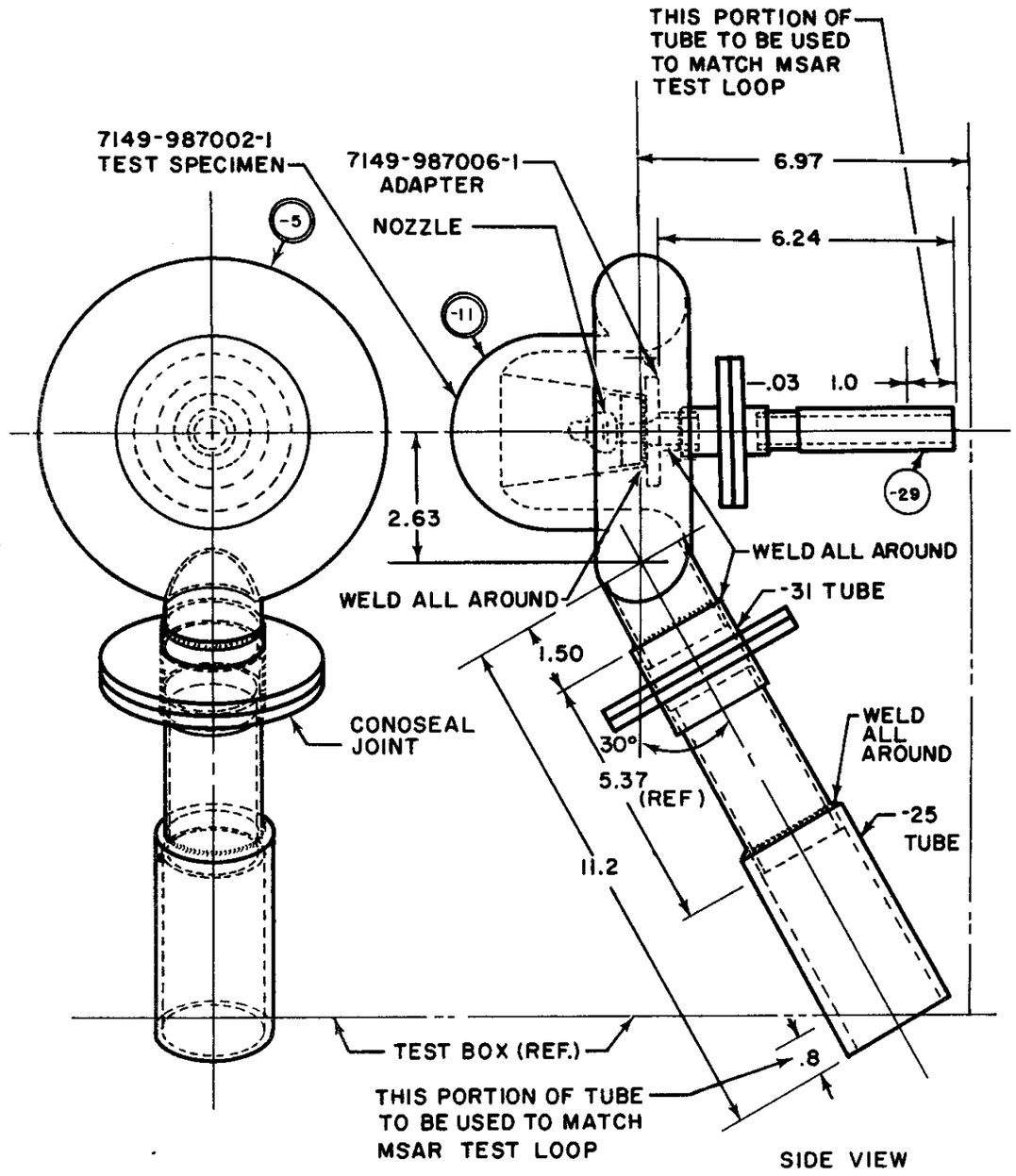

Figure 8. Installation Drawing for Series A and C Specimens

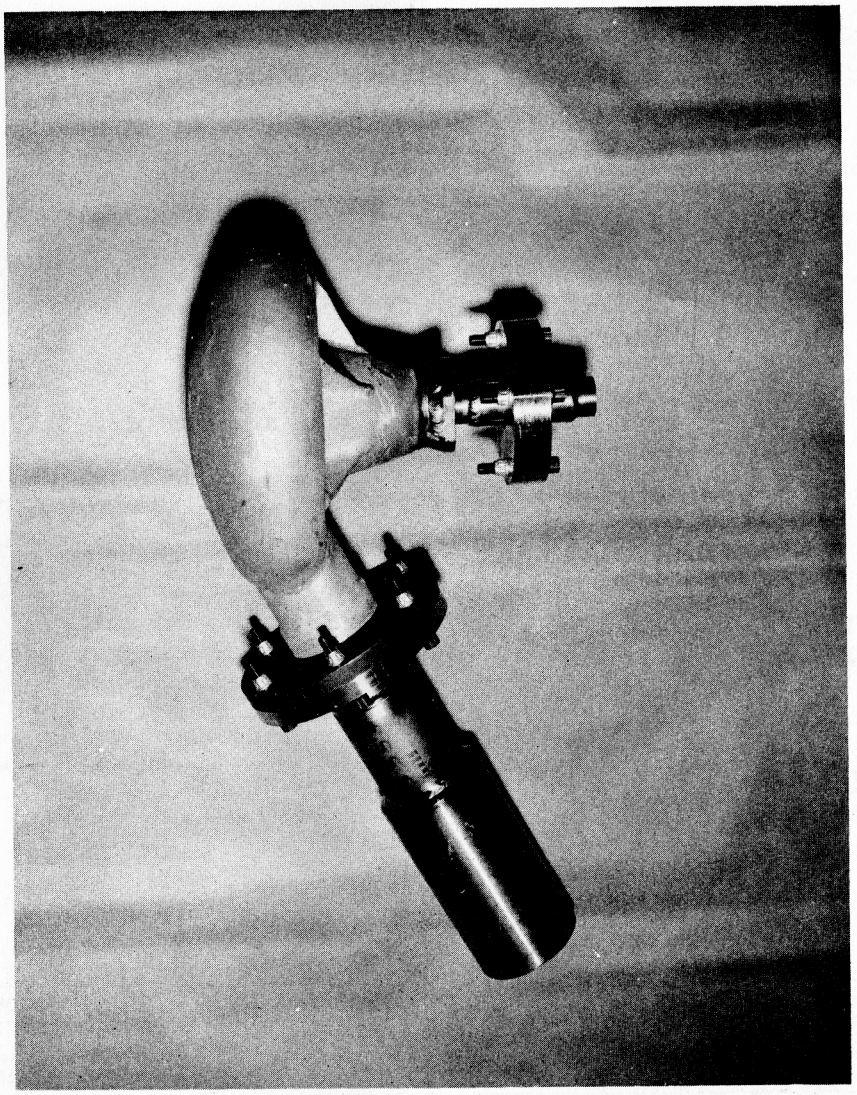

Figure 9. A Test Specimen After Coating

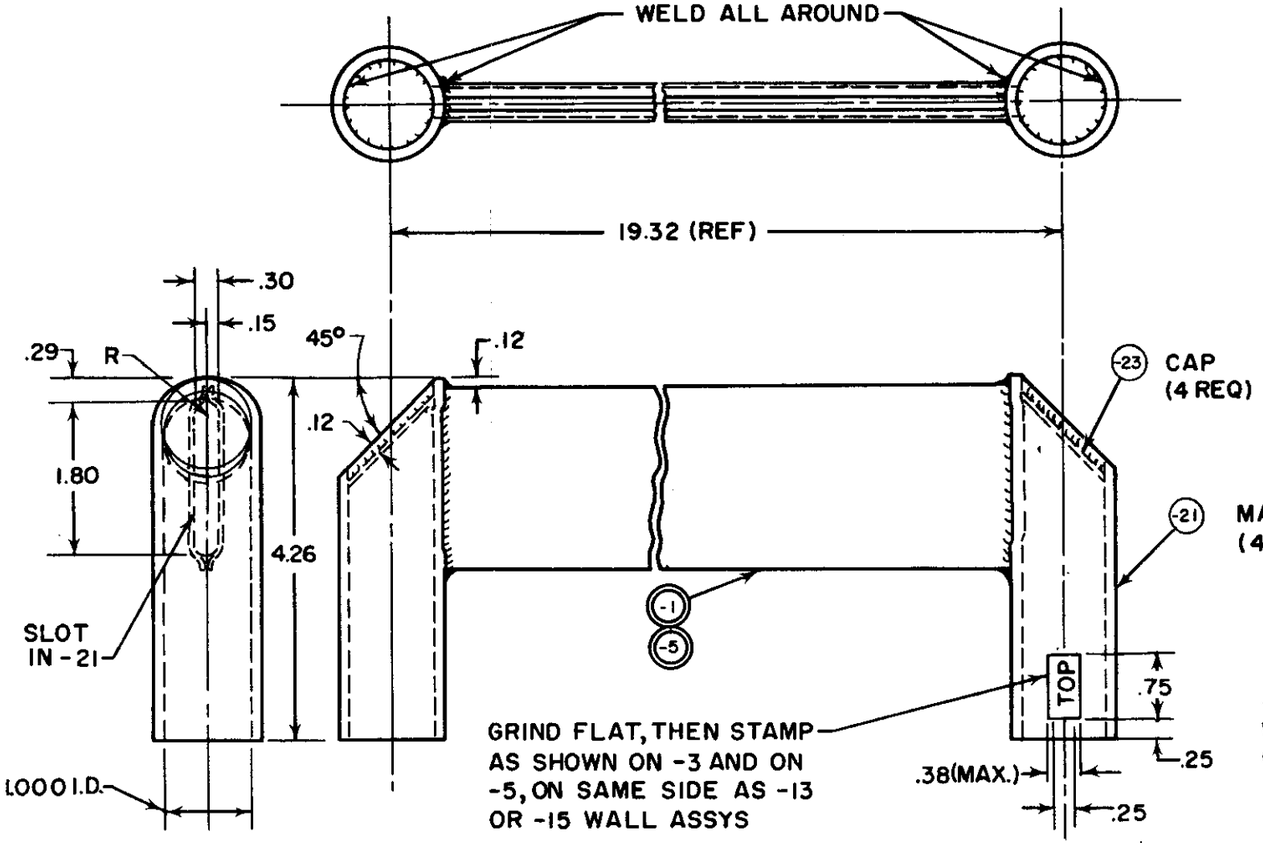

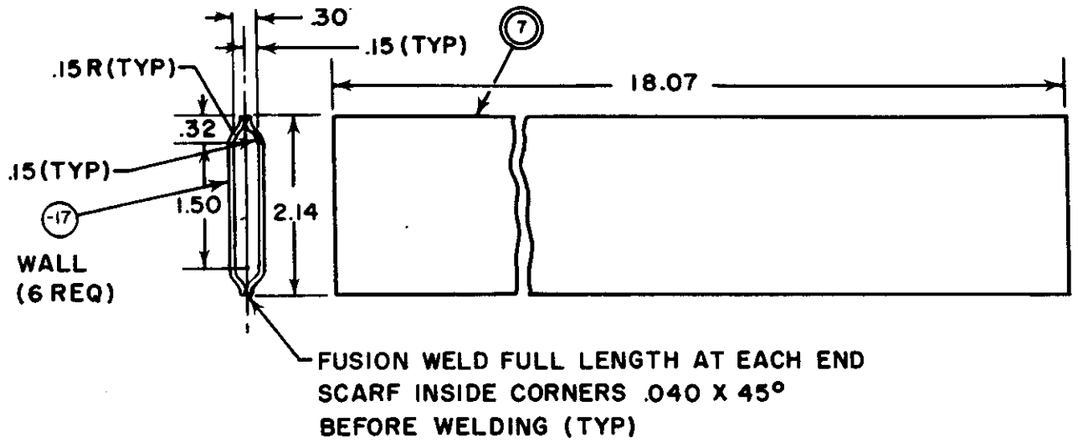

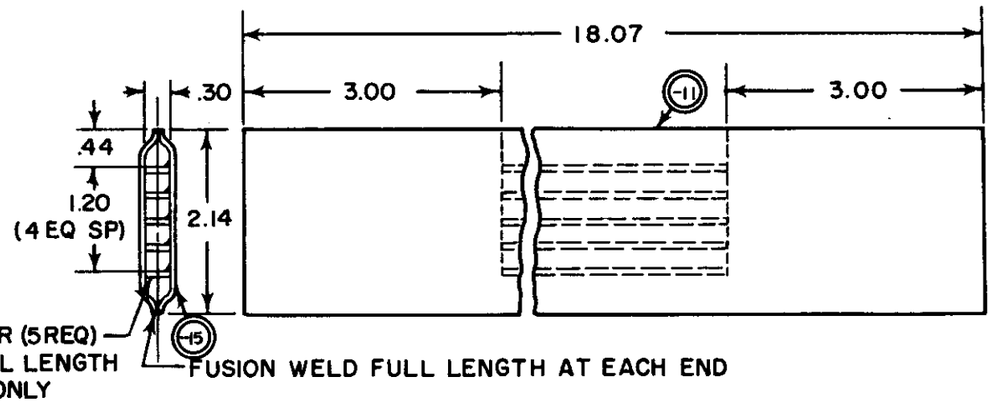

BAC DWG NO. 7149-987003

			2	2		-23	CAP	HAYNES ALLOY NO.25	AMS 5537-B		.063	1.9	1.9	145
			2	2		-21	MANIFOLD	HAYNES ALLOY NO.25	AMS 5537-B	1 1/4			4.6	
5						-19	SPACER	HAYNES ALLOY NO.25	AMS 5537-B		.063	0.5	12.5	145
1	1	2				-17	WALL	HAYNES ALLOY NO.25	AMS 5537-B		.063	3.0	18.5	145
	1					-15	WALL ASSY							
			1			-11	WELD ASSY							
				1		-7	WELD ASSY							
						-5	TEST SPECIMEN							
-15	-11	-7	-5	-1		7149-987003-1	TEST SPECIMEN							
QUANITY REQUIRED					CODE IDENT	PART OR IDENTIFYING NO.	NOMENCLATURE OR DESCRIPTION	MATERIAL OR NOTE	SPECIFICATION	DIA	THK	W	LG	1000 PSI

Figure 10. B Test Specimen Drawing

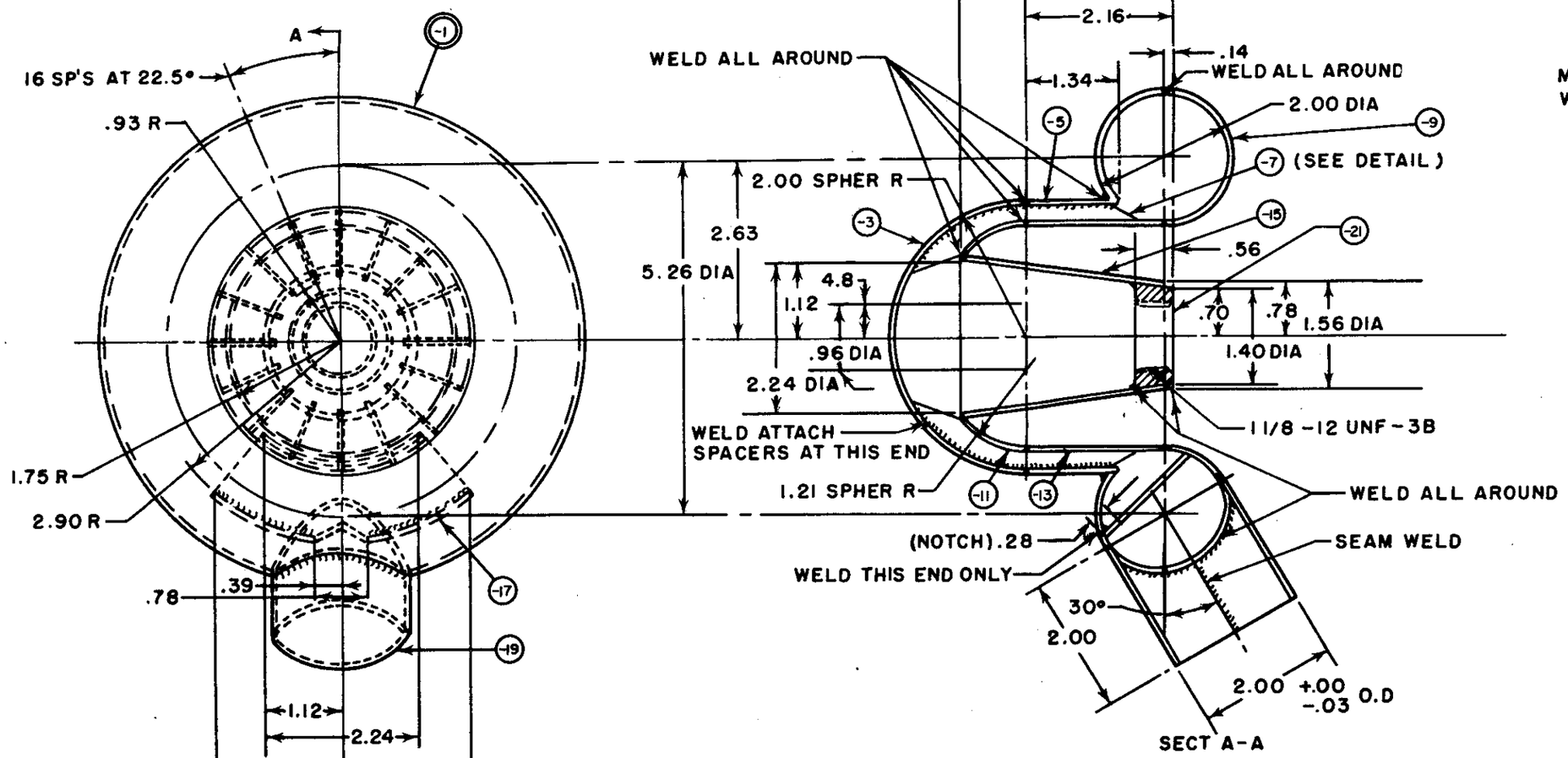

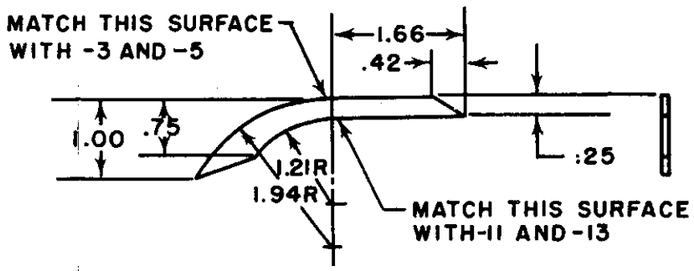

DETAIL OF -7 SPACER
(16 REQ)

BAC DWG NO. 7149-987002

	QTY REQD	CODE IDENT	PART OR IDENTIFYING NO.	NOMENCLATURE OR DESCRIPTION	MATERIAL OR NOTE	SPECIFICATION	DIA	THK	W	LG
				LIST OF MATERIALS OR PARTS LIST						
	-1		7149-987002-1	TEST SPECIMEN						
	1		-21	INSERT	COLUMBIUM-1% ZIRCONIUM		2.0			0.8
	1		-19	TUBE	COLUMBIUM-1% ZIRCONIUM			.060	2.4	7.4
	1		-17	BAFFLE	COLUMBIUM-1% ZIRCONIUM			.060	2.8	4.4
	1		-15	CONE	COLUMBIUM-1% ZIRCONIUM			.060	4.2	8.3
	1		-13	CYLINDER	COLUMBIUM-1% ZIRCONIUM			.060	2.3	11.5
	1		-11	SEGMENT	COLUMBIUM-1% ZIRCONIUM			.060	6.5	6.5
	1		-9	TORUS	COLUMBIUM-1% ZIRCONIUM			.060	9.4	18.8
	16		-7	SPACER	COLUMBIUM-1% ZIRCONIUM			.060	1.2	3.9
	1		-5	CYLINDER	COLUMBIUM-1% ZIRCONIUM			.060	1.8	13.1
	1		-3	DISC	COLUMBIUM-1% ZIRCONIUM			.060	7.3	7.3

Figure 11. C Test Specimen Drawing

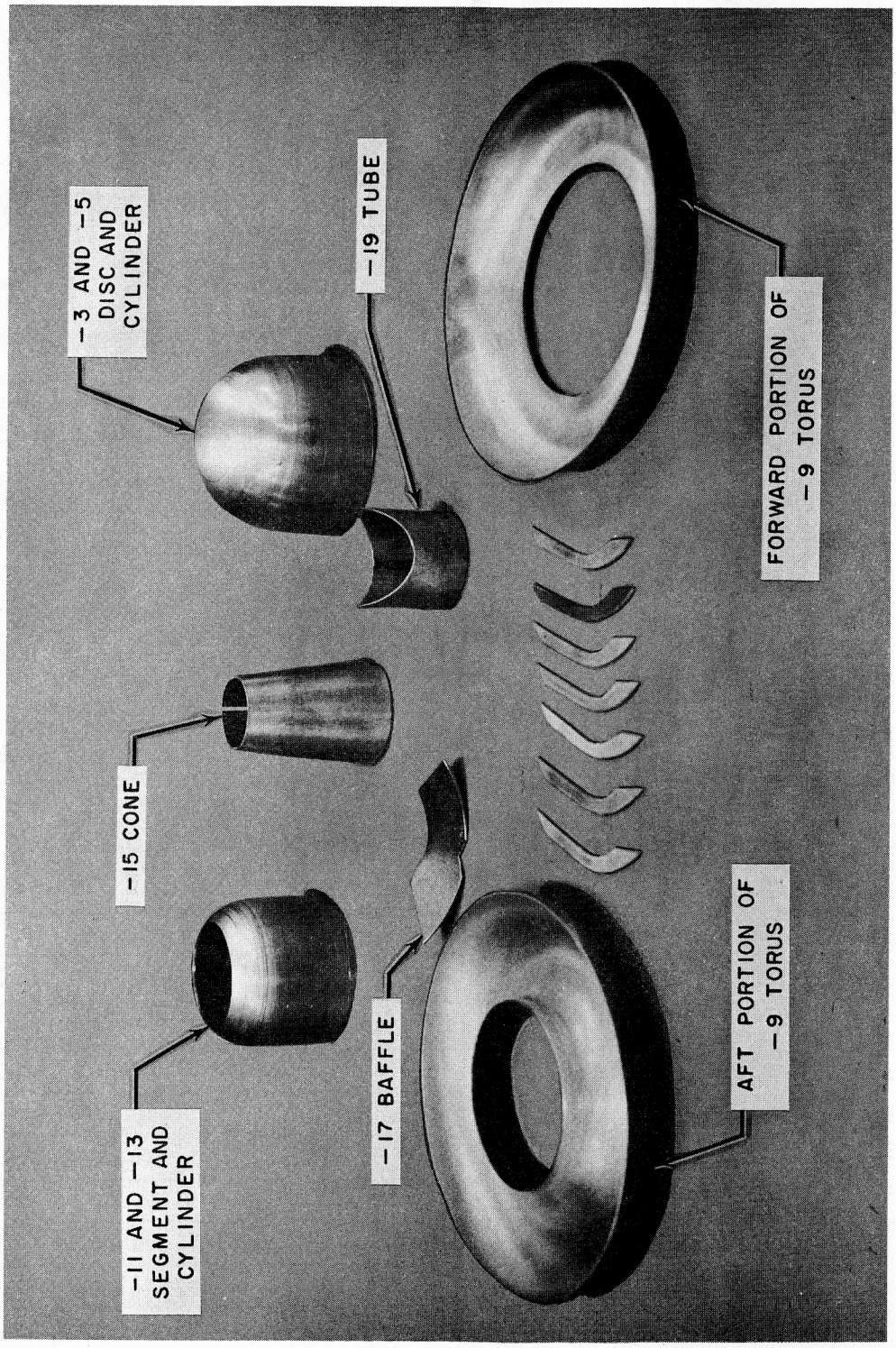

Figure 12. Major Parts of the C Specimen

Figure 13. C Specimen After Coating

5. Test Specimen Inspection

One of the most important factors to ensure the success of the test program was the requirement that the entire liquid metal system be absolutely leak tight to avoid contamination of the lithium by air leaking into the system. A stringent inspection procedure was involved, therefore, to insure that the specimen would be examined for leaks. The inspection procedure included the examination of each specimen under internal pressure with halogen leak detection equipment. In the case of the A and C specimens, the specimens were examined both before being shipped out for coating and after coating; this included the inspection of the Conoseal joints.

6. Test Specimen Instrumentation

The test specimen instrumentation was concerned with temperature measurement exclusively. The thermocouples were located with a dual purpose in mind:

(a) To protect the specimens from damage during testing.

(b) To determine the actual values of temperature at significant points on the specimens; in some cases to verify uniformity and in other cases to measure thermal gradients.

Since the operating temperature of the specimens was limited to 2200°F, 28 gage chromel-alumel thermocouples were used in all installations. The thermocouples were bonded to the A and C specimens with pyrochrome cement using the procedure outlined in Appendix I. The thermocouples were spotwelded directly to the B specimens.

The thermocouple locations for the test specimens are given in Figures 14, 15, 16, and 17.

7. Temperature Measurement and Recording System

The temperature measurement and recording system is shown in Figure 18. The required speed of response for certain tests indicated the use of an oscillograph (designated A in Figure 18) and the problem of record development dictated the use of a direct writing model, but the number of channels required exceeded the capacity of any available model. Accordingly, a multiplexing device (B) consisting of a number of relays was devised and built to enable each oscillograph galvanometer to alternately accommodate two thermocouples. The multiplexing device is controlled by a timer (C) which governs the duration of sampling times for the thermocouples, according to test requirements. A 24-channel thermocouple calibration and sensitivity control box (D) permits adjustment of each circuit to provide equal sensitivities for ease of data reductions. The potentiometer (E) is used in setting up the voltage inserted for calibration. A Series B test specimen (F) is included in Figure 18 to represent the source of the signals being measured and recorded.

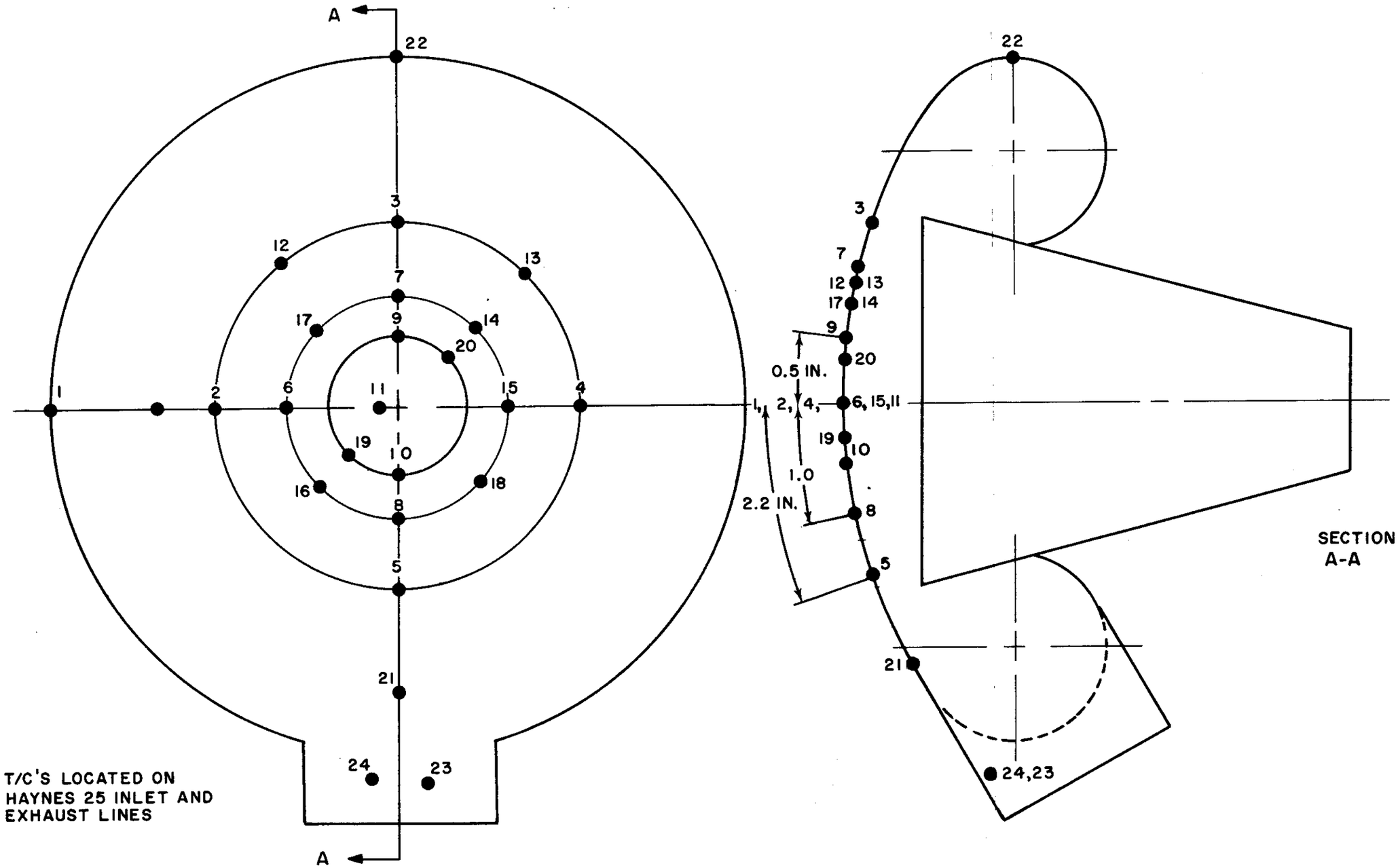

Figure 14. Thermocouple Locations - A Specimen

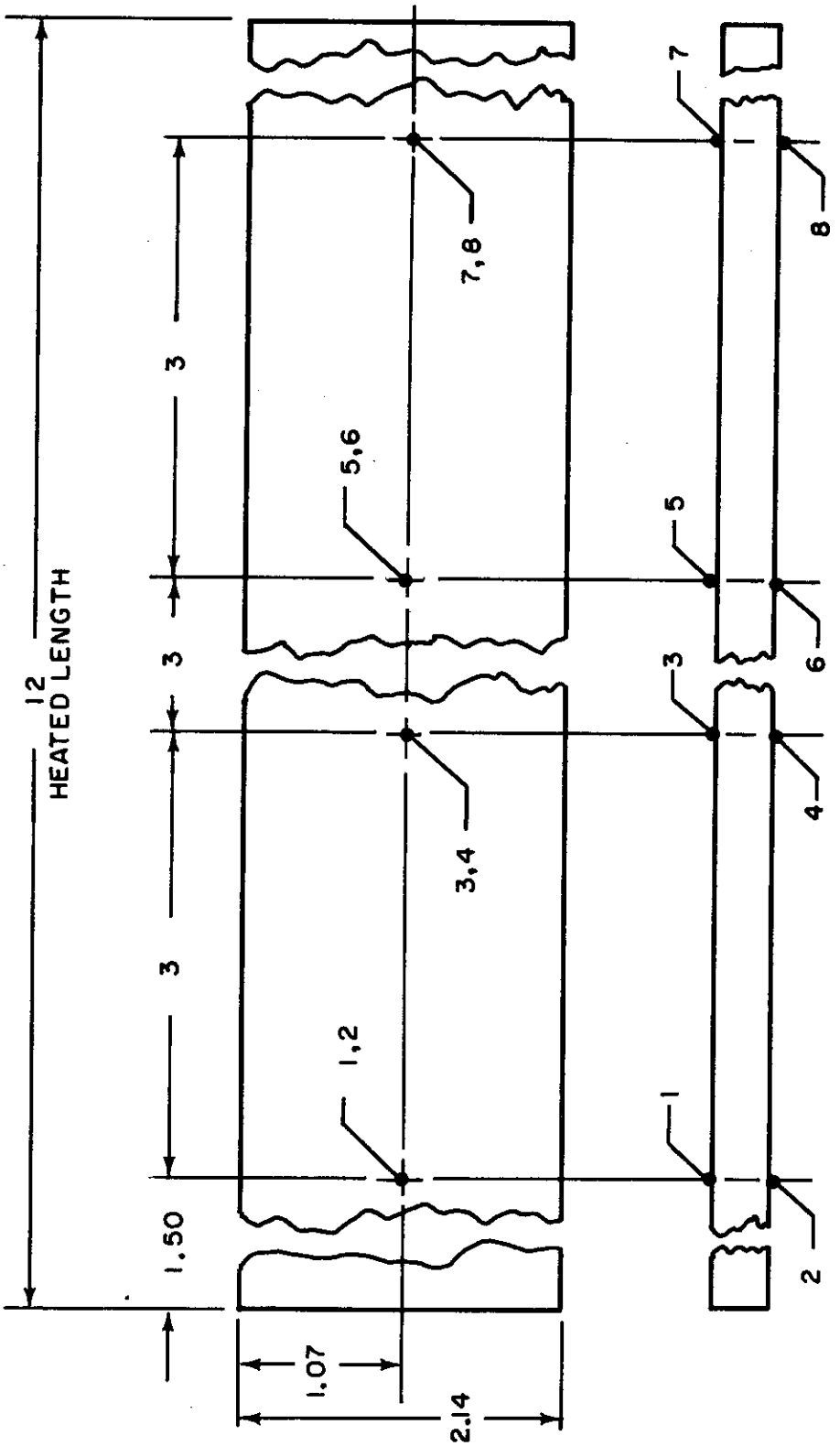

NOTE: SEE DRAWING 7149-987003 FOR DIMENSIONS

Figure 15. Thermocouple Locations — Specimen B-1

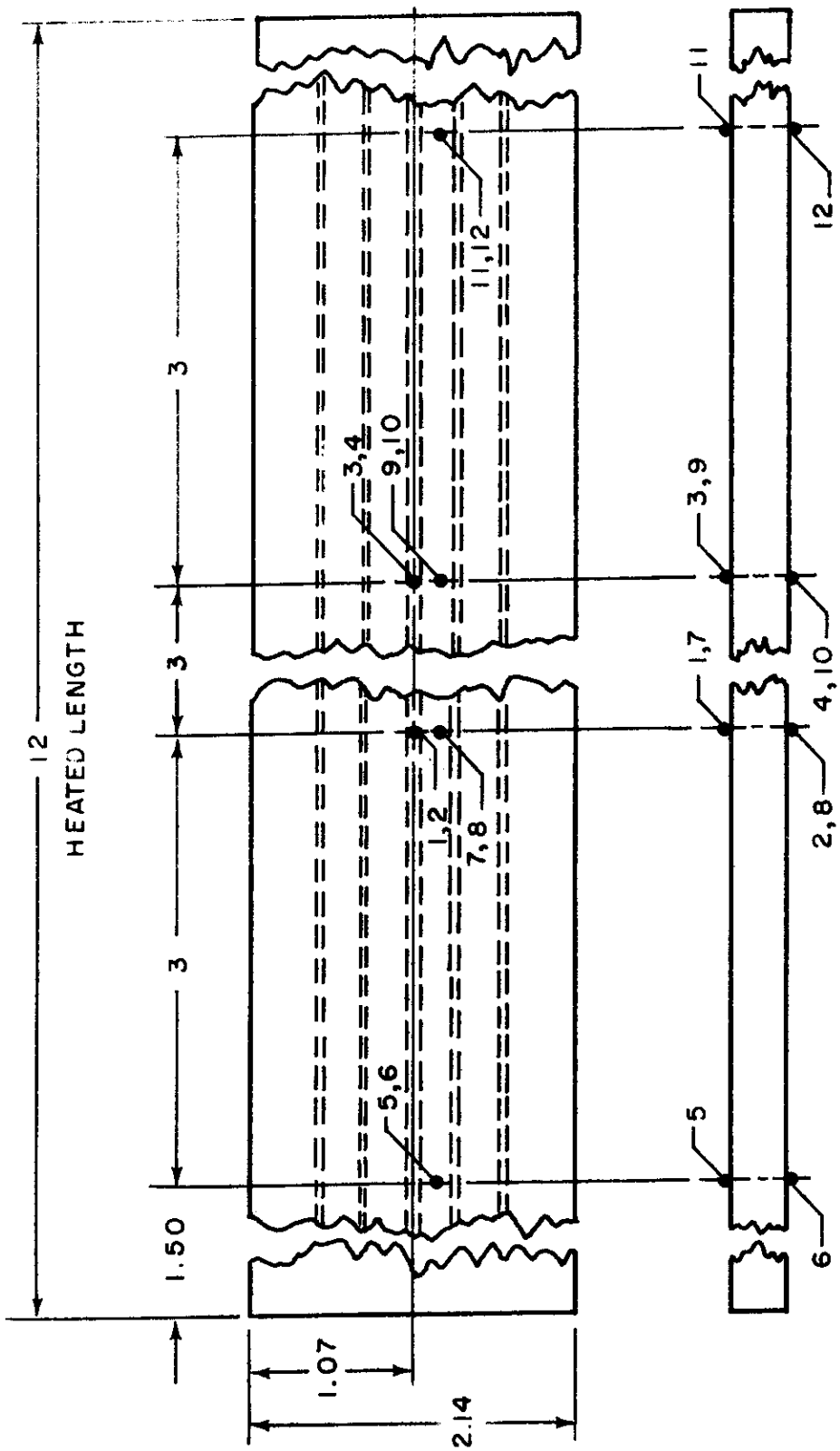

Figure 16. Thermocouple Locations — Specimen B-2

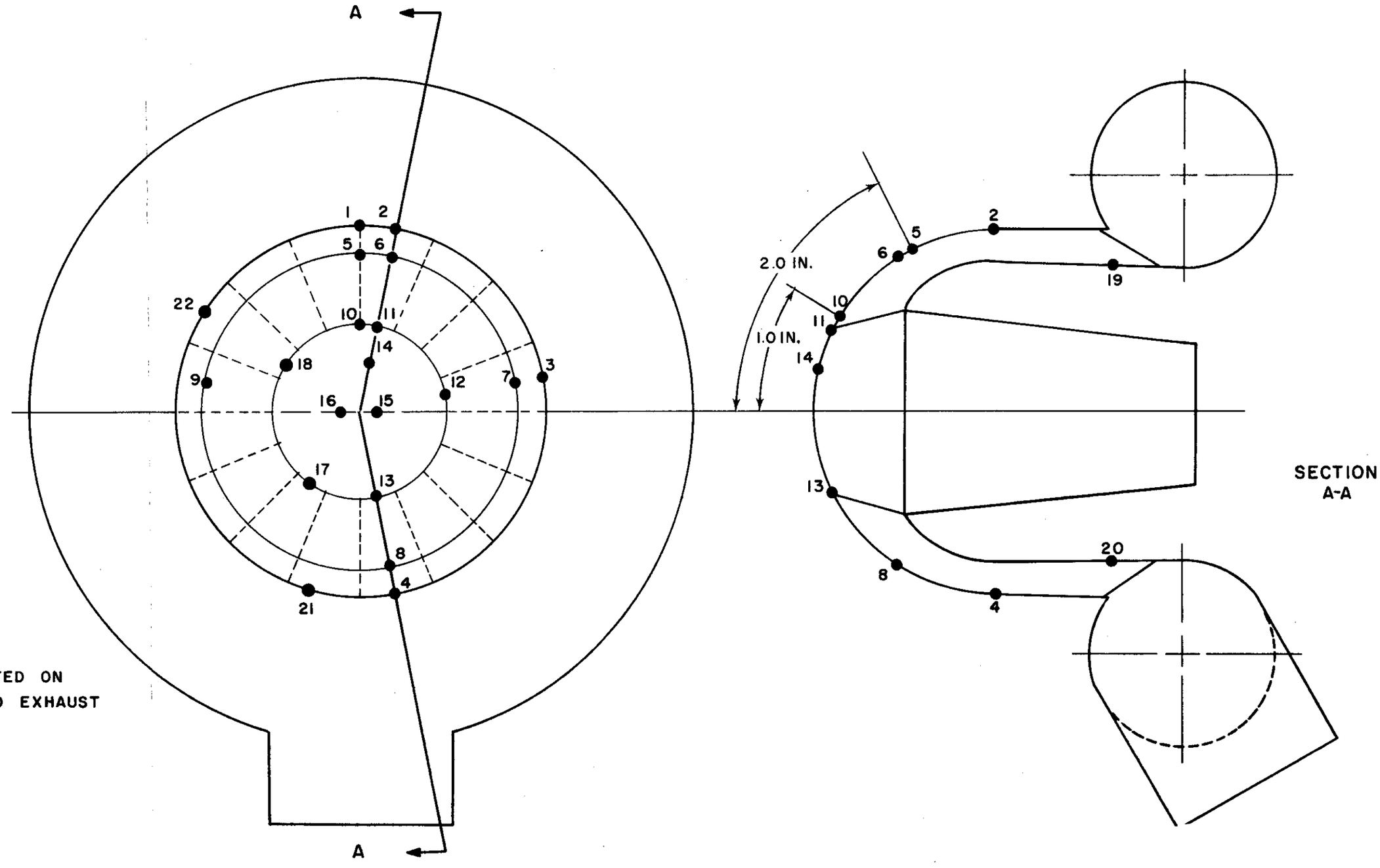

THERMOCOUPLES LOCATED ON HAYNES 25 INLET AND EXHAUST LINES ALSO

Figure 17. Thermocouple Locations - C Specimen

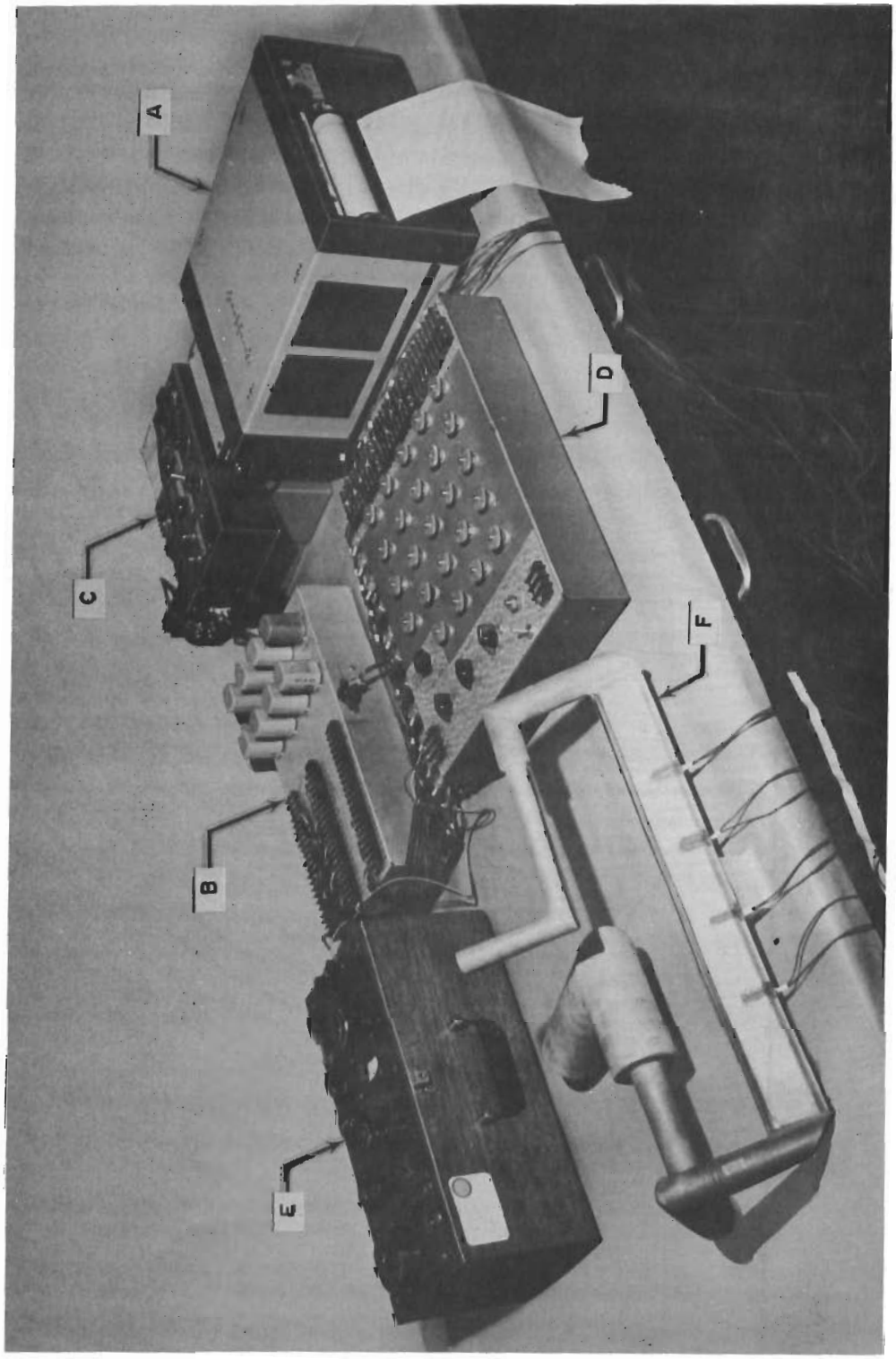

Figure 18. Temperature Measurement and Recording System

B. LITHIUM LOOP

1. General

The lithium loop was designed, built and operated by the MSA Research Corporation of Callery, Pennsylvania under a subcontract from Bell Aerosystems Company. A schematic of the loop is shown in Figure 19. The basic components of the loop include a supply tank, condenser, sump tank, electromagnetic (EM) pump, vacuum pump, and pressurization system. All pipe lines, as well as, the basic components, have electrical heaters and are insulated so that the outside insulation temperature did not exceed 140°F during operation. Haynes 25 and 316 stainless steel were used throughout the loop. A complete description of the loop is given in Reference 4.

2. Loop Instrumentation

Temperature, pressure, flow and liquid level transmitting elements were located throughout the loop. The instrumentation receivers and the manually operated powerstats for voltage adjustments to the preheating circuits were located on a panel board at one end of the loop. Thermocouple locations are shown in Figure 19. All thermocouple data were recorded on a potentiometer type strip chart recorder except the sump tank temperature which was indicated on a galvanometer type indicator with on-off control capabilities. The magnetic flow meter output, which is a millivolt signal that is proportional to the lithium flow rate, was recorded on a potentiometer type strip chart recorder.

The liquid level transmitters were located in the supply tank and the sump tank. The supply tank liquid level transmitter output, which was a millivolt signal that is proportional to the lithium liquid level, was recorded on a galvanometer type strip chart recorder. The sump tank element had to be raised or lowered manually to determine the liquid level.

3. Loop Construction

All phases of construction were performed by personnel thoroughly experienced in fabrication of liquid metal equipment. The welders were qualified under the ASME code and MSAR Specifications MPS-103 and 106. The root pass and final pass of all welds were dye checked, and some of the more difficult welds were X-rayed. All metal which would be in contact with lithium was cleaned to MSAR Specification MPS-104 and maintained in a clean condition throughout the construction phase. The completed system was mass spectometer tested in accordance with MSAR Specification MPS-105.

4. Loop Operation

The loop was charged by first evacuating the air from the loop by means of the vacuum pump and establishing an inert atmosphere with argon cover gas. The

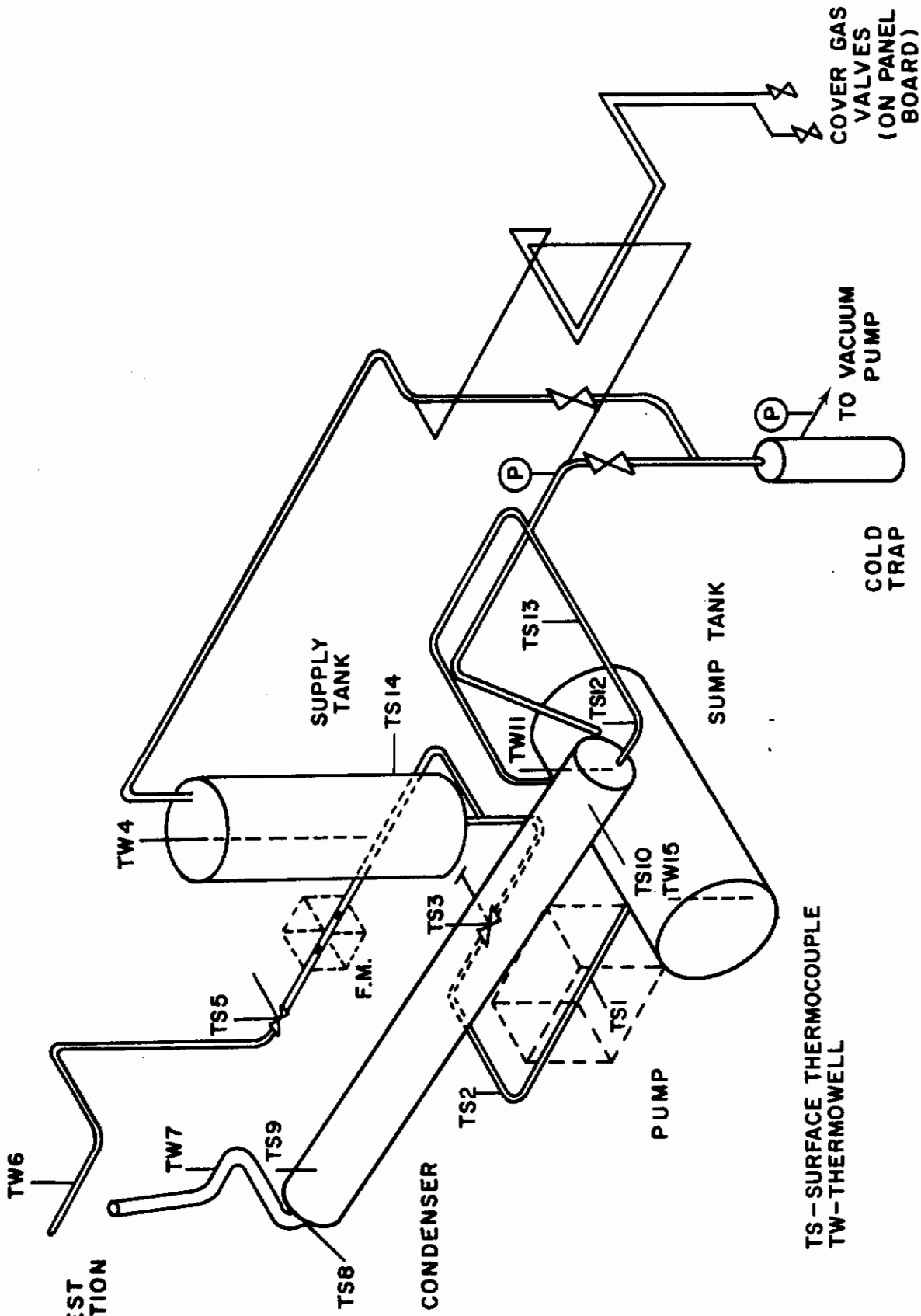

Figure 19. Lithium Nose Cap Cooling System Schematic

lithium, which was transported to the test site in a stainless steel barrel, was liquified by heating to 600°F with clamp-on drum heaters. The lithium was then pressurized from the stainless steel barrel into the sump tank.

The loop (basic components, and pipe lines) was preheated to 600°F by the electrical heaters and maintained "hot" during the entire testing phase. The pipe line heaters on the inlet and exhaust lines to the test specimens were turned off when specimens were changed.

The following procedure was used for charging the supply tank and operation of the loop during specimen testing. The lithium in the sump tank was heated to 600°F and then pumped by the electromagnetic pump into the supply tank. The valve between the sump tank and supply tank was closed and the pump turned off. The supply tank was pressurized by the argon cover gas and a vacuum was drawn on the condenser and sump tank to the desired test condition. The valve between the supply tank and test specimen was opened and flow through the spray nozzle in the test specimen was established. The flow was regulated by this valve until the test condition flow rate was established as determined by the flow rate indicator on the control board. The lithium passed through the test specimen where it was heated and exhausted into the condenser. In the condenser, it was cooled and passed into the sump. The same procedure was followed for each test run.

C. INDUCTION HEATING SYSTEM

1. General

The induction heating system used for the application of reentry level heat flux rates to the test specimens is located at the University of Florida, Gainesville, Florida, and all work concerning the induction heating portion of the test program was performed by personnel of the Induction Heating Project Laboratory, University of Florida, under a subcontract from Bell Aerosystems Company.

The system consists of two radio-frequency generators rated at 200 kw output each; each is capable of being adjusted for various operating conditions including operating frequency, output voltage, and current. The nominal operating frequency of the generators lies in the range of 200 to 400 kilocycles, although both generators have been operated with experimental tank circuits at frequencies above 2 megacycles but at reduced power. Each generator may be operated continuously at rated output, or the output can be varied by pulse control equipment developed at the University of Florida. Therefore, transient control may be achieved in accordance with specified control functions which are supplied by analog computer components. The latter equipment consists of variable-time-base function generators, analog multipliers, operational amplifiers, variable d-c voltage sources, helipots, two patch panels and static elements. Instrumentation data may be recorded on any one of several electromagnetic oscillographs.

2. Induction Heating Theory

A brief explanation of induction heating theory will be presented. A more detailed explanation is given in Reference 5.

If a given specimen is to be heated by high frequency induction, a sinusoidal time-varying magnetic field intensity is produced at the surface by passing high frequency currents through conductors (the conductor configuration is called a "work coil") located near the surface. This magnetic field penetrates the surface, producing currents which in turn produce heating. If the specimen is infinitely thick (this requirement will be relaxed later), the surface power density produced is given by:

$$P = H^2 (\pi \ f \ \mu \ \rho \ )^{1/2} \qquad \text{watts/unit area} \qquad (1)$$

where:

- **P** is the surface power density
- H is the rms (root-mean-squared) value of the surface magnetic field intensity in amperes/unit length
- f is the frequency of the sinusoidally varying magnetic field intensity in cycles per second
- μ is the magnetic permeability of the specimen material in the rationalized practical system of units = 3.2×10^{-8} henrys/inch for vacuum)
- ρ is the electrical resistivity of the specimen material in ohms-unit length

For (1) to hold practically, the specimen thickness, t, must only satisfy:

$$t \geq 2 \left(\frac{\rho}{\pi \ f \ \mu} \right)^{1/2} \qquad \text{unit length} \qquad (2)$$

In general, this restriction is not difficult to satisfy since, for example, if the specimen were copper and the frequency were 400 kilocycles, a thickness of only 0.008 inch would be required.

The magnitude of the magnetic field intensity at any point depends on the size and location of the work-coil conductors and is directly proportional to the magnitude of the work-coil current. Therefore, a given heating pattern can be produced by proper choice of the coil configuration and the current supplied by the generator.

3. Work-Coil Design and Fabrication

The extreme power density (1000 BTU/ft^2-sec) required in these studies is much greater than ever before attempted at the University of Florida in a sustained test. Therefore, some new techniques were required in this area.

Equation (1) shows the parameters involved in producing a given power density. The electrical properties, ρ and μ, of the specimen are not controllable once a given material has been selected. The frequency, f, is generally dictated by the capabilities of the generators available. The units at the University of Florida operate best in the range from 200 to 400 kilocycles per second. Therefore, the only parameter available for design is H, the surface magnetic field intensity.

In general, the magnitude of H for a given area is directly proportional to the product of the number of work-coil turns and the work-coil current. The maximum work-coil current is limited by the capabilities of the generators. The units at the University can produce up to approximately 1200 amperes for several minutes and this figure was used as a probable maximum in design calculations.

Even with this large current available, the magnitude of H necessary to produce the desired power density requires many turns in the coil. In order to get many turns in a given area, the conductors must be narrow. At the same time, the conductors must be large enough so that some type of cooling can be used to carry away the heat lost in the work coil.

The design requirements for the work coils were as follows:

(a) A specimen - provide a uniform heat flux over a four-inch diameter.

(b) B specimen - provide a uniform heat flux for an 18-inch length of the specimens on one side only.

(c) C specimen - provide a heat flux rate distribution over a hemispherical nose as a function of angular position relative to the nose stagnation point.

The final work coil, which is in the form of a spiral, was fabricated from 1/4 inch copper tubing which had been flattened to approximately 1/8 inch thickness. In order to obtain adequate water flow for cooling, the coil consists of four sections, each of which is a separate water path. These sections were fabricated by cutting the tubing on a 45° angle and soldering with a 1100°F melting point alloy to form 90° elbows. The sections were then soldered in series using a 1250°F melting point alloy. The tubing was then wrapped with TFE (Scotch No. 51) tape and formed in a spiral of approximately eight turns with a 3/8-inch inside diameter and a four-inch outside diameter.

The maximum allowable length of each section was determined by experimentation. With each section supplied with water at a pressure of 150 psi, high frequency currents were passed through the coil and the temperature rise rate of the water in each section was noted. These tests revealed the interesting situation that, with a constant current, the temperature differentials were less when the coil was adjacent to a simulated specimen than they were with the specimen removed. This is due, no doubt, to the difference in field distributions in the two cases. It meant,

however, that meaningful testing must be conducted with a specimen. Since it was not practical to build a simulated specimen which would absorb the maximum design powers, these tests had to be conducted at reduced power and the results extrapolated.

The final design resulting from these tests consisted of a four-inch section (at the center of the spiral), two 16-inch sections, and an 18-inch outer section. The center section was the most critical but it appeared adequate since it had a flow rate of 3.2 gallons per minute and a temperature increase of only 20°F at a work-coil current of 570 amperes. Extrapolating this temperature differential to the maximum test current of 980 amperes gave 60°F, a workable figure with a good safety margin. The outer sections had lower temperature differentials.

The contour of the coil which gave the best heating pattern was experimentally determined using the survey coil technique which is discussed in Reference 5 and a dummy specimen. This contour was slightly curved but not as great as that of the series A specimen. The desired contour was machined out of a flat plate by cutting a 10° slope for a radius of one inch and an additional 10° slope for the remaining radius. The coil was then pressured to this contour and potted with Scotchcast Resin No. 5. In the final tests, the coil was mounted using a phenolic collar around the potted coil.

The resulting work coil was used for both the A and C test specimens. This was possible since the shape of the specimen affects the resulting heating pattern. The spiral type coil used produced an area of reduced heating at the center and had to be accepted.

Figures 20 and 21 show a representative distribution of the H^2 (proportional to the surface power density for a constant f, μ and θ) as measured by the survey coil for the A and C test specimens, respectively. The magnitude of the power density depends upon the magnitude of the work coil current and the magnitude of f and θ . The H^2 distribution does not have axial symmetry because of the special effect. The distributions are for a specimen to work-coil spacing of 0.125 inch.

Preliminary design work was performed for a work coil suitable for the B test specimen. A coil was constructed and the resulting heating pattern measured. However, this work coil was never completely tested since the B specimens were not tested (see Section 4-C).

4. Insulation Between Work Coil and Specimen

In most induction heating applications, the specimen is at ground potential while the work coil is at some voltage other than ground. Some form of electrical insulation is therefore required between them. This insulation may consist of tape wrapped around the coil, it may be flat sheet insulation between the coil and specimen, or it may consist of both of these. Most available electrical insulating materials must also be protected from the high temperature of the specimen surface.

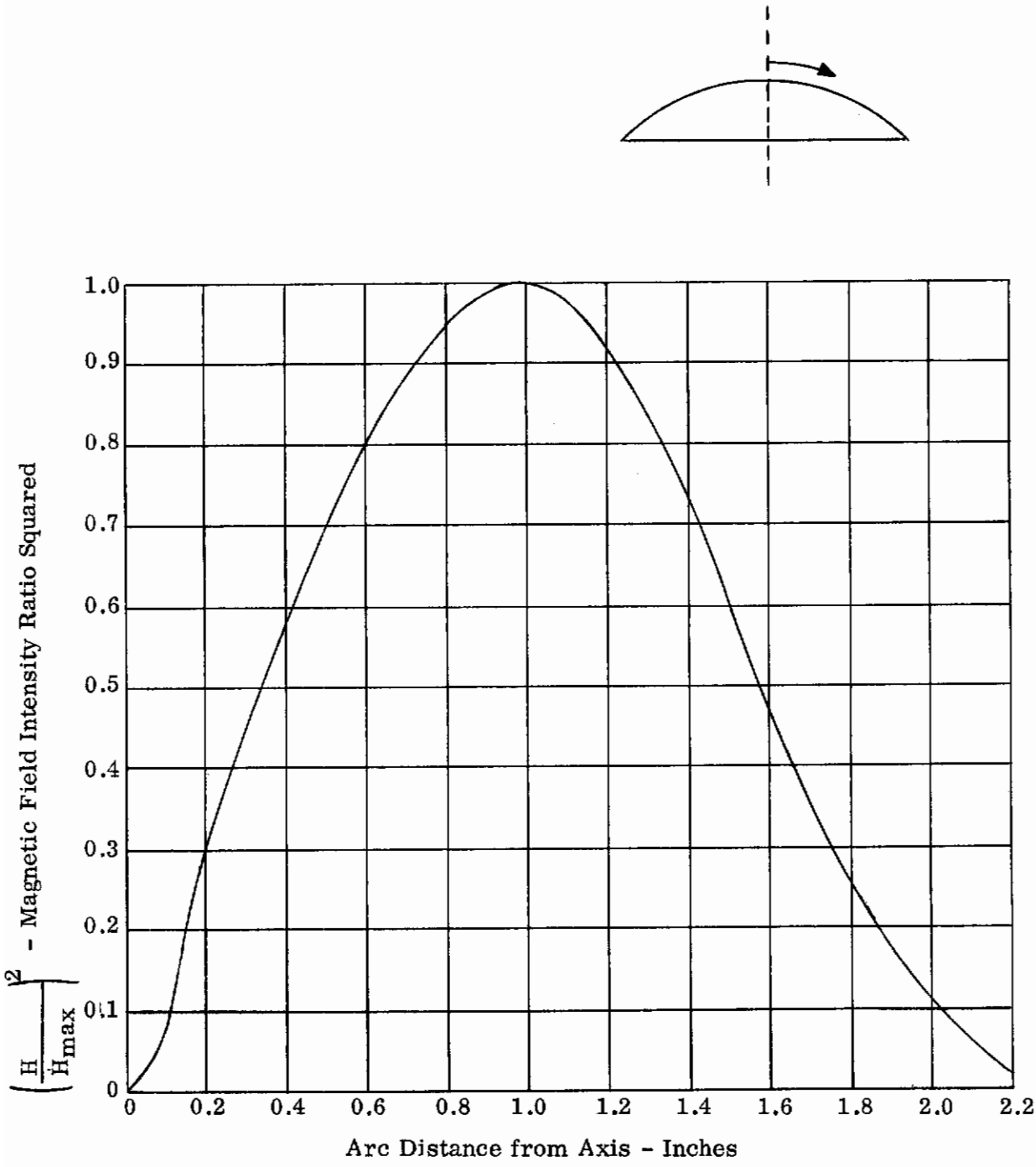

Figure 20. Representative Field Distribution for A Test Specimens

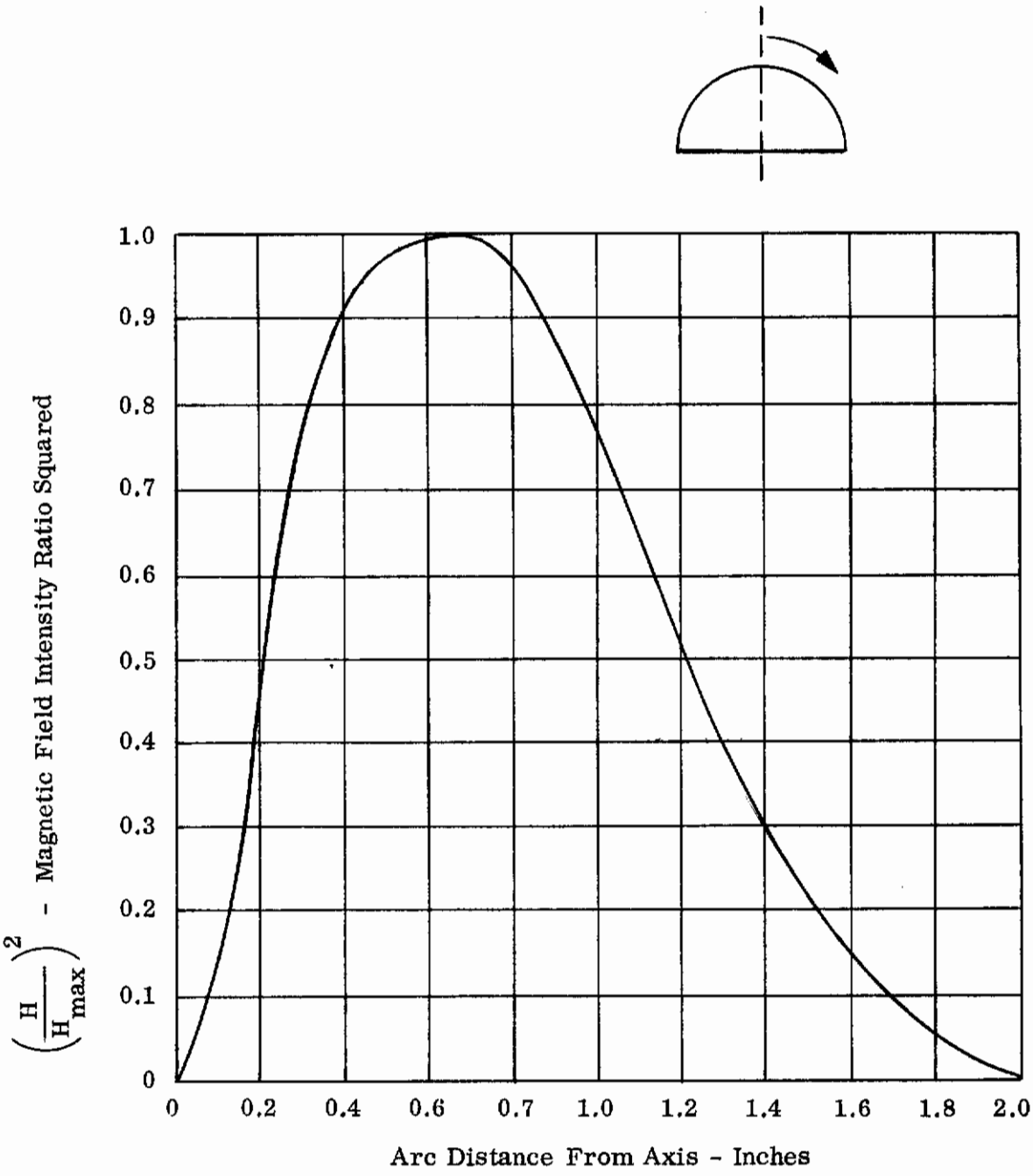

Figure 21. Representative Field Distribution For C Test Specimen

For the work coils used, TFE tape was wrapped around the conductors to provide insulation between turns. This wrapping also constituted the primary insulation between coil and specimen. However, the upper temperature limit of TFE is about 500°F, so thermal insulation was also required. Furthermore, if for any reason the work coil failed, destroying the TFE, it was required that any current be prevented from reaching the specimen. This made additional electrical insulation necessary between the coil and specimen. Previous tests of insulating materials (Reference 6) had shown that laminations of certain types of sheet insulation were most effective at high temperatures. In this technique, sheets of electrical insulation are placed adjacent to the work coil and sheets of thermal insulation next to the specimen. For these tests, sheets of silicone impregnated Isonica (3M Company, Type T1-20) were used as the electrical insulation. This material is an excellent RF insulator and withstands up to 1200°F. As thermal insulation, sheets of Tipersul, fibrous potassium titanate (E.I. DuPont) were used, Tipersul is effective up to 2200°F.

It had been found that three or more sheets of Tipersul 0.025 inch/sheet, adjacent to a 2200°F surface would adequately protect a 0.024-inch thickness of T1-20 (12 sheets, 0.002 inch/sheet) adjacent to a 200°F surface. For these tests, four sheets of Tipersul were used with 12 sheets of T1-20, giving a total insulation thickness of 0.124 inch.

For the tests on the first A specimen, the Tipersul was shaped over the curved specimen, while the T1-20 was held by compression to the lesser curvature of the work coil. This protection system was later revised during the actual test program as is discussed in Section 4-B.

5. Automatic Cutoff Meter

In order to protect the test specimens from damage due to possible overheating, an automatic cutoff meter for shutting down the equipment was installed. The meter relay would operate from one of the test specimen thermocouples and if a preset temperature was exceeded, the cutoff meter would automatically throw the circuit breakers to the induction heating equipment. The cutoff meter was installed at the RF control console to provide continuous temperature monitoring in addition to the shutoff feature.

6. Control System for Transient Heating

The method of closed loop control which was used for the transient heating tests warrants some discussion. The most desirable method would utilize a sensor of actual surface power which could be compared with the desired power versus time function. Unfortunately, there is no device for directly measuring surface power at high levels. Therefore, some secondary means must be used.

A quantity which is reasonably conveniently measured is work-coil current, or better, the square of the current, which can be directly related to surface power if the work-coil geometry and specimen temperature are known. By this method, the

desired power curve must be corrected for specimen temperature if accurate simulation is required.

It was originally planned to use the above technique of control with the output of the thermal RF ammeter as the feedback element. However, the output of this device was extremely noisy, and therefore unsatisfactory for use in the control loop. Fortunately, in the proportional pulse control system which was used, the percentage of duty cycle is also related to the power output. Using the duty cycle as a feedback signal is somewhat less accurate than a current control, but for the purposes of these preliminary tests it was considered satisfactory. A duty cycle meter was available and was modified to provide a feedback signal, the level of which was proportional to duty cycle. The control system was aligned so that the peak RF current desired (700 amps) was very nearly 100% duty cycle. The actual RF current (squared) was recorded as described in Section 4-C.

SECTION 4

EXPERIMENTAL PROGRAM

A. PRETEST CHECKOUT

Initial operation of the lithium loop system was conducted, with a B specimen installed, for the purpose of overall checkout. Lithium was charged into the sump tank, the NaK inert gas purifier was charged and connected to the system, and the electrical equipment and instruments were activated.

1. Lithium Loop

Lithium was pumped into the supply tank at 500°F and was then pressured through the specimen and condenser and back to the sump tank. After three runs, it was impossible to get flow through the supply tank inlet line or outlet line and it was assumed that the valves were not opening. These valves utilized springs to lift the plug off the seat and if the springs were overheated they would no longer lift the plug. Visual examination of the valves verified that they had been overheated. This overheating resulted from the surface thermocouples not being bottomed in their wells, thereby indicating a temperature which was possibly 300°F below actual temperature when the lines and valves were being preheated. This type of valve was used to speed up the original delivery of the system because the high temperature positive lift valve was not available.

Checkout was again initiated after a Hoke valve was installed in the supply tank inlet line and a special Haynes 25 throttle valve was installed in the supply line. Installation was difficult because the lines were full of lithium which made cleaning a problem and made it impossible to get an argon purge at the open ends. Every effort was made to reduce air contamination but without success on the supply line, as determined later.

Lithium was pumped into the supply tank several times to check calibration on the liquid level instrument at 700°F, then the tank was charged and the pressure increased to 50 psig. At this time a leak was noted in the button head near the thermowell. The leak occurred in a crack in the flanged portion of the head adjacent to the thermowell weld. The tank was removed, washed with water, the crack repaired, dried and replaced in the system.

After recharging the supply tank, flow could not be established through the supply line so it was cut out for cleaning. The lithium was melted out and a plug was found at the valve inlet. The entire line was washed with water, dried and replaced. Flow could then be maintained without difficulty. Several runs were made to calibrate the flowmeter against the supply tank liquid level instrument. While the calibration runs were successful, it was found that the CEC Haynes 25 valve leaked slightly across the seat. However, it was not felt that the leak rate was not high enough to cause trouble. The valve had been calibrated at MSAR to determine the flow and pressure drop at various positions and it was leak tight during these tests.

The B specimen was replaced with the first A specimen in preparation for the first run. The first flow calibration run was started at 700°F and 50 psig on the supply tank. After a short time, the flow was increased by increasing the pressure on the supply tank and at approximately 55 psig a leak occurred at the same place as the previous leak. The tank was drained and all the lines were blown clear of lithium.

Since the crack was adjacent to the repair weld and there was no assurance of making a successful repair, the decision was made to replace the tank with one made from Type 316 stainless steel (see Appendix II). This material could now be used since the maximum operating temperature had been lowered from 2000 to 1500°F. The new tank was made from a 23-3/8-inch long section of 1/4-inch plate rolled into a 14-inch OD cylinder with two ASME flanged and dished heads. It also differed from the Haynes 25 tank in that the thermowell enters the top head instead of the bottom head, and the supply line tied into the 1/2-inch nozzle at the bottom rather than the bottom head.

The new supply tank was installed, along with a new Type 316 stainless steel supply line which included a Hoke HY477 valve. This was done to replace the CEC valve which leaked across the seat. Several calibration runs were made which indicated that the system was ready for test operation.

2. Test Specimen Instrumentation Recording System

During the checkout period, the instrumentation recording equipment was placed in operation. Filters were placed in the circuits to prevent RF pickup from the induction generators. The number of thermocouples used on the test specimen exceeded the number of available galvanometers in the oscillograph and by using the multiplexing unit, it enabled each galvanometer which was multiplexed to alternatively accommodate two thermocouples. The multiplexing unit is controlled by a timer which governs the duration of sampling time for the thermocouples. Twelve of the oscillograph galvanometers were multiplexed. The remaining five galvanometers were not, thus allowing for continuous recording of temperature data on these galvanometers.

The oscillograph uses a photographic type of paper. A light beam from each of the galvanometers is focused on the oscillograph paper. As the paper moves out of the oscillograph and the thermocouple millivolt output deflects the galvanometer, a line appears on the paper when it is exposed to light. With 17 galvanometer, 17 lines appear on the paper and each line must be identified with a galvometer number. Each galvanometer trace is a continuous line except for the break which will occur opposite a number along one edge of the oscillograph paper. This number corresponds the galvanometer number. If two galvanometer traces are superimposed, no break will appear for either galvanometer and trace identification is difficult or impossible when this occurs with more than one pair of traces. For the multiplexed galvanometer, the traces are not continuous because sampling of two thermocouples whose millivolt outputs are not the same will cause abrupt changes in the traces. The same method of trace identification is used as for the continuous traces but, in addition, the trace indicates which side of the galvanometer is being sampled.

For the checkout, the baselines for each galvanometer were displaced 0.1 inch from each other to aid in trace identification. The multiplex timer was set for one second sampling time for each thermocouple on a multiplexed galvanometer.

The results from these checkout runs made two problems evident. One of the functions of the specimen thermocouples was to ensure that the specimen temperature did not exceed 2200°F, as a safety precaution, since burnout of the test specimen would allow air to enter the lithium loop and contaminate the lithium or start a fire. The galvanometers were calibrated so that a four-inch deflection was equivalent to 2200°F. It was found that the oscillograph paper developed too slowly to identify galvanometers during a test run, or determine the magnitude of temperature due to galvanometers not starting from the same baseline. The multiplexing presented an additional problem in identifying galvanometers because of the short time duration of sampling of each thermocouple on the multiplexed galvanometers.

To circumvent these problems, all of the galvanometers were started from the same baseline. At ambient temperature, all of the galvanometer light beams are superimposed and appear as a single light dot. By placing a calibrated scale for temperature on the oscillograph above the light dots, the temperature could be visually monitored and when any thermocouple indicated 2200°F, the induction heating unit would be shut down. The multiplexing unit would become essentially a two-position switch. All primary thermocouples would be placed on one side of the switch and all secondary thermocouples on the opposite side; changing of the switch position would be done manually. When power was increased to the induction heating work coil, the primary thermocouples would record continuously and data for the secondary thermocouples would be recorded only after the specimen had reached thermal equilibrium at each constant heat flux level. Galvanometer-trace identification would be made after a test run was completed when the oscillograph paper could be fully developed.

It was realized that trace identification would be difficult since the specimen thermocouples were located in concentric rings from the specimen center and the thermocouples in the same ring should indicate the same temperature since they would be at points of the same heat flux. This meant the likelihood of traces being superimposed was great but the prevention of specimen damage was vastly improved, and more important, danger to test personnel was greatly reduced.

B. TEST SETUP

1. Mounting of Induction Heating Work Coil

Since the test specimen as well as the lithium loop would be subjected to thermal growth, the mounting of the work coil presented a problem. Power density distributions were based on a 0.125 inch work coil to specimen spacing. Attempting to maintain this spacing as the test specimen and loop elongated did not appear feasible. It was decided to set back the work coil and allow the thermal growth to bring the specimen up to the required spacing at temperature.

Originally it was planned to anchor the inlet and outlet lines to the test specimen and mount the work coil independent of the lithium loop and test specimen so that only the specimen thermal growth had to be accommodated. Analysis of the resulting thermal deformations, which would result in the test specimen because of the relatively cool inlet line and hot exhaust line, indicated high thermal stresses would result in the test specimen. In addition, the work coil could be set back to compensate for the specimen axial growth, but the resulting specimen rotation from the unequal growth of the inlet and exhaust line could not be compensated.

The work-coil mounting problem was finally resolved by using the work-coil mount shown in Figure 22. The specimen exhaust line is anchored and the inlet line is free. A horizontal bar is welded to the inlet line and the work coil is cantilevered from this bar. It will be noted that any specimen rotation will be accommodated since the work coil is essentially mounted to the test specimen and as the test specimen rotates so will the work coil. The thermal growth which must be compensated is from the point at which the bar is welded to the inlet line to the specimen face. The work coil would be set back equal to this elongation. At the lower heat fluxes, when the test specimen was not up to temperature, the actual heat fluxes would be lower than the indicated heat fluxes due to the work coil to specimen spacing being greater than 0.125 inch.

2. Test Specimens

The test specimens were joined to the loop through Haynes 25 welds. After completion of tests on a specimen, the specimen was removed from the loop by cutting the inlet and exhaust lines to the loop. To prevent contamination of the lithium during this removal process and installation of a new specimen, a high purge of argon cover gas was maintained through the test section until the final closure weld was made.

C. TEST PROGRAM AND PROCEDURE

1. General

Due to instrumentation problems with the test specimens, the originally planned test program had to be curtailed. After the first run on each specimen, a number of the cemented thermocouples became detached from the specimen surface and after each succeeding run, additional thermocouples became detached. Duplicate thermocouples had been added to areas of the test specimens which would be highly heated, since previous experience with cemented thermocouples indicated that cemented installations are subjected to spalling in an erratic manner. The tight test schedule precluded any attempt to replace thermocouples during the testing phase. This problem reduced the number of test runs which could be conducted on each specimen, since the thermocouples were essential in determining if and when specimen burnout was occurring.

The B test specimens which were fabricated from Haynes 25 sheet were not tested. After the Haynes 25 supply tank failure, the integrity of the B specimen welds

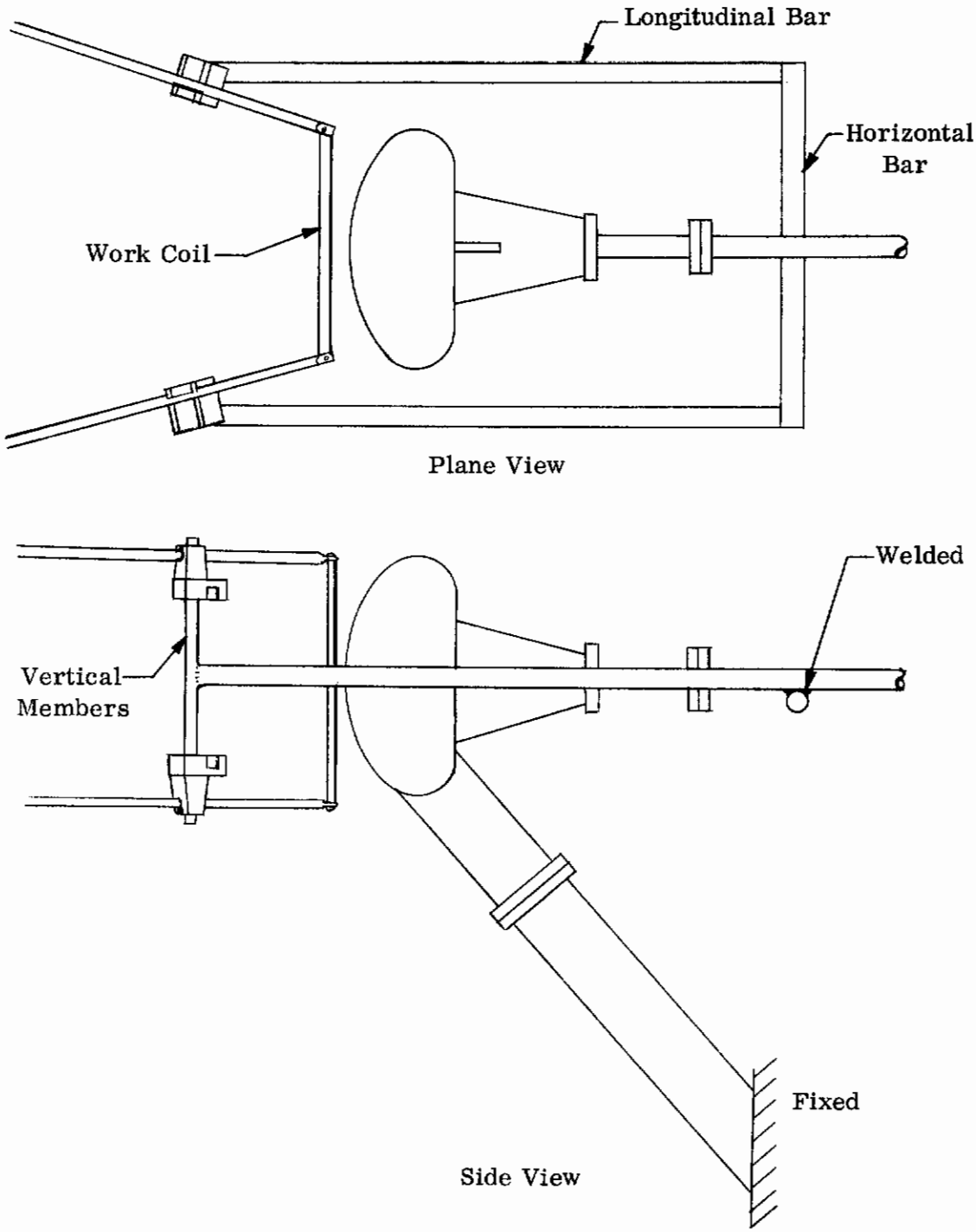

Figure 22. Schematic of Work-Coil Mount

was questionable and it was advisable not to test the specimens. A failure of the test specimens would allow the lithium to leak out and ignite. This would cause failure of the water cooled induction heating work coil and would result in a reaction between the lithium and water.

2. Test Program

The test conditions for each of the specimen test runs are shown in Table 1. The test runs on the A specimen, Type I, were conducted to determine the maximum heat flux that could be tolerated. The test runs on the A specimen, Type II (knurled), were also conducted to determine the maximum heat flux but in addition: run No. 1 was conducted to determine if knurling had any effect on the heat flux by comparison with the test runs on the A specimen, Type I; run No. 2 was conducted to determine the effect of vapor pressure on the heat flux by comparison with run No. 1; and run No. 3 was conducted to determine the effect of the flow by comparison with run No. 1.

The C test specimen, which was a scale model of a prototype hemispherical nose, was to be used for the application of a transient heating cycle. In addition, the heat flux distribution over the model was to be varied as a function of the angular position relative to the nose stagnation point. The vapor formed when the spray made contact with the heated surface would flow to the rear and cool the remainder of the hemisphere not covered by the spray by convective cooling. Since the testing of the B specimens was eliminated, the determination of the ability of a wet vapor mixture to pick up heat was unknown. The heated area of the C specimen was reduced accordingly, so that only a small area was not covered by the lithium spray. Figure 23 shows the variation of heat flux over a hemispherical nose with the test heat flux superimposed. This is the heat flux distribution which was used for the transient heating cycle.

The transient heating cycle was based on the time history of stagnation point total heating rate experienced by a 12-inch radius nose in flight, and not on the radius of the test model. While a goal of 1000 BTU/ft^2-sec had been set for the heat flux rate at the stagnation point to be accommodated by lithium spray cooling, a lesser value established experimentally would have to be accepted. Consequently, all values of Figure 5 were ratioed by the peak heat flux and the dimensionless curve of heat flux rate variation with time, Figure 24, was obtained. This includes both convective aerodynamic and equilibrium gas cap radiation. Figure 24 provided the basis for the transient heating cycle, regardless of what the peak heat flux rate determined experimentally from the steady state tests turned out to be.

Run Nos. 1, 2, and 3 were steady-state tests, conducted on the C specimen to determine the peak heat flux for the transient heating cycle. Two transient cycle runs were made.

TABLE 1

SUMMARY OF TEST CONDITIONS

Specimen Type	Condenser Pressure psia	Lithium Inlet Temperature °F	Supply Tank Pressure psig	Maximum Work Coil Current Amperes	Flow Rate lb/hr	Remarks (Cause of Shutdown)
A Specimen, Type I						
Run No. 1	0.5	683	93	560	60	T/C No. 4 indicated rapid temperature rise
Run No. 2	0.5	660	82	500	60	T/C No. 13 indicated 2200°F
A Specimen, Type II						
Run No. 1	0.5	690	118	650	60	T/C No. 13 indicated 2200°F
Run No. 2	0.1	700	115	520	60.8	T/C No. 17, 11, 19, indicated rapid temperature rise
Run No. 3	0.5	690	155	550	67.6	T/C No. 9, 6, 15 indicated rapid temperature rise
C Specimen						
Run No. 1	0.5	720	137	775	79.5	Ran out of usable lithium
Run No. 2	0.5	715	135	760	79.5	Work coil over heated
Run No. 3	0.5	700	74	750	49.8	T/C No. 10 indicated rapid temperature rise
Simulated Flight						
Run No. 1	0.5	735	70	685	54	
Run No. 2	0.5	-	70	685	53.2	

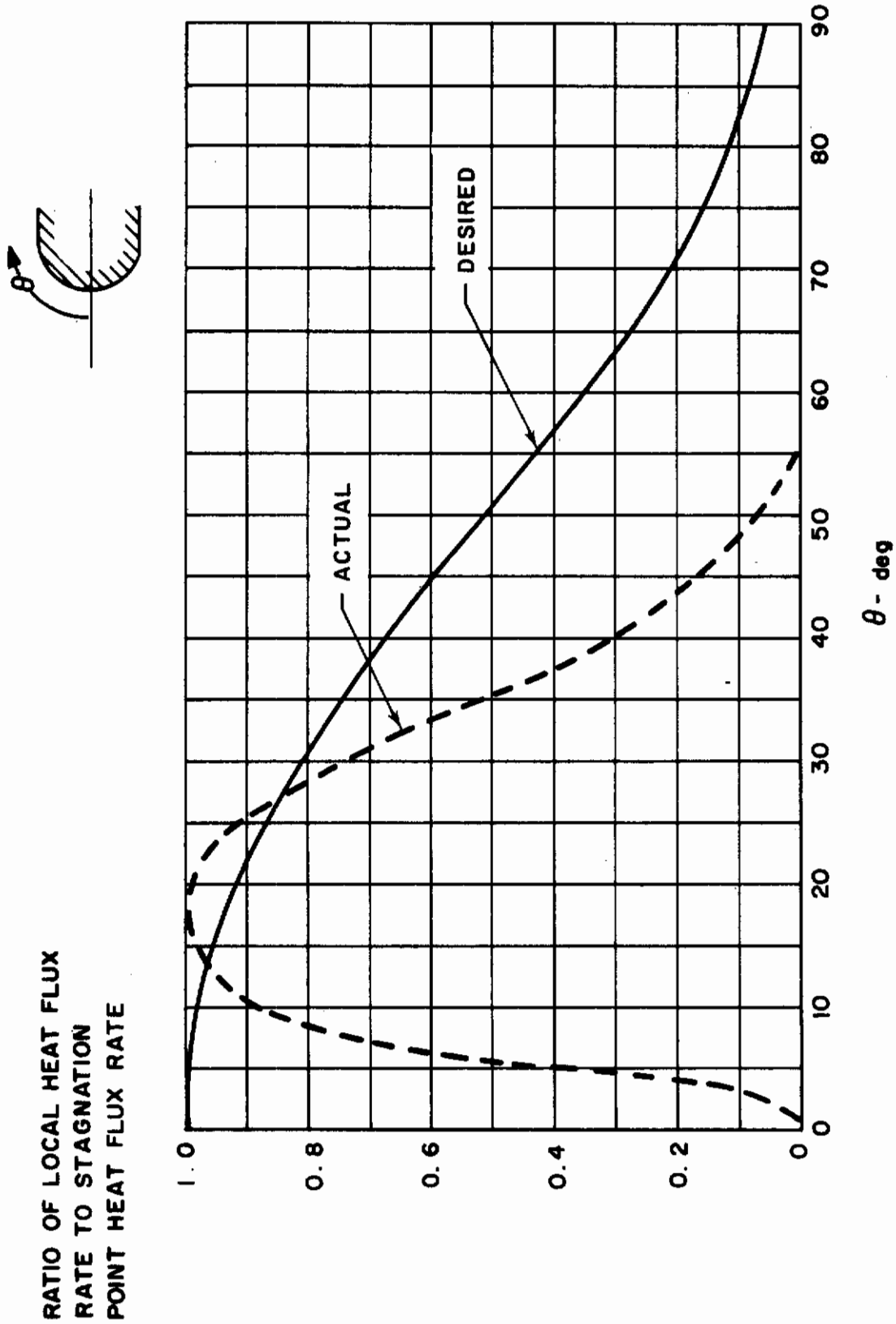

Figure 23. Comparison of Desired and Actual Heat Flux Dixtribution over the C Test Specimen

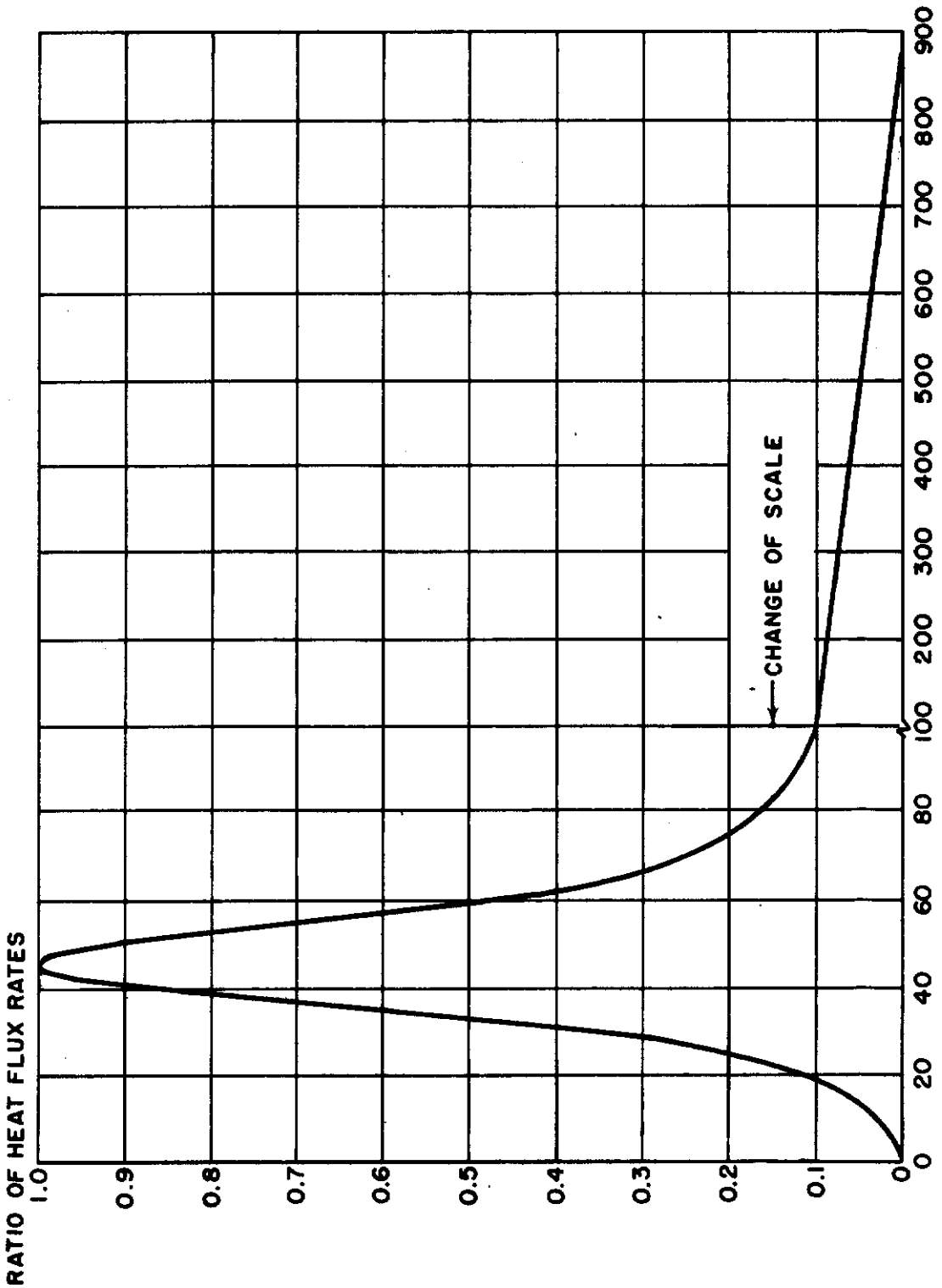

Figure 24. Dimensionless Heat Flux Variation with Time for Transient Heating Cycles

The test conditions shown in Table 1 are at the beginning of a test run, during the course of the run, the lithium inlet temperature varied, and the flow rate. The maximum power input to the work coil is also included and the reason for the termination of a test run.

3. Test Procedure

As a safety precaution, it was established that when a five-minute supply of lithium remained in the supply tank, a run would be terminated. Instantaneous burn-up of the test specimen would occur at the higher heat fluxes with a loss of coolant. In addition, during all of the testing, the lithium flow rate was held constant or nearly constant. The valve between the supply tank and test specimen was manually operated and did not have the fineness of control which would be required to vary the flow during a test run.

Before the lithium flow was started for a test run, the test specimen target area was preheated to 700-900°F. This was to prevent the test specimen and the thermocouple installations from being subjected to thermal shock when the 700°F lithium hit the front face of the test specimen. With the target area up to temperature, the lithium flow was initiated and adjusted to the desired level.

Power control to the work coil was attained by use of the plate voltage taps in the induction generators with proportional control manually operated. Each tap has a separate power level and by proportional control it gave vernier adjustment up to the maximum power level of a given tap. The power input to the work coil was slowly increased to each test point, so that the thermocouples could be monitored. The power input was held constant at the test point until thermal equilibrium had been established and data recorded. In the test data, Appendix III, it will be noted that the work-coil current is the same for some of the test points for a specimen test run. This is the point where the maximum power level of a tap had been reached and a change to a higher power tap was made. For a tap change, the induction generators had to be shut down. To prevent thermal shock, the current was slowly reduced, the unit turned off, the tap change made, the unit turned on and the current increased slowly to the previous test point value.

Due to the combined effects of random hot spots, which are discussed in Section 5, and the thermocouple failures, the automatic cutoff meter was decided to be unreliable, since it was possible for a unwanted shutdown to occur due to its thermocouple becoming deflective. Instead, the test personnel who monitored the oscillograph were provided with a manual switch to cut off power when necessary.

For the simulated flight tests, it was necessary to provide a recording of the square of the RF current so that an accurate time-history of heat flux could be obtained. One galvanometer of the oscillograph which was used for thermocouple recording was adapted for this purpose. The galvanometer trace was calibrated against the indicating meter (work-coil power input) at various current levels during the steady-state tests on the C specimen. By measuring the galvanometer deflection

during the steady-state tests, a plot of current versus galvanometer deflection could be made. During the simulated flight tests, the current was recorded continuously on the oscillograph trace along with the thermocouple data. The oscillograph paper traveled at a preset speed, in the case of the simulated flights one inch per second, so that a check of specimen temperature, work-coil power input (heat flux) versus time could be made.

Only the first 100 seconds of the heat flux rate-time history was simulated. The lithium flow rate was held constant for the entire test duration.

SECTION 5

TEST RESULTS

The test data from the test specimen and the lithium loop is presented in Appendix III. Before discussing the test results, it is advisable to identify some of the problems concerning the test specimen instrumentation.

The oxidation protective coating used on the A and C test specimens had an Al-Sn base and after the coating process free tin still remained in the coating. Upon exposure of the test specimens to temperature, the free tin extruded from pinholes in the coating to form spheriods on the specimen surface. The tin spheriods became highly heated by the induction heating work coil. Some of the test runs were terminated by a tin spheriod forming near a thermocouple. When the thermocouple sensed the tin spheriod, a rapid rise in temperature was indicated, causing shutdown of the induction heating equipment.

In an attempt to reduce the amount of extruded tin, after testing of the first A specimen, the knurled A specimen and the C specimen were subjected to a bakeout run. The test specimens were preheated to approximately 1000°F and held at this temperature for five minutes. The induction heating work coil was removed and the extruded tin was removed. This procedure reduced the amount of extruded tin during a test run, but the problem still existed.

After the first test run and each succeeding test run on a test specimen, a number of thermocouples became detached from the test specimen surface. This was due in part to the thermal shock to which the thermocouple installations were subjected by shutdown of the induction heating equipment. When the power to the induction heating system was shut down, lithium flow was still maintained, and the 700°F lithium rapidly cooled the test specimen. The cemented thermocouple installations were subject to spalling in an erratic matter. Duplicate thermocouples had been added in anticipation of such a problem.

It was found after the bakeout run on the C test specimen that all but two of the thermocouple installations were shorted to ground. The thermocouple installation procedure in Appendix I insulates the thermocouple bead and leads from the test specimen surface. A short to ground indicated that the thermocouple was touching the test specimen at the thermocouple bead or somewhere along the length of the leads. The test runs on the C test specimen were conducted realizing this condition existed, but with the large number of thermocouples in the heated area, it was chanced that some of the thermocouples were grounded at the thermocouple bead and temperatures could be monitored. It was not possible to determine where the shorts were located so that location of the temperatures in Appendix III for the C specimen is questionable. The grounding of the thermocouples leads was probably caused by too thin a layer of pyrochrome cement being used to insulate the thermocouple leads or flaking

off of the pyrochrome cement due to extruded tin from the specimen surface and allowing the tin to come in contact with the thermocouple leads. Prior to the bakeout run, the thermocouple installations were checked and they were all satisfactory.

For all of the test runs, it was found after the thermocouple data was reduced that the thermocouples on galvanometers 13, 14, 15, 16, and 17 indicated temperatures which were abnormally low. All of the galvanometers were calibrated before each specimen test; therefore, the problem did not exist in the galvanometers but has not been resolved. The above mentioned galvanometers were for continuous recording of temperature data and were not connected to the multiplexing unit.

The determination of heat transfer coefficients requires instrumentation which has a higher degree of sophistication than was afforded by the cemented thermocouple technique and the instrumentation recording system. The temperature drop used in the calculation of the heat transfer coefficient is normally taken as the temperature of the surface in contact with the fluid less the saturation temperature of the fluid. In the nucleate boiling range these temperature differences are small. For sodium the temperature difference at the initiation of nucleate boiling is approximately 10°F. Due to the insulating effect of the cemented thermocouples, the indicated specimen temperature is lower than the actual specimen temperature. This precluded any attempt to calculate the temperature drop through the specimen wall to determine the inside wall temperature with the accuracy required. The accuracy of reducing thermocouple data from the oscillograph traces was ±10°F.

A. PRESENTATION OF TEST DATA

The heat flux supplied to the test specimens by the induction heating system was not uniform but varied as is shown in Figure 20, for the A specimens and Figure 21 for the C specimen. The dimensionless ratio $\left(\frac{H}{H_{max}}\right)^2$ on the ordinate is also a dimensionless ratio of heat flux for any power input to the work coil.

Since the heat flux distribution over the test specimen surface was not uniform, a consistent manner of graphical representation of the test data was required. Therefore, at each test point, the peak heat flux of the nonuniform distribution was used to indicate temperature trends of the thermocouples, regardless of the location of the thermocouples on the specimen surface. The heat flux which is induced in a test specimen is also related to the specimen surface temperature. The effect of specimen surface temperature on the induced heat flux versus work-coil power input is shown ir Figures 25 and 26 for A and C specimens, respectively. The curves shown in Figures 25 and 26 are for a work coil to specimen spacing of 0.125 inch.

The following procedure was used to determine the peak heat flux at each test point. The thermocouple at the point of maximum power density, which indicated the maximum specimen temperature, was used as the specimen surface temperature to determine the heat fluxes from Figures 25 and 26. No corrections were applied to

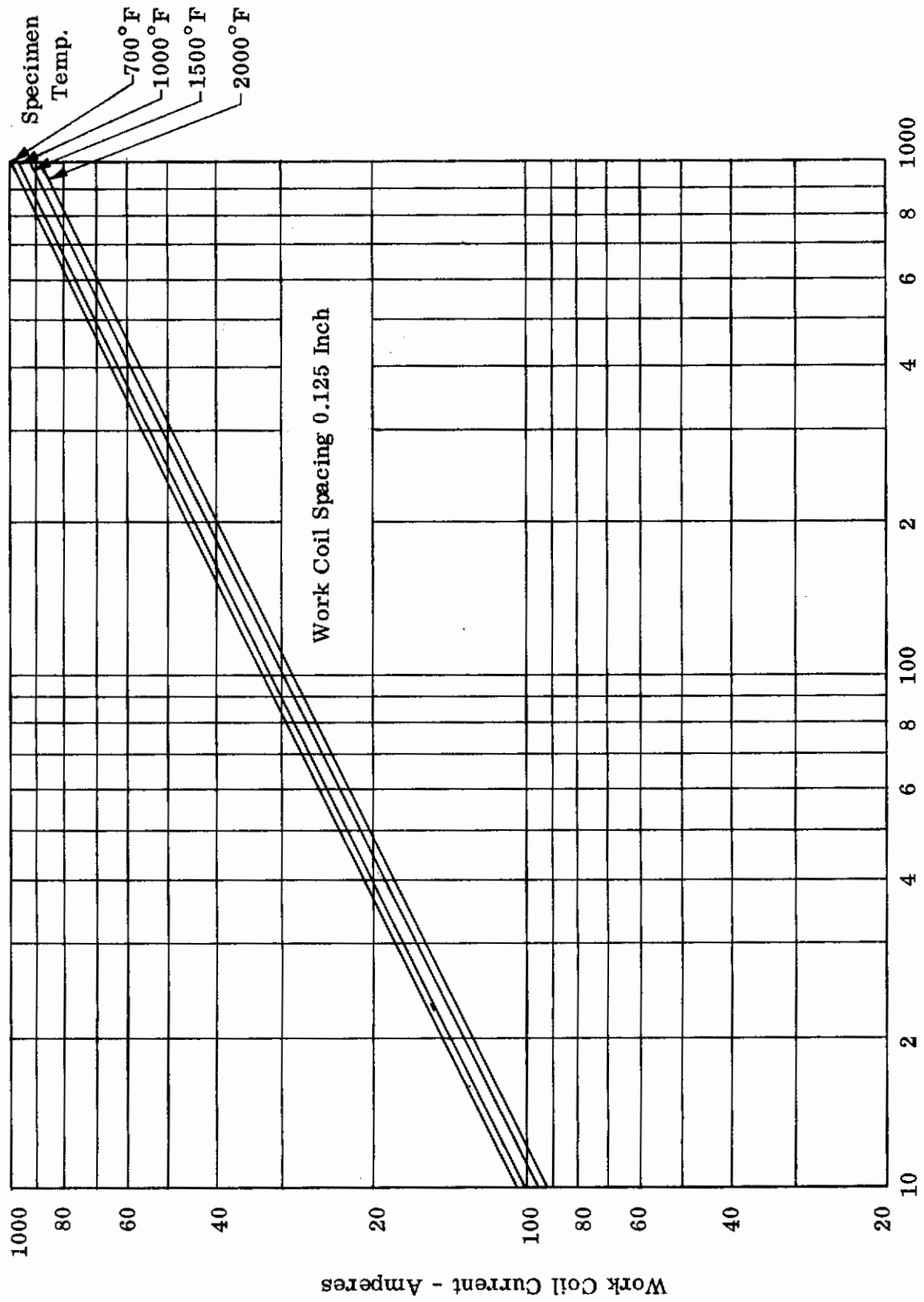

Figure 25. Work-Coil Current versus Heat Flux for A Specimen

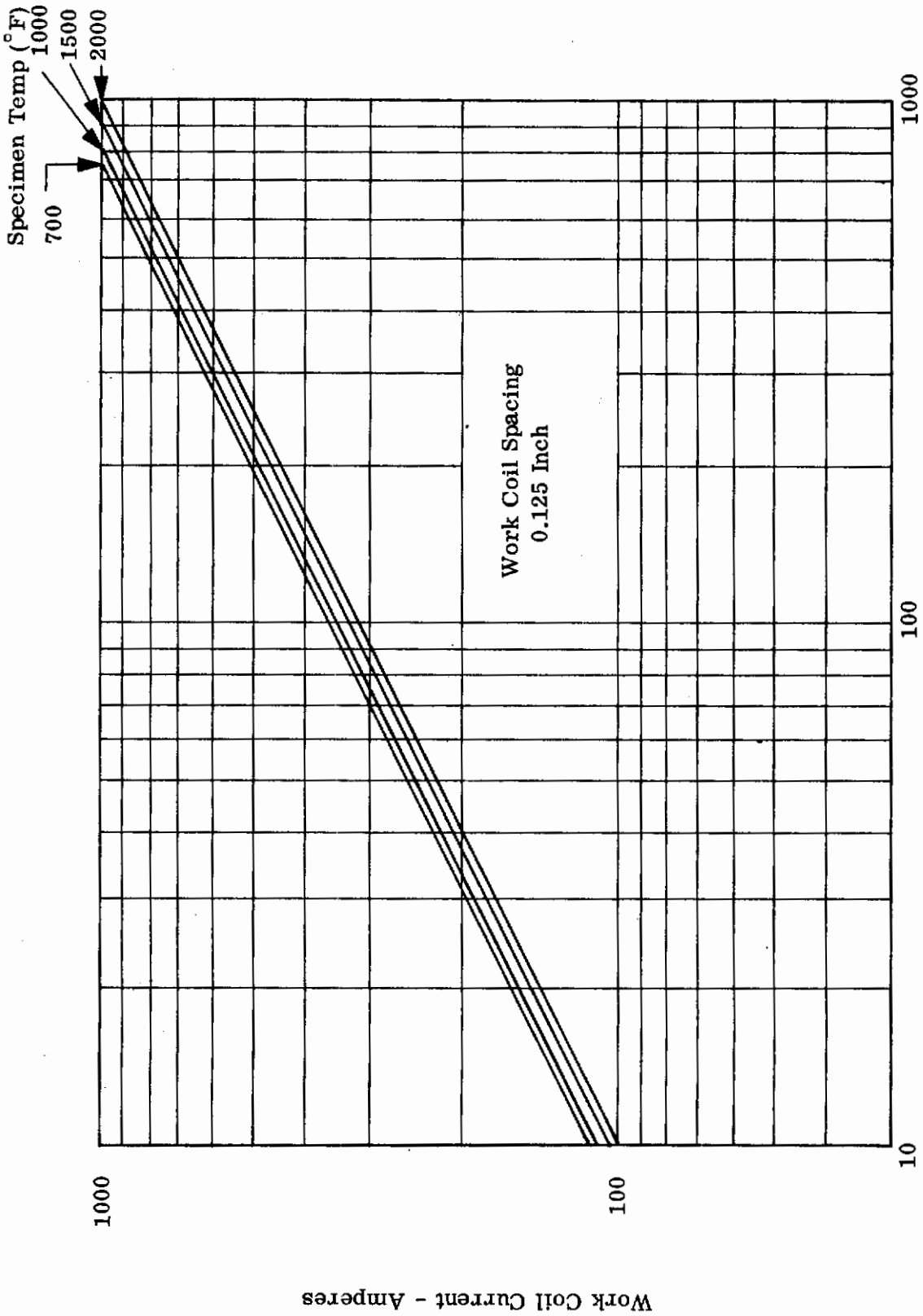

Figure 26. Work-Coil Current versus Heat Flux for C Specimen

lower heat fluxes due to the specimen to work-coil spacing for thermal expansion compensation. This effect is discussed later. The selection of the maximum indicated surface temperature rather than an average value is probably valid since the cementing technique used for the thermocouples insulated the thermocouple from the specimen surface; therefore, the indicated surface temperature would be lower than the actual surface temperatures. Visual observations of the test specimen verified this conclusion.

B. DISCUSSION OF TEST RESULTS

1. Spray Boiling

The mechanism for spray boiling is not considered to be the same as that of pool boiling. The spray continuously supplies fluid to the heated surface, whereas in pool boiling, the fluid is displaced from the heated surface by natural convection and bubble formation.

It may be well to describe the expected behavior of the lithium spray as it impinges on the heated surface. If the spray particles which hit the center of the heated surface are considered first, these particles would pick up heat and flow radially outward along the heated surface. (Prior to initiation vaporization, some of the particles would flow downward due to gravity.) As the particles flow radially outward, there would be a mixing of these particles with the lithium spray before it hits the heated surface, raising the temperature of the incoming lithium spray. There would be a pickup of heat as the lithium flowed radially outward. At the outer edge of the inductively heated surface, where the heat flux is essentially zero, it would be expected that the thermocouples in this region would, as the lithium flows radially outward, indicate a temperature rise for each heat flux step and then remain at a constant temperature after the vaporization temperature of the lithium had been reached.

The full cone spray which is generated with the type of spray nozzle used may be compared to the spray from a common household aerosol can. The spray is a mist which has negligible velocity of impact. The spray nozzle used in the test specimens was a commercial spray nozzle for water. The spray cone angle for water was 63° and based upon the density and viscosity of lithium, the spray cone angle for lithium was considered to be the same.

2. A Specimen, Type I

Two test runs were conducted on the A specimen, Type I, with the same test conditions. The lithium flow rate was 60 lb/hr and the condenser pressure was 0.5 psia corresponding to a lithium saturation temperature of approximately 1700°F. Duration of testing for run No. 1 was 30 minutes and for run No. 2, 20 minutes.

Test run No. 1 was terminated when a rapid temperature rise was indicated by thermocouple No. 4. Upon removal of the work coil, a tin spheriod was formed adjacent to the thermocouple. Examination of the Tipersul insulation between the

work coil and test specimen showed that the insulation had melted in small areas which matched the location of the tin spheriods on the test specimen. The T1-20 insulation was also charred at these spots. The Tipersul melts at about 2500°F. This indicated that the molten tin was being inductively heated. The tin spheriods were removed from the specimen surface and the insulation was replaced.

Test run No. 2 was terminated when thermocouple No. 13 indicated a temperature of approximately 2200°F. Examination again showed a tin spheriod adjacent to the thermocouple and the Tipersul insulation was damaged. A small bump on the specimen surface was probed and approximately one square inch of the coating was removed. Apparently the temperature limitation of the coating had been exceeded by a hot spot caused by a tin spheriod. This resulted in local damage to the coating and allowed oxidation of the columbium substrate. The test specimen was cut out of the loop and the Conoseal joints examined. No indication of leaks was evident. With the exhaust line Conoseal joint disassembled, the interior of the columbium exhaust line was visible. The inside surface showed no evidence of reaction with the lithium.

The specimen surface temperature versus the peak heat flux of each test point is presented in Figures 27, 28, and 29. Temperature data from thermocouple No. 6 was used in conjunction with the work-coil current to determine the peak heat flux at each test point from Figure 25.

Since the sprayed lithium would pick up additional heat as it flowed radially outward over the heated surface it was desirable to calculate the peak heat flux which would initiate boiling at each concentric ring of thermocouples, for comparison with values determined from the experimental data. The total heat input from the induction heating work coil as a function of the distance from the center of the test specimen is shown in Figure 30 for a peak heat flux of 1 BTU/ft^2-sec. This curve was obtained by graphically integrating Figure 20, a dimensionless ratio of heat flux versus distance from the test specimen center, for a peak heat flux of 1 BTU/ft^2-sec.

Considering the spray distribution to be uniform and covering only the heated surface, the following method was used to determine the peak heat flux to initiate boiling of lithium to occur at the locations of each concentric ring of thermocouples.

The heat input required to raise 60 lb/hr of lithium from 700 to 1700°F (saturation temperature) is

$$Q = Mc_p \Delta T = 60 \text{ lb/hr} \times 1 \text{ BTU/lb} - {}^\circ\text{F} \times (1700 - 700)$$

$$= 16.67 \text{ BTU/sec}$$

From Figure 30, the heat input to the test specimen up to a point 0.5 inch from the specimen center is 0.0025 BTU/sec for a peak heat flux rate of 1 BTU/ft^2-sec. The percentage of the total lithium spray which covers this area was calculated

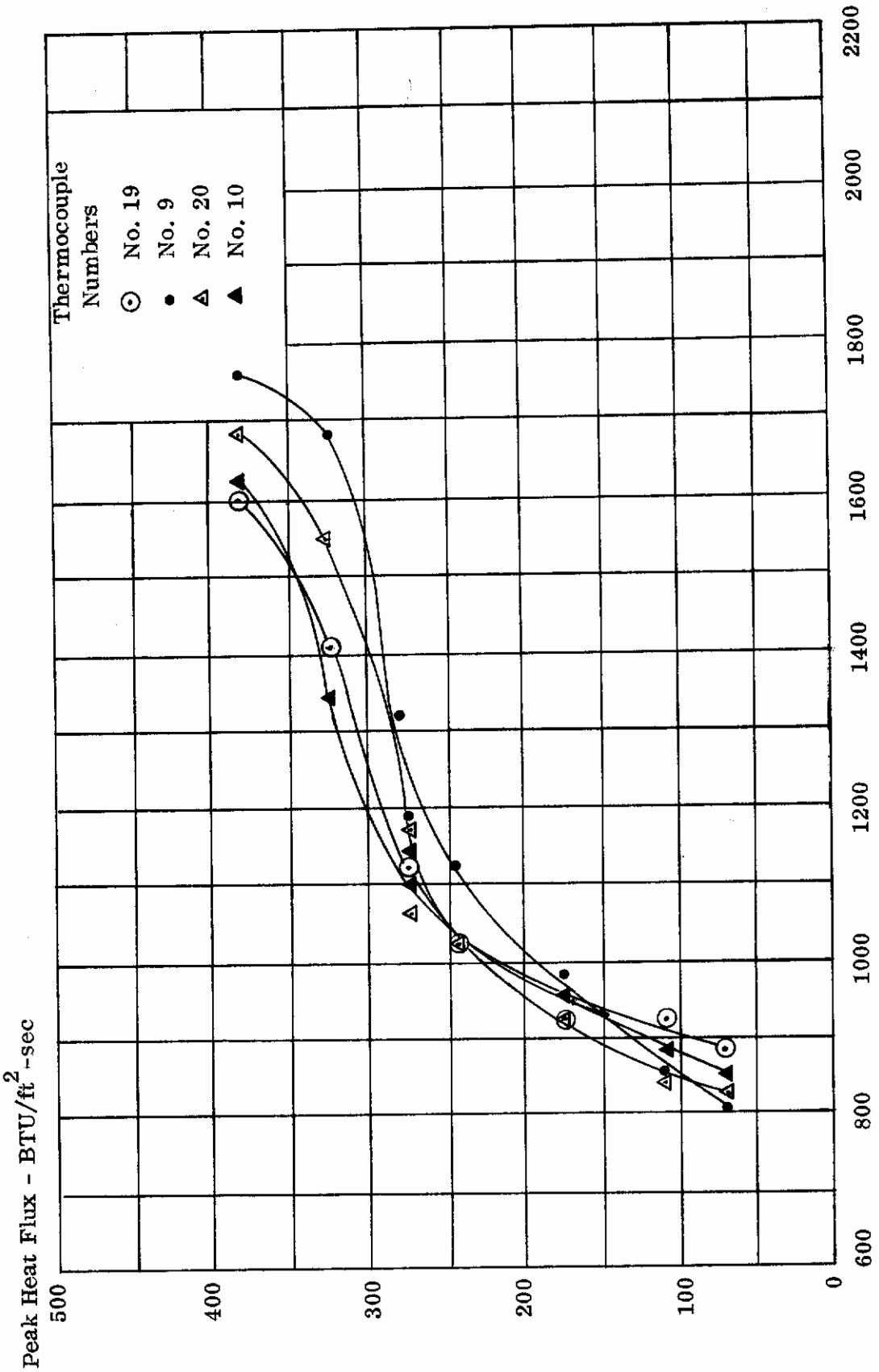

Figure 27. A Specimen, Type I, Run No. 1 Temperature Data 0.5 Inch from Specimen Center

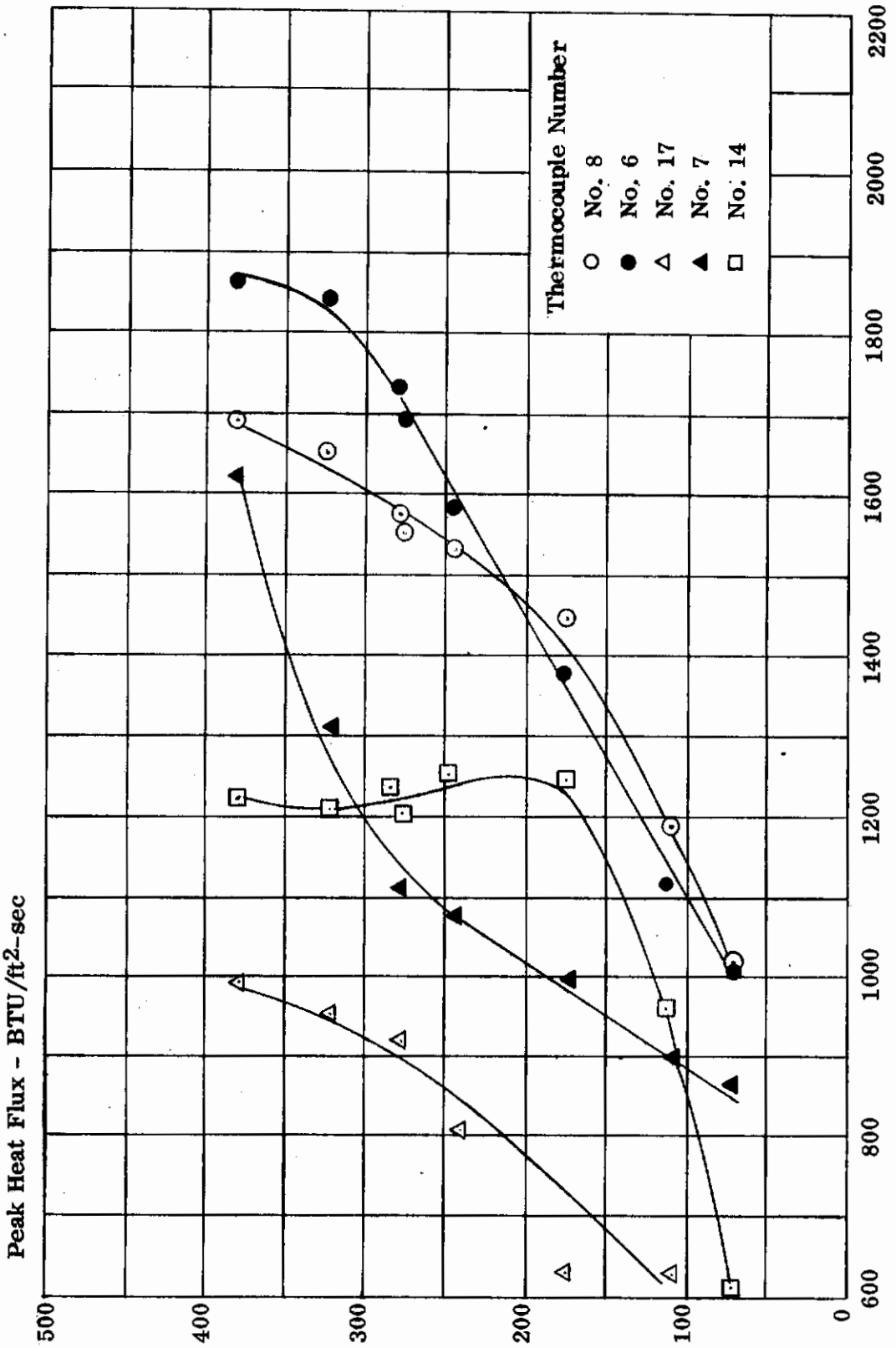

Figure 28. A Specimen, Type I, Run No. 1 Temperature Data 1.0 Inch from Specimen Center

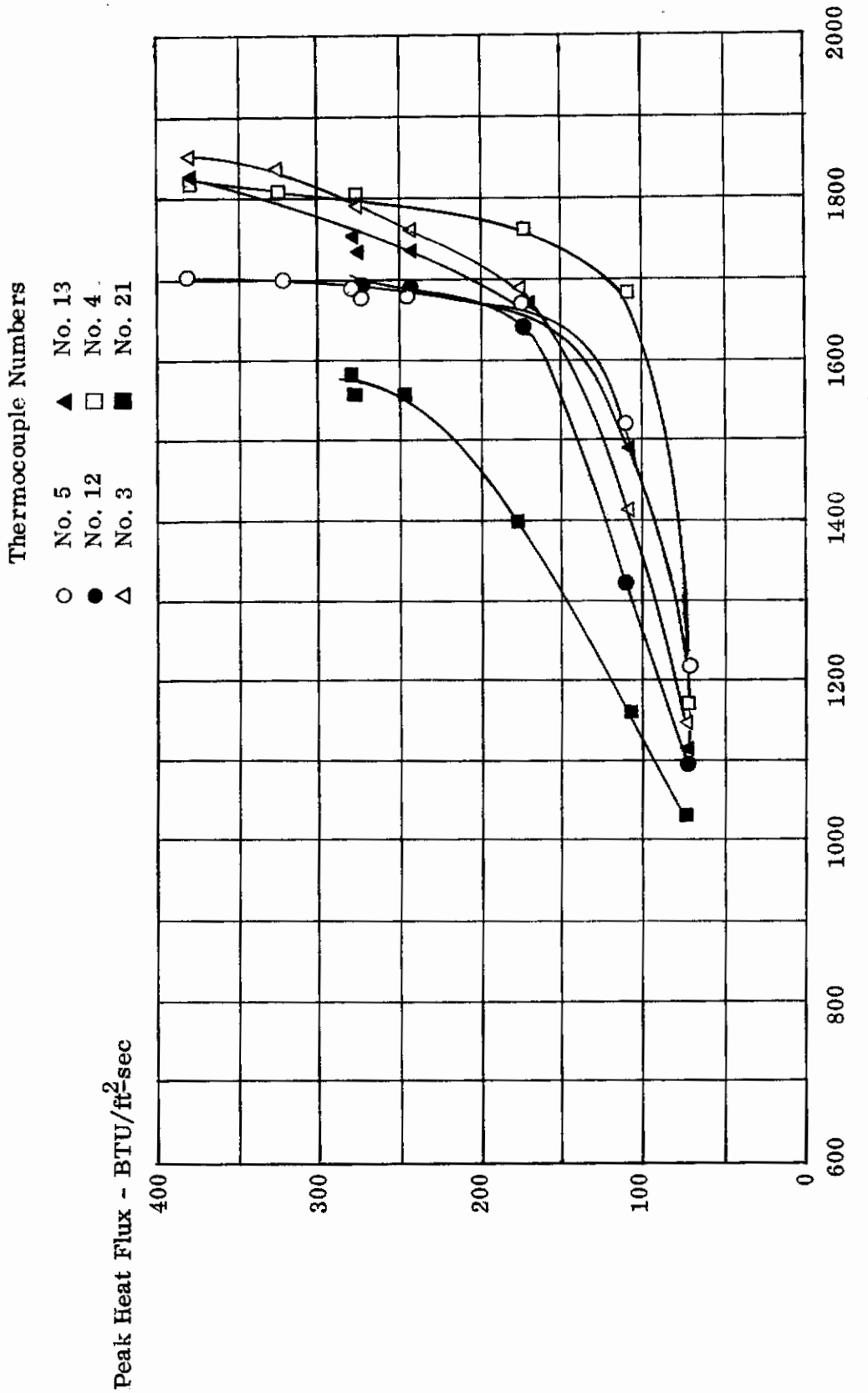

Figure 29. A Specimen, Type I, Run No. 1 Temperature Data 2.2 Inches from Specimen Center

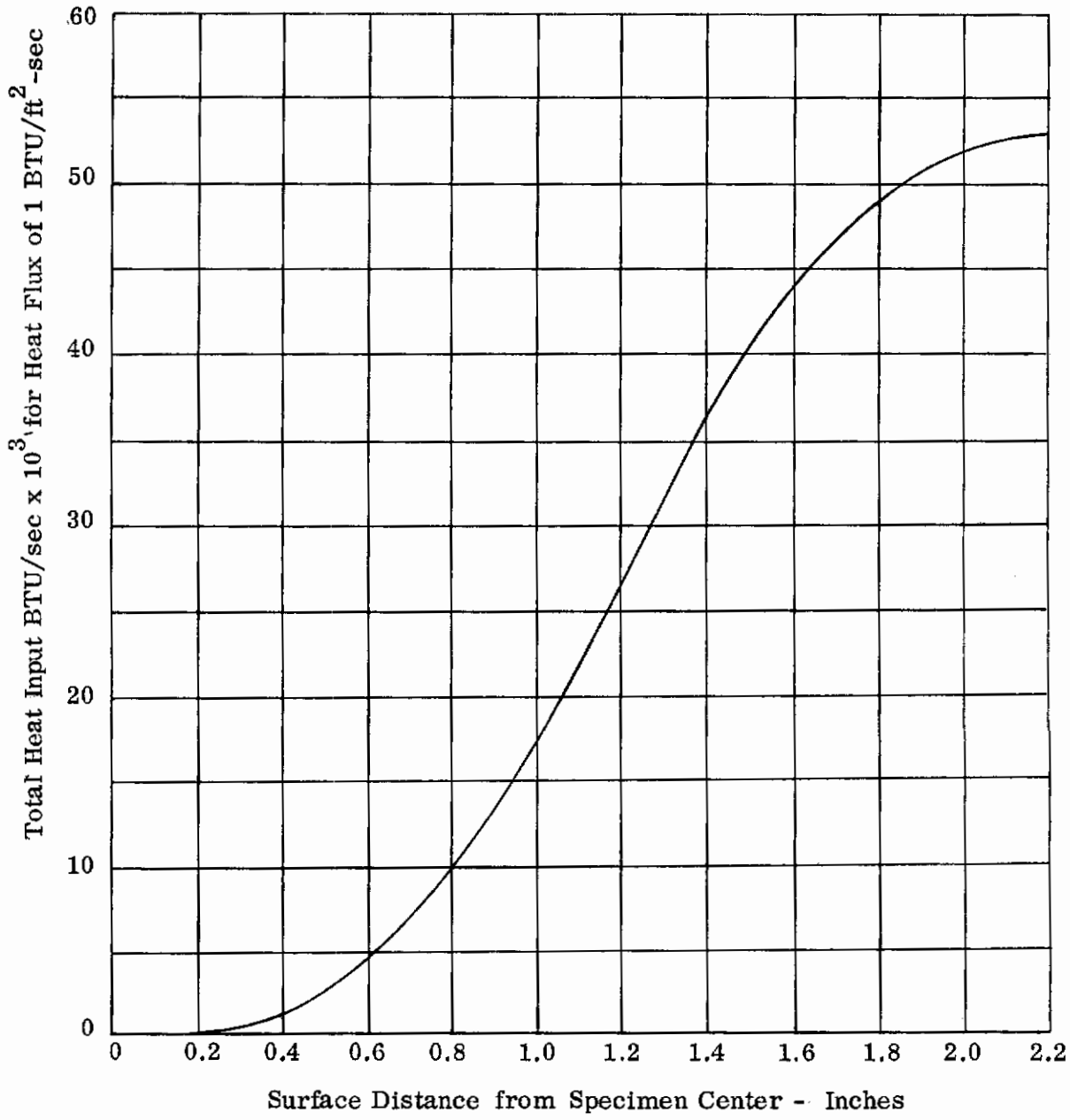

Figure 30. Total Heat Input To A Specimen For a Heat Flux of 1 BTU/ft^2-sec

to be 5.3%. The heat input required to raise this amount of lithium to the saturation temperature is:

$$Q = 16.67 \text{ BTU/sec} \times 5.3\%$$

$$= 0.884 \text{ BTU/sec}$$

Peak heat flux to initiate boiling at a surface distance of 0.5 inch from the specimen center is:

$$q = \frac{0.884 \text{ BTU/sec}}{0.0025 \text{ BTU/sec}} \times 1 \text{ BTU/ft}^2\text{-sec}$$

$$= 355 \text{ BTU/ft}^2\text{-sec}$$

Peak heat flux to initiate boiling at a surface distance 1.0 inch from the specimen center is:

$$Q = 16.67 \text{ BTU/sec} \times 21\%$$

$$= 3.50 \text{ BTU/sec}$$

$$q = \frac{3.50 \text{ BTU/sec}}{0.014 \text{ BTU/sec}} \times 1 \text{ BTU/ft}^2\text{-sec}$$

$$= 205 \text{ BTU/ft}^2\text{sec}$$

Peak heat flux to initiate boiling at a surface distance of 2.2 inches from the specimen center is:

$$Q = 16.67 \text{ BTU/sec} \times 100\%$$

$$= 16.67 \text{ BTU/sec}$$

$$q = \frac{16.67 \text{ BTU/sec}}{0.0525 \text{ BTU/sec}} \times 1 \text{ BTU/ft}^2\text{-sec}$$

$$= 315 \text{ BTU/ft}^2\text{-sec}$$

Figure 27, the specimen surface temperature versus peak heat flux for thermocouples located 0.5 inch from the specimen center, shows two slopes before boiling is initiated. The temperature data indicates boiling initiated at a peak heat flux of 325-350 BTU/ft^2-sec which is in good agreement with the calculated value of 355 BTU/ft^2-sec.

Figure 28, the temperature data at the point of peak heat flux on the specimen surface, shows boiling to have initiated at a heat flux of 175-300 BTU/ft^2-sec. The test value to indicate boiling shows fair agreement with the calculated value of

205 BTU/ft^2-sec. There was no indication of burnout at the maximum test heat flux of 380 BTU/ft^2-sec. The temperature data of thermocouple Nos. 6 and 8 indicate boiling has been initiated. The data of thermocouple No. 7 does not indicate boiling and the trend is similar to the data in Figure 27. This trend and the range of heat fluxes to initiate boiling may be due to an uneven lithium spray distribution.

The temperature data for thermocouple Nos. 14 and 17, which was connected to galvanometer Nos. 15 and 16, are also included in Figure 28. The output from these galvanometers indicated abnormally low temperatures throughout the entire test program.

The temperature data at the point of approximately zero heat flux is shown in Figure 29. The trend of curves shows good agreement in what was expected to occur in this area. There is a temperature rise as the lithium is heated to its saturation temperature followed by an approximate constant temperature for increases in heat flux. The calculated heat flux for the lithium to reach its saturation temperature is 315 BTU/ft^2-sec versus a value of 125-175 BTU/ft^2-sec from the curves in Figure 29. This disagreement in the boiling heat flux indicates that the lithium spray covered an area which was greater than the heated area; therefore, boiling would be indicated at a lower heat flux.

Thermocouple No. 4, which caused termination of the test run as the heat flux was being increased to the next test point, shows no indication of burnout about to occur, nor would burnout be expected in an area of approximately zero heat flux.

3. A Specimen, Type II

Three test runs were conducted on the knurled A specimen. For test run No. 1, the initial lithium flow rate was 60 lb/hr and the condenser pressure was 0.5 psia. For test run No. 2, the initial lithium flow rate was 60.8 lb/hr with a condenser pressure of 0.1 psia. In test run No. 3, the initial flow rate was 67.6 lb/hr and the condenser pressure 0.5 psia. The lithium saturation temperature is approximately 1700 and 1550°F for a condenser pressure of 0.5 and 0.1 psia, respectively. Duration of testing was 37, 12, and 17 minutes for test runs 1, 2, and 3, respectively.

As has been previously discussed, a bakeout run was conducted on this specimen to reduce the amount of tin extruded during a test run. In addition. to minimize damage to the Tipersul insulation, the Tipersul insulation was not shaped over the test specimen as was done for the A specimen, Type I, but was held by ceramic pins; therefore, it covered only a small portion of the test specimen. Figure 31 shows the Tipersul insulation shaped to the A specimen, Type I and the Tipersul insulation held by ceramic pins on the knurled A specimen. It was expected that this would allow the extruded tin to drip away.

Test run No. 1 was terminated when thermocouple No. 13 indicated a temperature in excess of 2200°F after a heat flux of approximately 500 BTU/ft^2-sec had been reached and the heat flux was being increased to the next test point. Test run

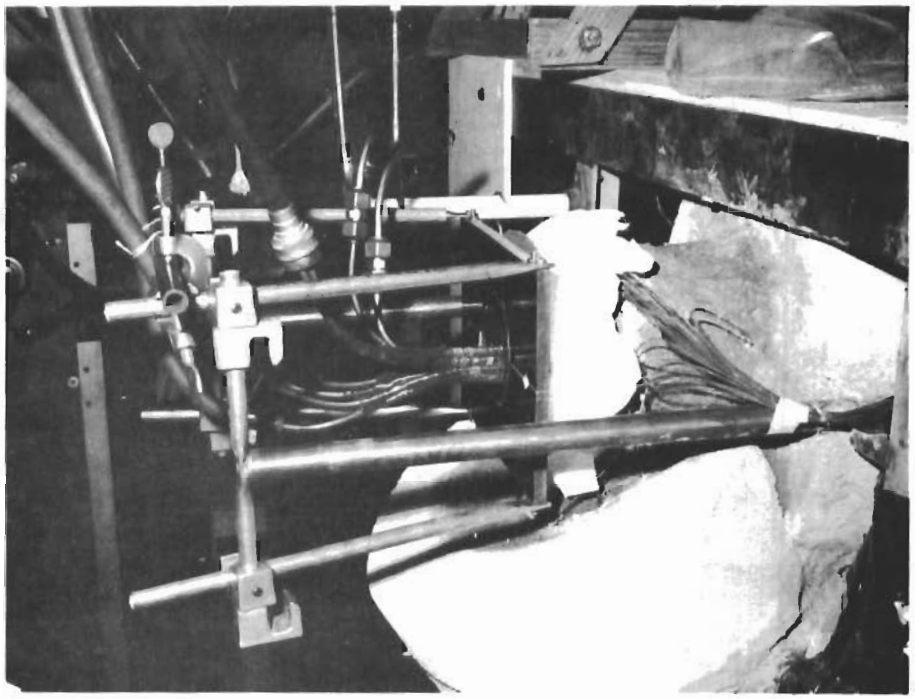

Before

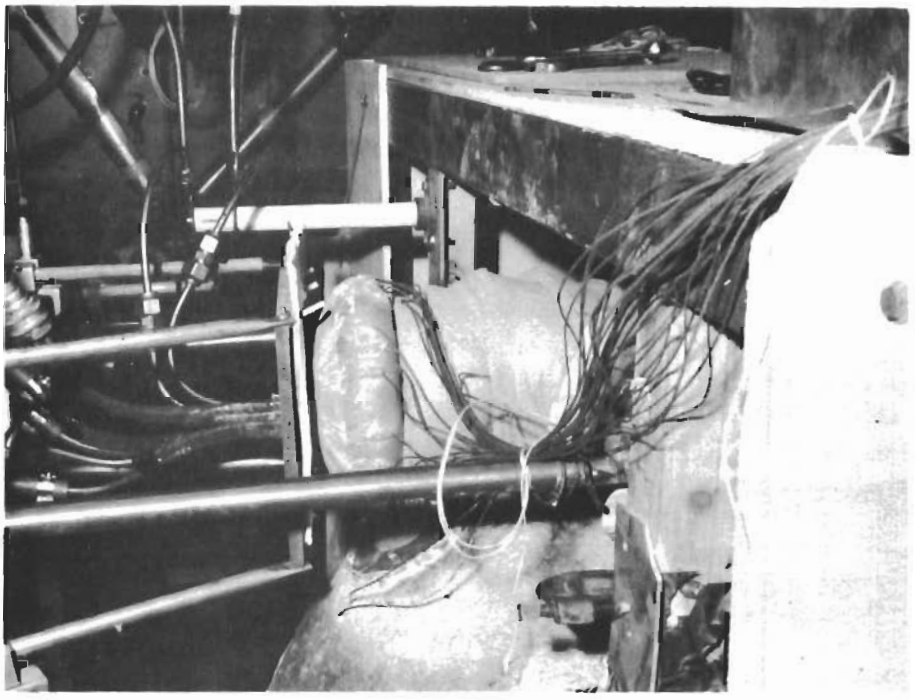

After

Figure 31. Change in Method of Attaching Tipersul Insulation Between Work Coil and Test Specimen

Nos. 2 and 3 were terminated when several thermocouples during each test run indicated a very rapid temperature rise. After test run No. 3, the test specimen was removed from the loop and the Conoseal joints on the inlet and exhaust lines were disassembled. Examination of the exhaust Conoseal showed definite signs of leakage. There was erosion of the Haynes 25 flanges and there was some evidence of oxidation of the columbium coupling. This is shown in Figure 32.

The temperature data for test run No. 1 is shown in Figures 33, 34, and 35. The temperature data from thermocouple No. 7 was used to calculate the peak heat flux at each test point. The calculated heat fluxes to initiate boiling for A specimen, Type I, are the same for this test run, since the test conditions are identical. The temperature data for the thermocouples located 0.5 inch from the specimen center is shown in Figure 33. The curves in Figure 33 show the same double shape before boiling is initiated as was observed for thermocouples located in the same area in the A specimen, Type I. The temperature data in Figure 33 indicates that boiling was initiated at a peak heat flux of 350-375 BTU/ft^2-sec versus a calculated value of 355 BTU/ft^2-sec which is in good agreement.

Figure 34, the temperature data at the point of maximum heat flux on the specimen surface, shows boiling to have initiated at a heat flux of 375-425 BTU/ft^2-sec. The calculated value is 205 BTU/ft^2-sec and the comparison is not favorable. The trend of thermocouple No. 7 is typical for boiling of a subcooled liquid. There is a rapid temperature rise as the lithium is heated to its saturation temperature, followed by boiling at which point for an increase in heat flux, there is a small rise in temperature. The disagreement between the calculated and test boiling heat fluxes may be due to an uneven spray distribution or to the increase in effective area (by a factor of about 1.5) as a result of knurling.

At the point of zero heat flux, Figure 25, boiling is initiated at a heat flux of 100-175 BTU/ft^2-sec. The calculated value is 355 BTU/ft^2-sec. Again, it may be assumed that the spray is covering an area greater than the heated area or that all of the lithium is not hitting the heated surface but is being carried outward by the exhaust vapor.

At this point, another factor which may account for discrepancies in the calculated and test indicated boiling heat fluxes should be presented. During the course of some of the runs, the lithium flow rate increased and the supply tank pressure was reduced to maintain the desired flow rate. The lithium loop test data in Appendix III indicates when the increased flow occurred and the supply tank pressure was reduced. The increase of flow was at first believed to be due to enlarging of the spray nozzle orifice diameter as a result of a temperature rise. This would reduce the pressure drop across the orifice for a given flow. The orifice diameter is 0.030 inch and the increase of diameter due to temperature would not be of the magnitude to cause a significant decrease in pressure drop across the nozzle. This increase in flow is believed to be the result of the spray nozzle attachment to the columbium adaptor. With reference to Figure 8, an engineering drawing of the A and C test

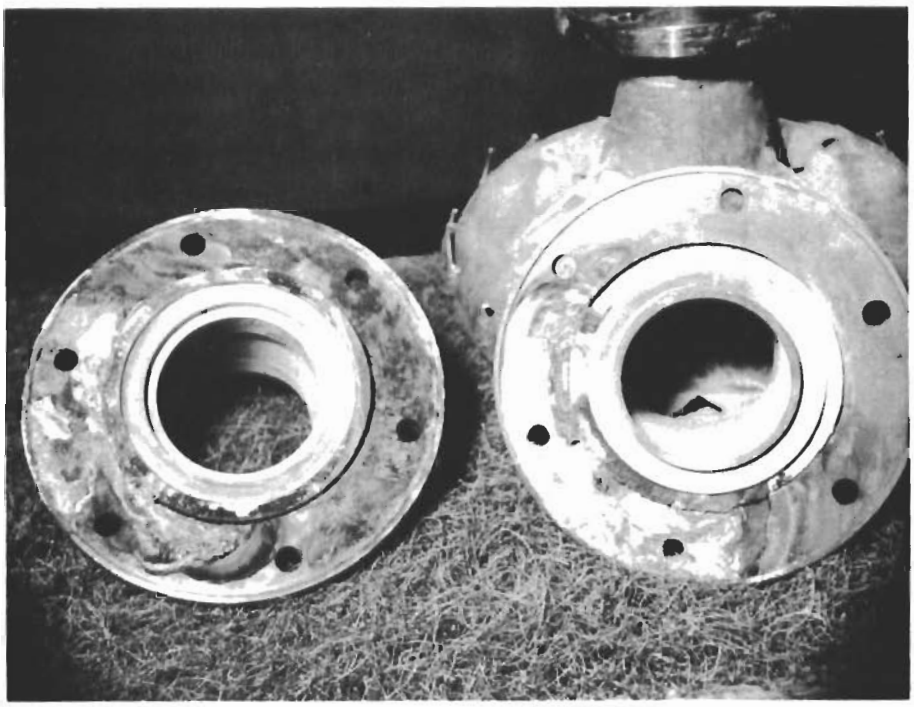

Figure 32. A Specimen, Type II, Disassembled Conoseal Joint

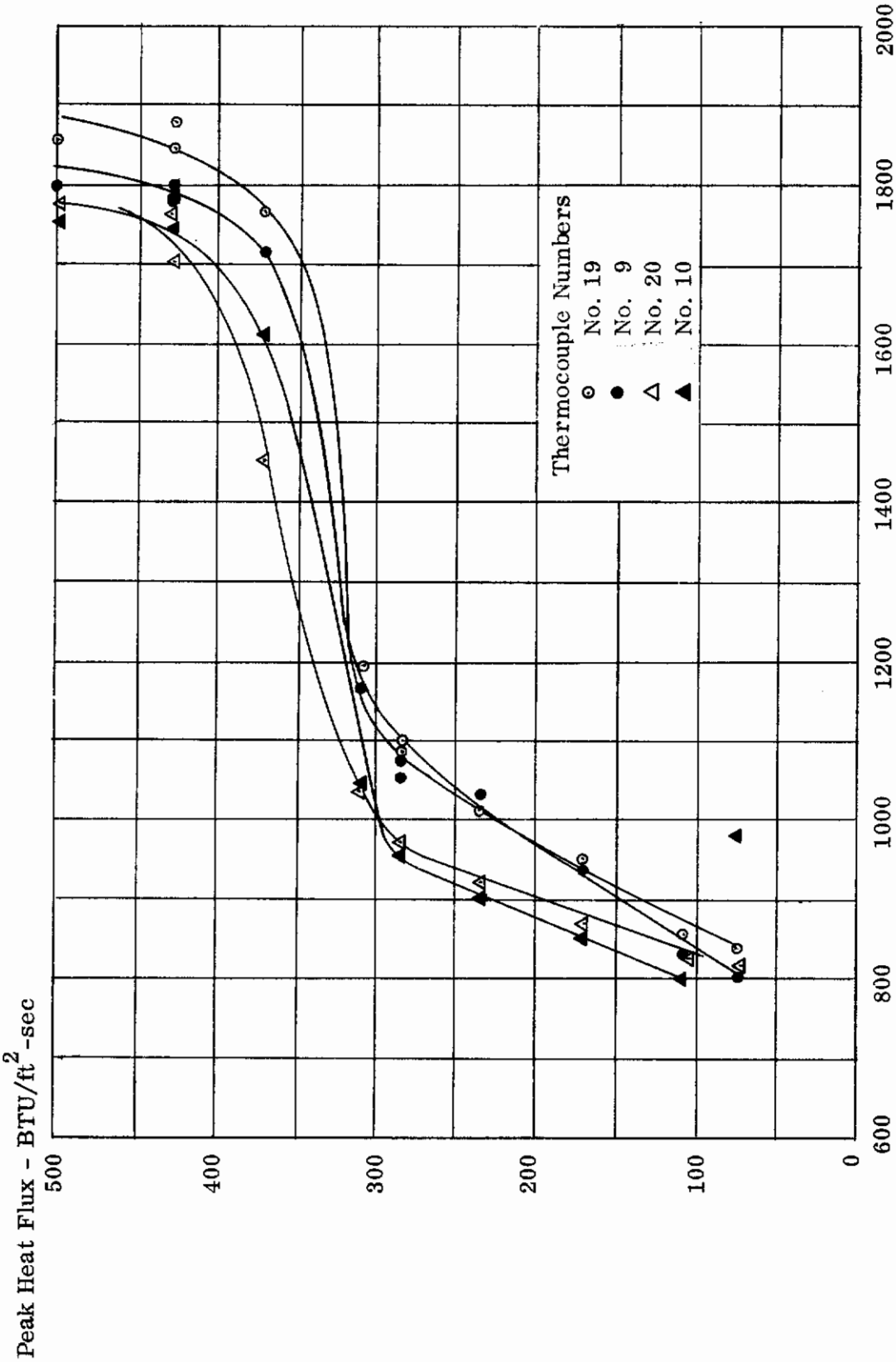

Figure 33. A Specimen, Type II, Run No. 1, Temperature Data 0.5 Inch from Specimen Center

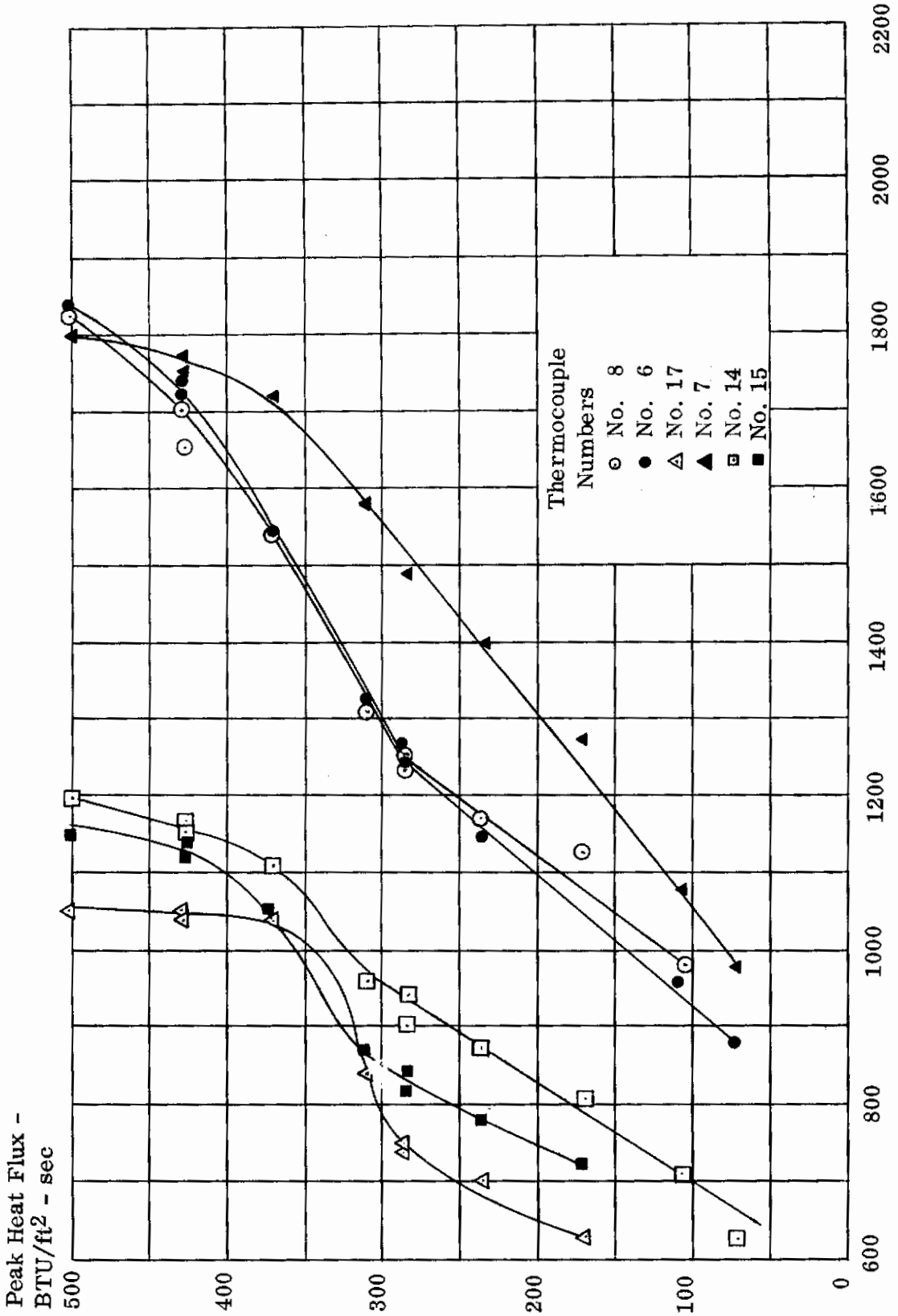

Figure 34. A Specimen, Type II, Run No. 1 Temperature Data 1.0 Inch from Specimen Center

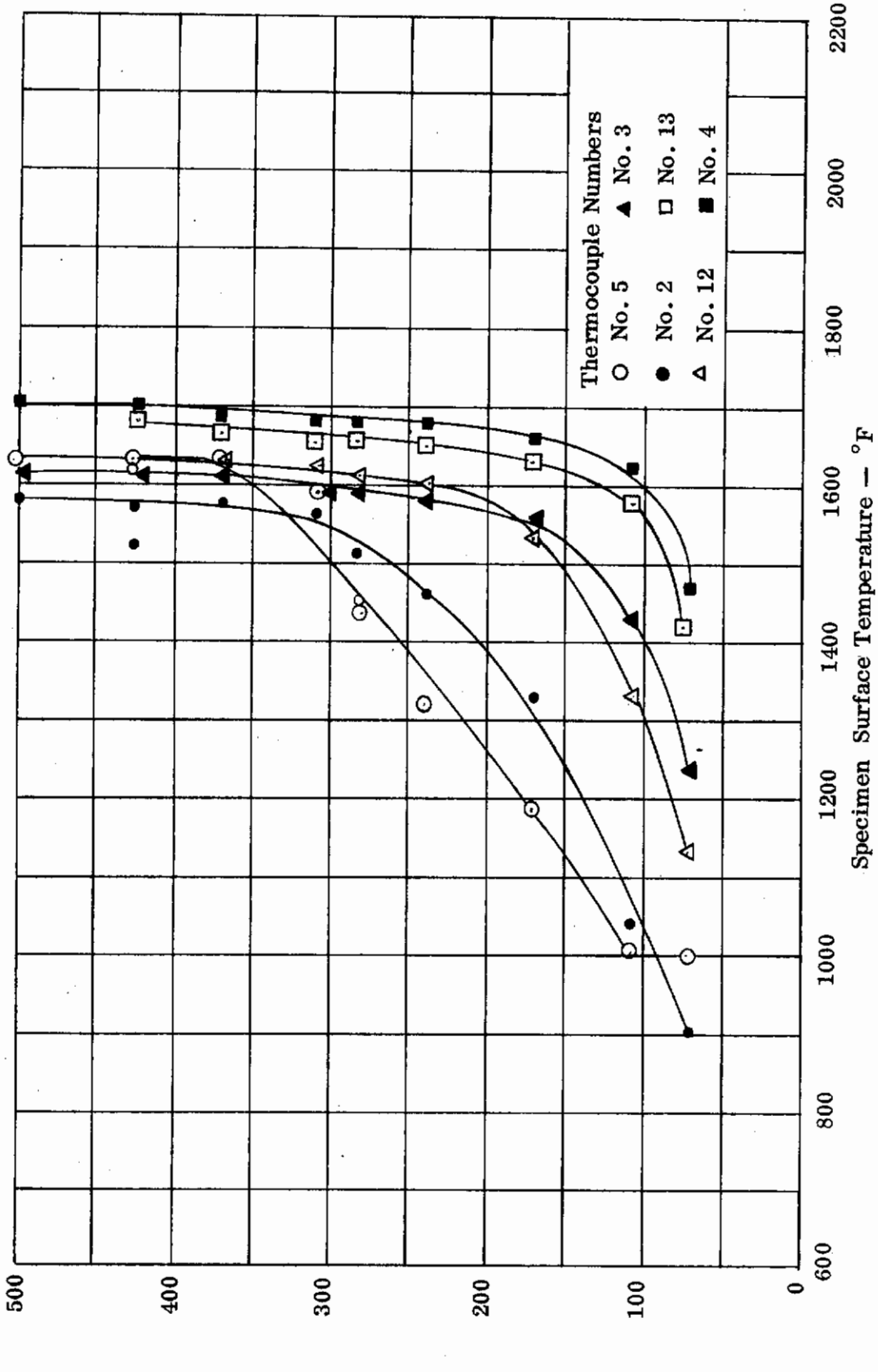

Figure 35. A Specimen, Type II, Run No. 1 Temperature Data 2.2 Inches from Specimen Center

specimens, the attachment of nozzle to the adapter is through screw threads. Pipe threads were used and when tightened an interference fit results. A threaded type joint was justified here, since the joint was contained with the test specimen. Leakage at this joint would not result in contamination of the lithium. The spray nozzle is stainless steel and it is postulated that due to the differential expansion between the spray nozzle and the columbium adaptor, the interference fit was relieved and the joint leaked. This may also indicate that the joint was not fully tightened when assembled.

The flow meter indicated the rate of flow to the test specimen. Although there was an indication of increased flow to the test specimen and the supply tank pressure was reduced, in reality the amount of sprayed lithium which hit the heated surface was reduced since the quantity of lithium which leaked from the joint would not come in contact with the heated surface. The calculated value of the heat flux to initiate boiling at the point of zero heat flux assumed that all of the lithium was striking the heated surface and flowing outward. The reduced lithium flow, along with the other postulations made with regard to the test heat flux to initiate boiling, would account for the variation between the test value and the calculated value of heat flux to initiate boiling. The leak may have also affected the spray density distribution as well.

The temperature data for test run No. 2 was not plotted but is presented in Appendix III. This run was conducted to determine the effect of vapor pressure on the maximum heat flux which the lithium spray could tolerate. The test conditions for run No. 2 were not as critical as for run No. 1, since the saturation temperature of the lithium would be lower. The lithium would boil at 1550°F; hence, the specimen surface temperature would be lower for a given flux. Run No. 2 was terminated by a rapid temperature rise indicated by thermocouple Nos. 11, 17, and 19. The rapid temperature rise of these thermocouples may have been due to the Conoseal joint leak which would allow the pressure in the test specimen to increase, hence increasing the saturation temperature of the boiling lithium.

In Figures 36 and 37 temperature data for test run No. 3 is shown. The temperature data for thermocouple No. 10 was used to calculate the peak heat flux. Shutdown occurred at a heat flux of 315 BTU/ft^2-sec. This test run was not as critical as test run No. 1 due to the higher lithium flow rate. The test run was terminated by a rapid temperature rise indicated by thermocouples Nos. 6, 9, and 15. The Conoseal joint leak is believed to have resulted in the shutdown. In addition, there may have been reduced lithium flow to the heated surface. Figure 37, the temperature data at the point of zero heat flux, indicates boiling to have initiated at a heat flux of 100-150 BTU/ft^2-sec. This value is higher than the heat flux of run No. 1, which could be expected due to the higher lithium flow rate.

Figure 38 is a photograph of the knurled A specimen after test. The black area at about 10 oclock appeared to be the beginning of coating failure at the point of maximum heat flux. This damage occurred after the second test run. The nature of

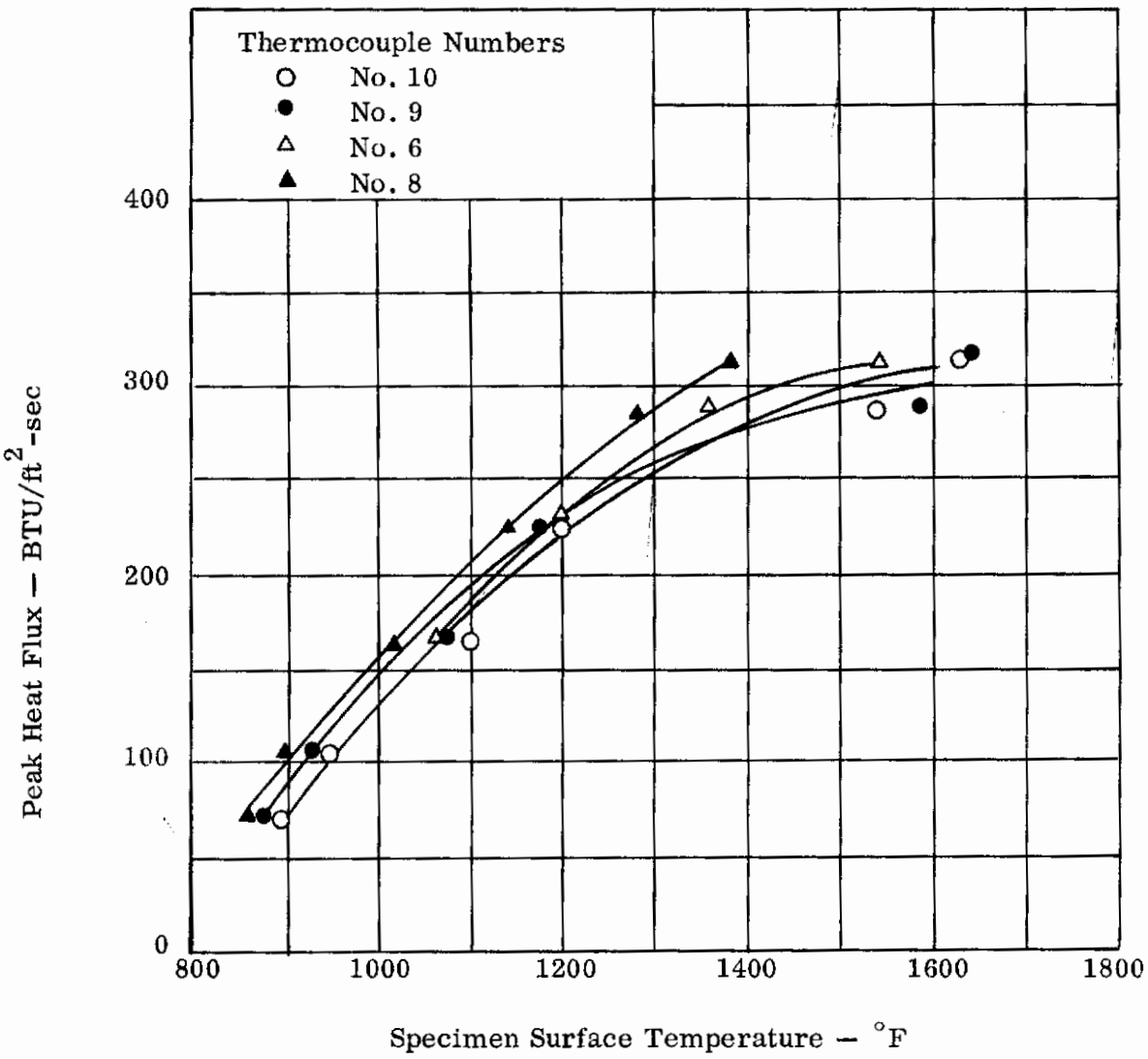

Figure 36. A Specimen, Type II, Run No. 3 Temperature Data 0.5 and 1.0 Inch from Specimen Center

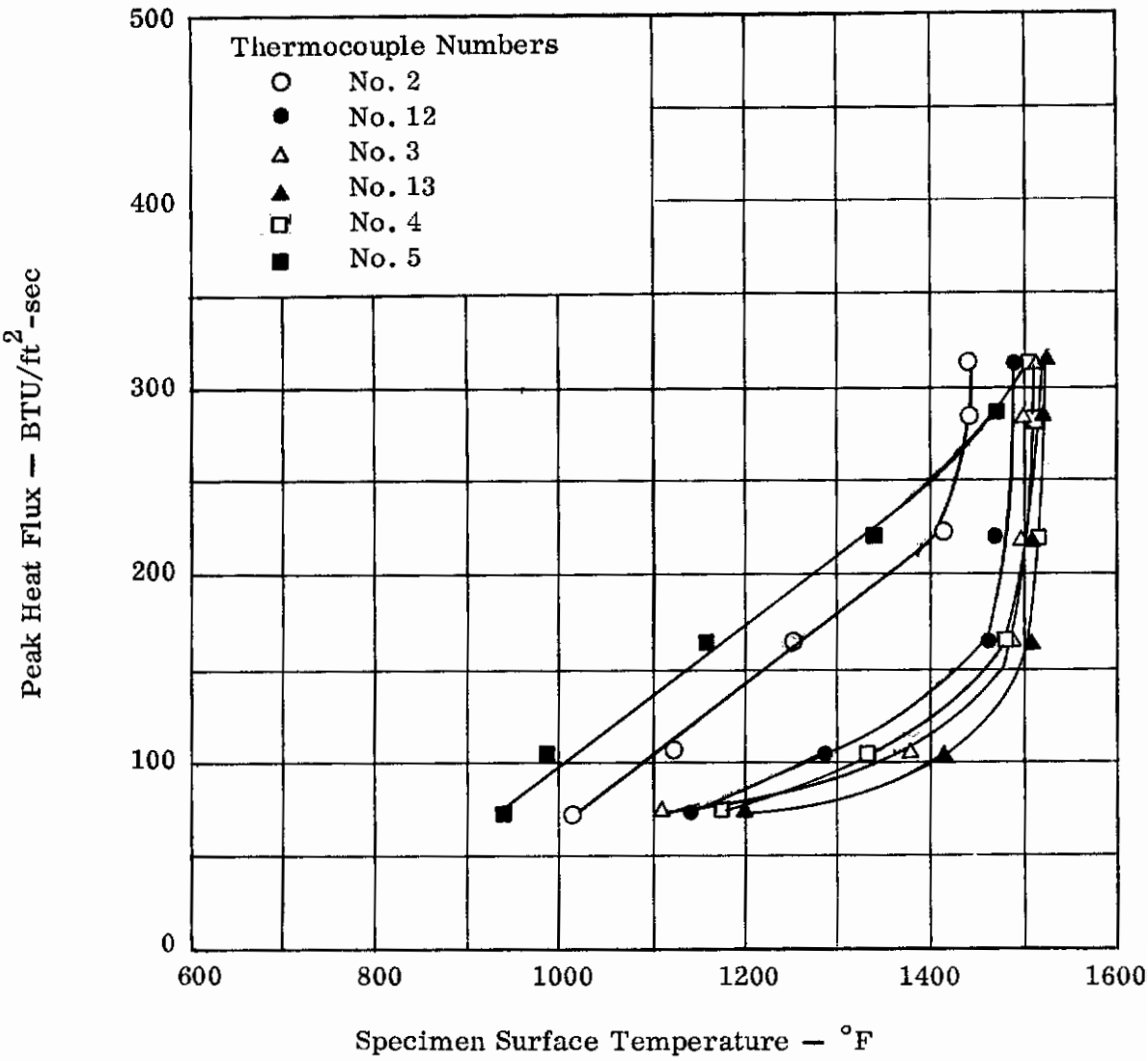

Figure 37. A Specimen, Type II, Run No. 3 Temperature Data
2.2 Inches from Specimen Center

Figure 38. A Specimen, Type II, After Testing

the failure suggested overheating. This could be the direct result of the Conoseal joint leak which increased the vapor pressure and hence the temperature of the sample. The way in which the cemented thermocouples became detached from the specimen surface is clearly visible.

Again it must be emphasized that the test conditions for test No. 1 were critical for the knurled A specimen and a higher heat flux was sustained, therefore this would substantiate the conclusions presented for the cause of the termination of test runs No. 2 and No. 3.

From the test data at the point of maximum heating for A specimen, Type I, and A specimen, Type II, there appears to be a definite effect of knurling on the heat flux to initiate boiling. The heat flux required to initiate boiling in the A specimen, Type II (knurled), is approximately 1.5 times that of A specimen, Type I. The increase in effective heat transfer area by knurling would account for the increase.

4. C Test Specimen

Three test runs and two transient heating cycle test runs were conducted on the C test specimen.

Since the primary function of the test program was to determine the maximum heat flux which could be accommodated by the lithium spray, it was decided for test run No. 1 on the C specimen to increase the lithium flow to the maximum flow which was attainable. The flow rate of 79.5 lb/hr was used for test run Nos. 1 and 2. The flow rate for test run No. 3 was 49.8 lb/hr and for the two transient cycle test runs 54 lb/hr. The condenser pressure was maintained at 0.5 psia for all of the C specimen testing. The total test time for run Nos. 1, 2, and 3 was 31, 14, and 13 minutes, respectively.

Test run No. 1 was terminated at a heat flux of 610 BTU/ft^2-sec because of the amount of lithium being used. Test run No. 2 was terminated when an audible cracking noise was heard in the vicinity of the work coil. The work coil was removed and it was noted that the inside section of the work coil had overheated and cracked the resin potting. This coil was no longer usable and a spare coil was installed which operated with no difficulty during the remaining tests. This spare coil, although basically identical with the first coil, had a slightly greater water flow rate in the center section.

Test run No. 3 was suspended when thermocouple No. 10 indicated a rapid temperature rise. Examination of the test specimen showed that the thermocouple had become detached and was inductively heated. This thermocouple was removed and the two transient cycles were conducted with no problem.

Based on a spray cone of 63°, the lithium spray would cover the surface area swept by an arc length of 1.40 inch from the specimen center. From Figure 21,

the dimensionless ratio of the heat flux distribution, the test specimen is inductively heated for a surface distance of 2.00 inch from the specimen center. The lithium spray would not cover the entire heated surface, but as the lithium flowed radically outward from the test specimen center, the lithium would cool this area. The total heat input to the C specimen versus surface distance from the center of the specimen for a heat rate of 1 BTU/ft^2-sec is shown in Figure 39. The heat input was obtained by graphical integration of Figure 21 for a peak heat flux of 1 BTU/ft^2-sec.

The peak heat flux to initiate boiling at 1.00 and 2.00 inch from the center of the test specimen is determined as follows. The heat input required to raise 79.5 lb/hr of lithium from 700 to 1700°F (saturation temperature) is

$$Q = Mc_p \Delta T$$

$$= 79.5 \text{ lb/hr} \times 1 \text{ BTU/ft}^2\text{-sec} \times (1700\text{-}700)^\circ\text{F}$$

$$= 22 \text{ BTU/sec}$$

From Figure 39, the heat input to the test specimen at a point 1.00 inch from the specimen center is 0.019 BTU/sec for a peak heat flux rate of 1 BTU/ft^2-sec. The percentage of the lithium spray which covers this area was calculated to be 50%. The heat input required to raise this amount of lithium to the saturation temperature is

$$Q = 22 \text{ BTU/sec} \times 50\%$$

$$= 11 \text{ BTU/sec}$$

Peak heat flux to initiate boiling 1.00 inch from the center of the test specimen is

$$q = \frac{11 \text{ BTU/sec}}{0.019 \text{ BTU/sec}}$$

$$= 580 \text{ BTU/sec}$$

At a point 2.00 inches from the center of the test specimen, the heat flux is zero, and the heat input to the test specimen is 0.0335 BTU/sec for a peak heat flux of 1 BTU/ft^2-sec. All of the sprayed lithium would be effective in cooling the specimen at this point. Therefore, the peak heat flux to initiate boiling is:

$$q = \frac{22 \text{ BTU/sec}}{0.0335 \text{ BTU/sec}} \times 1 \text{ BTU/ft}^2\text{-sec}$$

$$= 655 \text{ BTU/ft}^2\text{-sec}$$

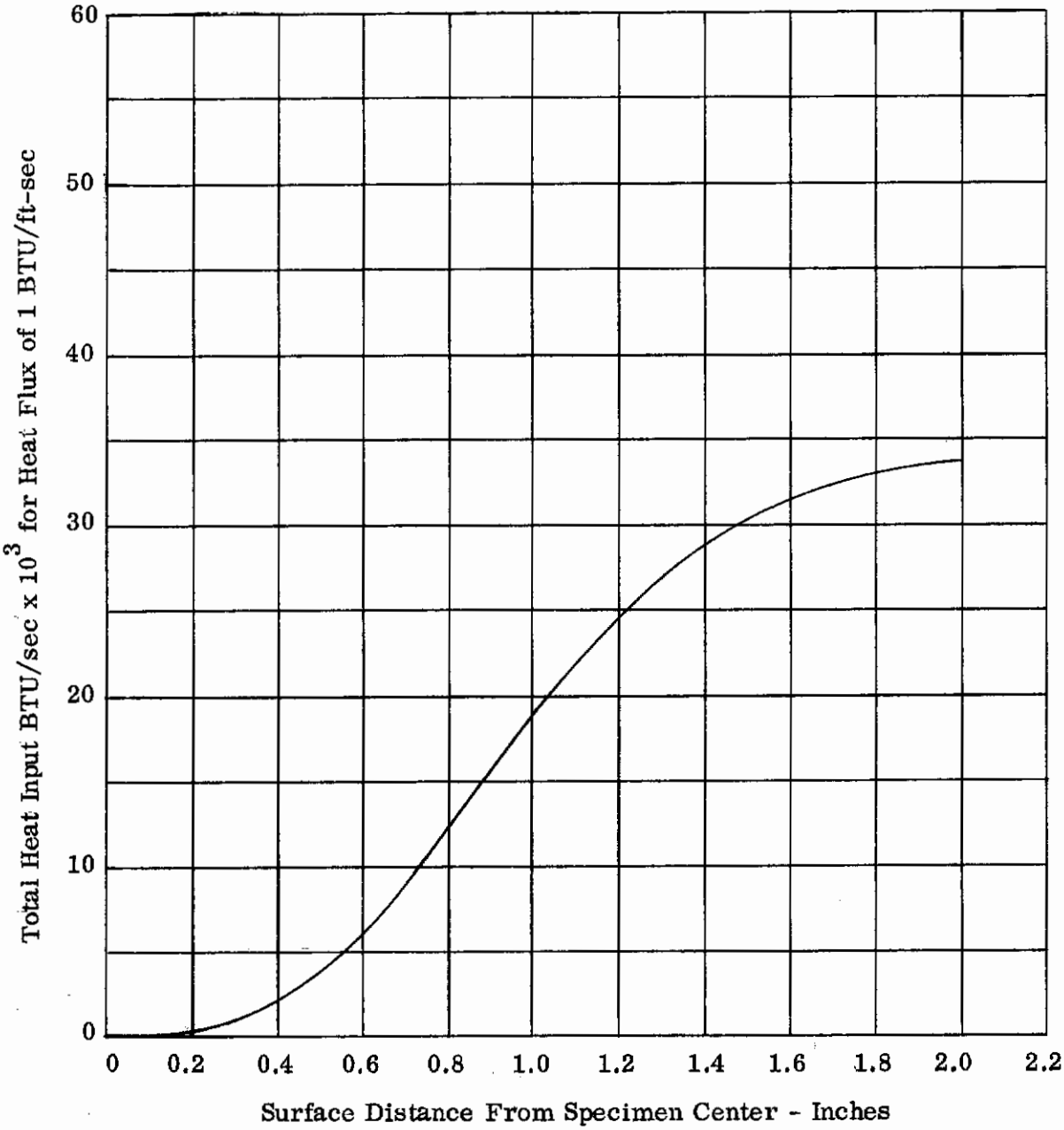

Figure 39. Total Heat Input To C Specimen For a Heat Flux of 1 BTU/ft^2-sec

After the bakeout run on the C specimen, the specimen thermocouples became shorted to ground, as has been previously discussed. Therefore, the temperature data for the C specimen may have serious inaccuracies. During one of the preheat runs, the specimen thermocouples indicated a maximum surface temperature of 1000°F, but viewing the specimen color, indicated a temperature of approximately 1300°F.

Temperature data versus the peak heat flux for test run No. 1 is shown in Figures 40 and 41. Temperature data from thermocouple No. 17 was used to determine the peak heat flux at each test point. The maximum peak heat flux achieved during test run No. 1 was 610 BTU/ft^2-sec.

Figure 40, the temperature data 1.00 inch from the center of the test specimen, indicates boiling to have initiated at a peak heat flux of 325-425 BTU/ft^2-sec. The calculated value at this point is 580 BTU/ft^2-sec. At 2.00 inches from the center of the test specimen, the temperature data in Figure 41 shows boiling to have initiated at a peak heat flux of 350-475 BTU/ft^2-sec. The calculated value is 655 BTU/ft^2-sec. The discrepancies between the calculated values and the test values of boiling heat flux may be due to leakage at the nozzle to columbium adapter joint, which would reduce the amount of sprayed lithium impinging on the heated surface. The change in slope of the temperature data for thermocouple Nos. 10 and 7 in Figures 40 and 41 may indicate that the shorts to ground for these thermocouples were eliminated during the test run and perhaps true temperatures were recorded at the higher heat fluxes.

The temperature data for test run No. 2 was not reduced since it was a duplication of test run No. 1. The amount of usable lithium was limited for a test run and for this reason, test run No. 1 was terminated. For test run No. 2, larger initial heat flux steps were taken to insure an adequate supply of lithium to continue testing beyond the heat flux achieved in test run No. 1. At approximately the same point reached in test run No. 1 shutdown occured by the overheating of the center section of the induction heating work coil.

Test run No. 3 was conducted at an initial lithium flow rate of 49.8 lb/hr. For this test run, when the flow meter indicated an increase of flow, the supply tank pressure was not reduced to maintain constant flow. At shutdown, the flow meter indicated a flow of 62.5 lb/hr. Due to the leak at the nozzle attachment to the columbium adapter, it may be assumed that the flow rate of the sprayed lithium was at a lower value than the initial flow rate of 49.8 lb/hr. Shutdown occurred when a maximum peak heat flux of 560 BTU/ft^2-sec was achieved, but temperature data was not recorded at this point.

By applying the ratio of flow rates for test run Nos. 1 and 2 to the peak heat flux values calculated for test run No. 1 to initiate boiling, 1.00 and 2.00 inch from the specimen center, the corresponding values at the same points for test run No. 3 are 365 and 410 BTU/ft^2-sec.

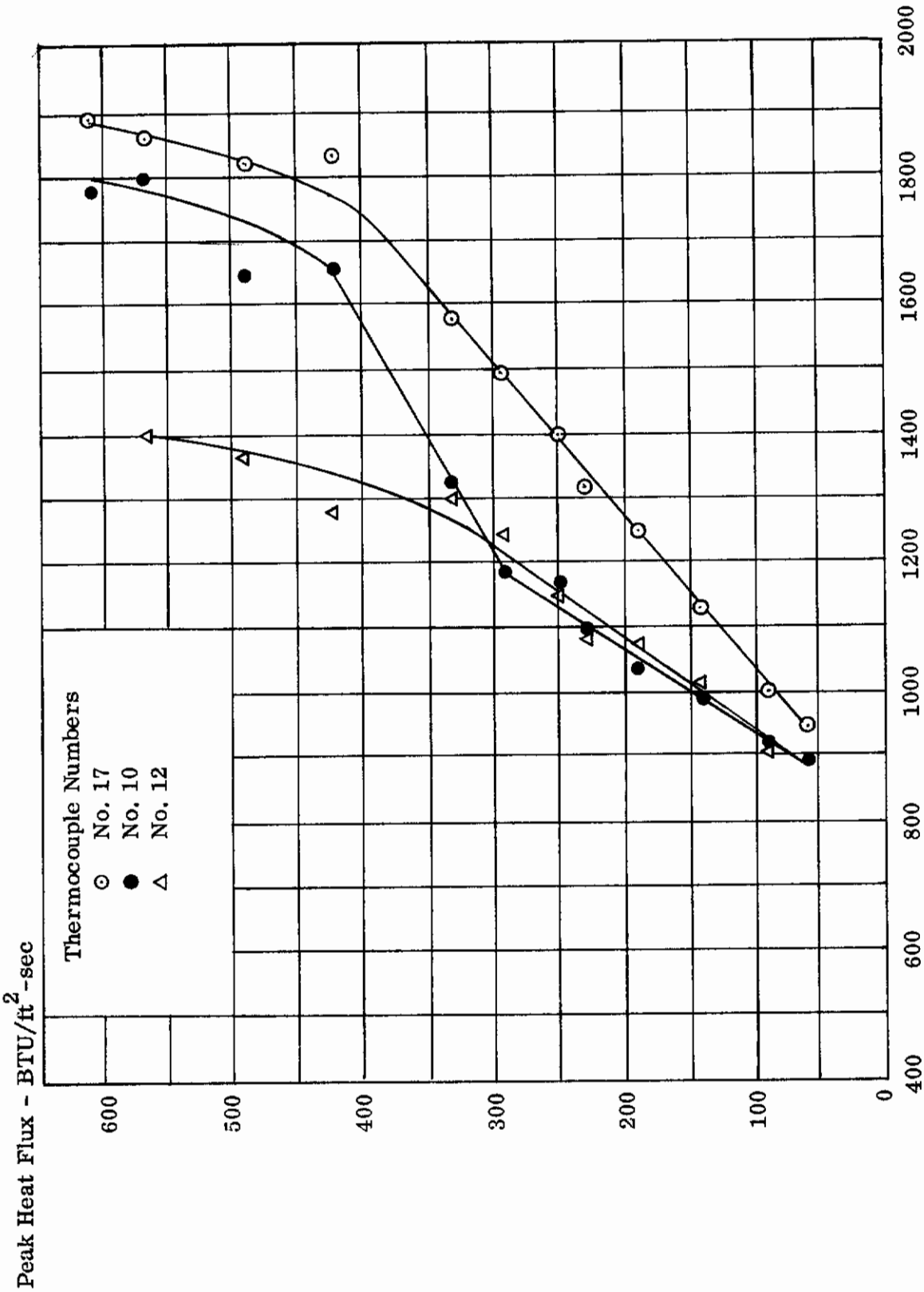

Figure 40. C Specimen Steady-State Run No. 1 Temperature Data 1.0 Inch from Specimen Center

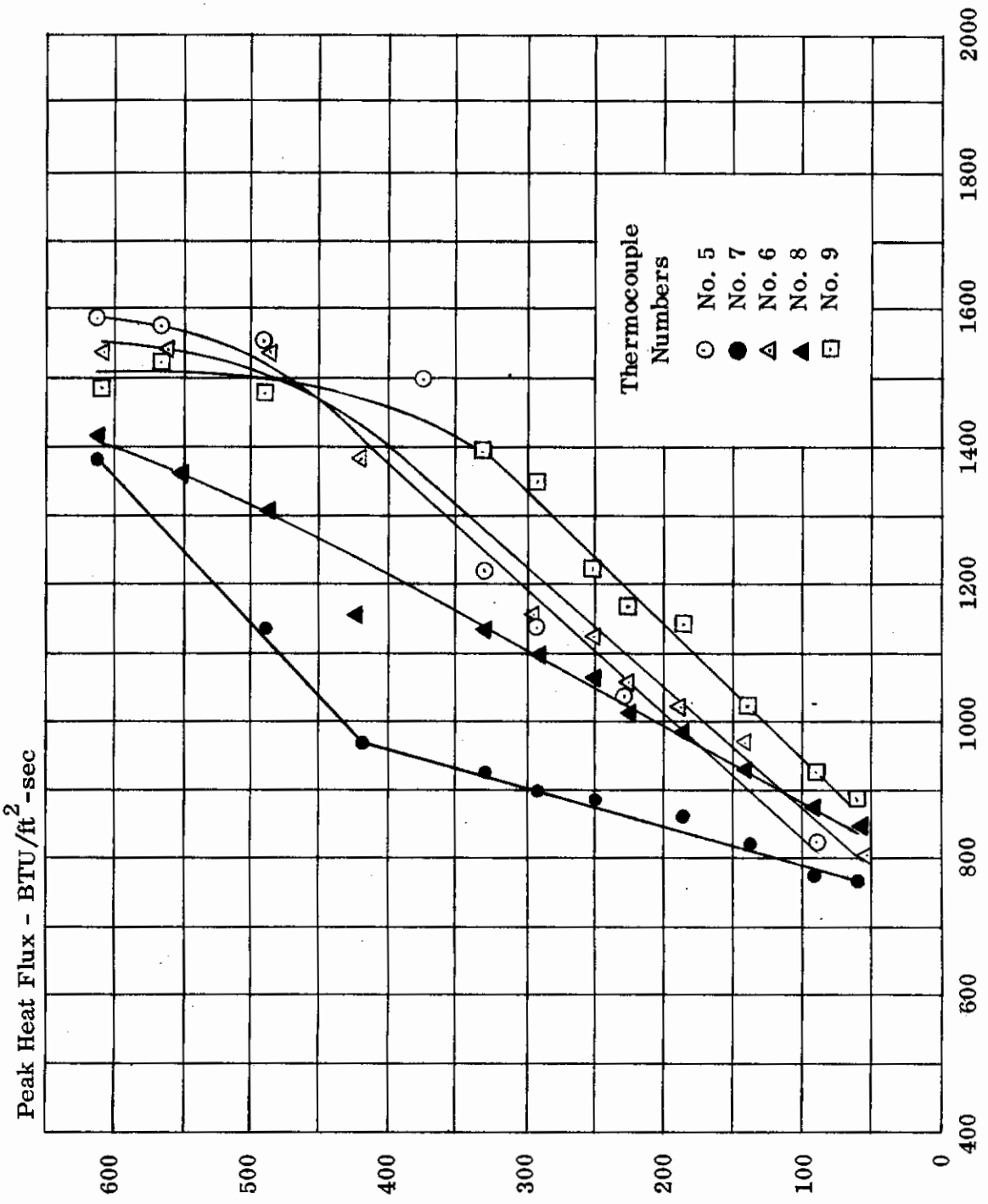

Figure 41. C Specimen Steady-State Run No. 1 Temperature Data 2.0 Inches from Specimen Center

Temperature data for test run No. 3 is shown in Figure 42. Thermocouple No. 10, which is located 1.00 inch from the center of the test specimen, indicates boiling initiated at a peak heat flux of 350 BTU/ft^2-sec. The calculated value is 365 BTU/ft^2-sec. Thermocouple Nos. 5, 6, and 9 indicate boiling to have started at a heat flux of 375 BTU/ft^2-sec at 2.00 inches from the center of the test specimen. The calculated value is 410 BTU/ft^2-sec. The good agreement between the test and calculated values of boiling heat fluxes substantiates the conclusion that the spray nozzle attachment to the columbium adapter did leak during test. During previous runs the reducing of the supply tank pressure to maintain a constant flow, as indicated by the flow meter, apparently was reducing the supply of lithium to the heated surface.

5. Transient Heating Cycle

Two transient heating cycles were conducted on the C test specimen primarily to determine the simulation of the heat flux versus time by the induction heating system for reentry. The temperature data for the first cycle was reduced and is presented in Appendix III.

Due to the thermocouple problem, it was necessary to be conservative in the application of the maximum heat flux during the transient heating cycle. Based upon the results from test run No. 3, a maximum work coil current of 685 amperes corresponding to a heat flux of 460 BTU/ft^2-sec was selected. The lithium flow rate was 54 lb/hr and the supply tank pressure was not regulated during the test run.

As has been discussed in Section 4-C, the work coil current was recorded continuously on the oscillograph traces along with the thermocouple data for the transient heating cycles. A calibration curve of work-coil current as a function of galvanometer deflection was obtained from the test data for test run No. 3 and is shown in Figure 43. The peak heat flux as a function of work current for test run No. 3 is shown in Figure 44. By the use of these curves, the galvanometer deflections obtained during the transient heating cycle for the work-coil current were converted to heat fluxes at the times indicated in Table 9, Appendix III. A dimensionless ratio of heat flux was obtained by dividing the heat flux at each time increment by the maximum heat flux. The dimensionless ratio of test heat flux as a function of time is shown in Figure 45, along with the desired distribution. The simulation is good. As may be seen from Figure 45, the test distribution subjected the test specimen to a more severe thermal loading during the beginning and end of the transient cycle test run than the desired thermal loading.

After completion of the C specimen tests, the specimen was removed from the loop and Conoseal joints disassembled. The joints had remained leak-tight during the tests and the external appearance of the specimen was excellent.

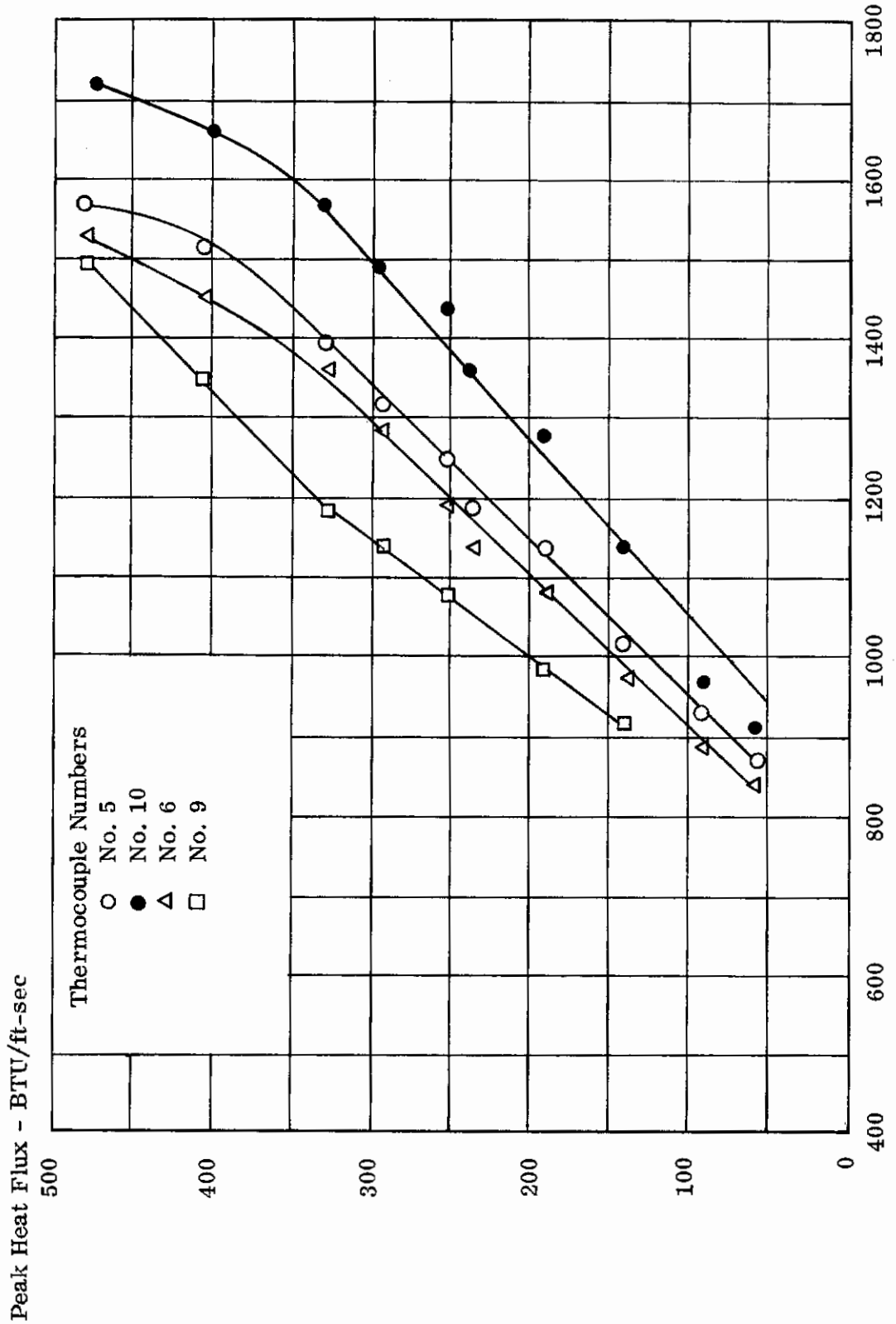

Figure 42. C Specimen Steady-State Run No. 3
Temperature Data 1.0 and 2.0 Inches from Specimen Center

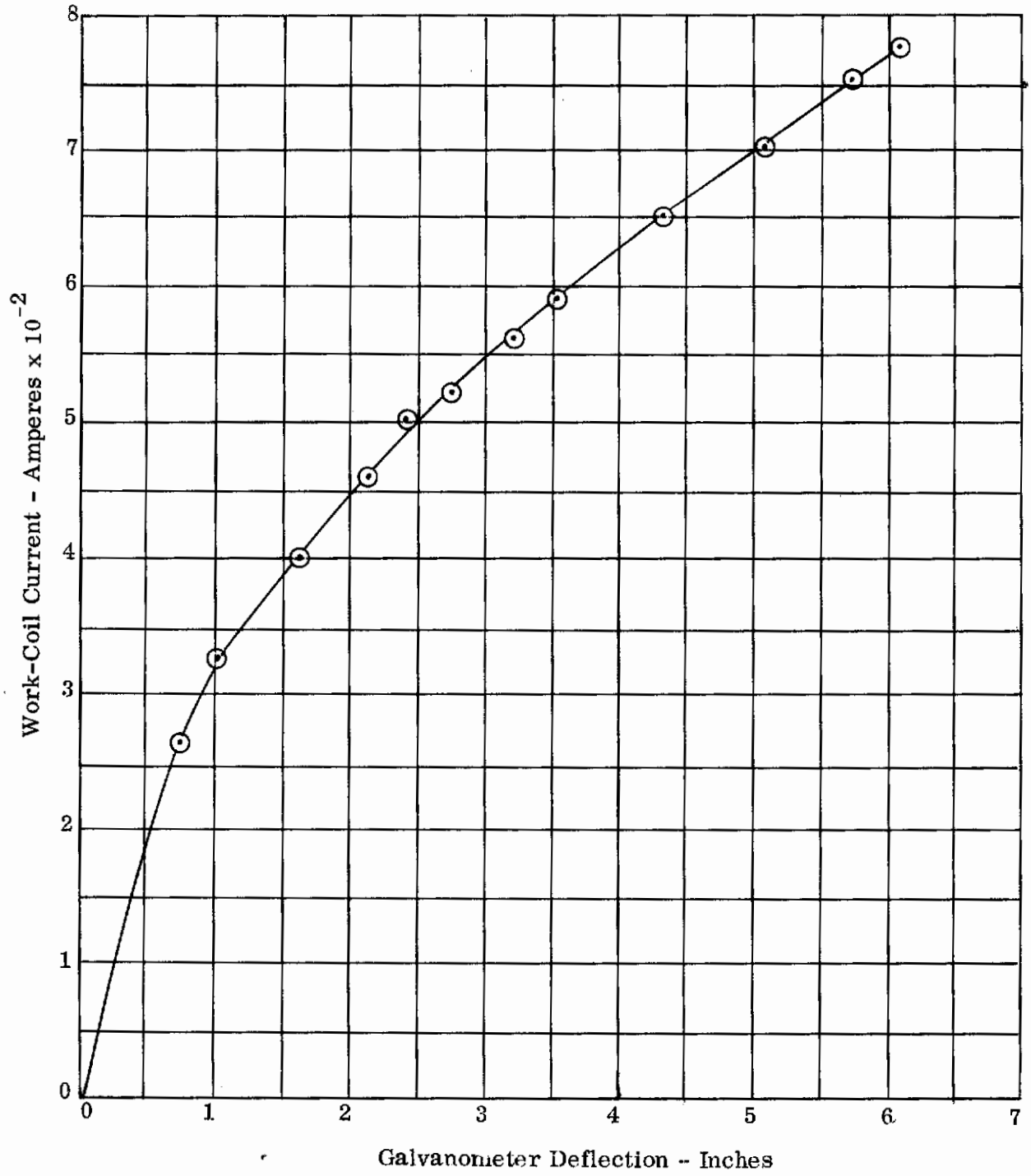

Figure 43. Calibration Curve of Galvanometer Deflection versus Work-Coil Current

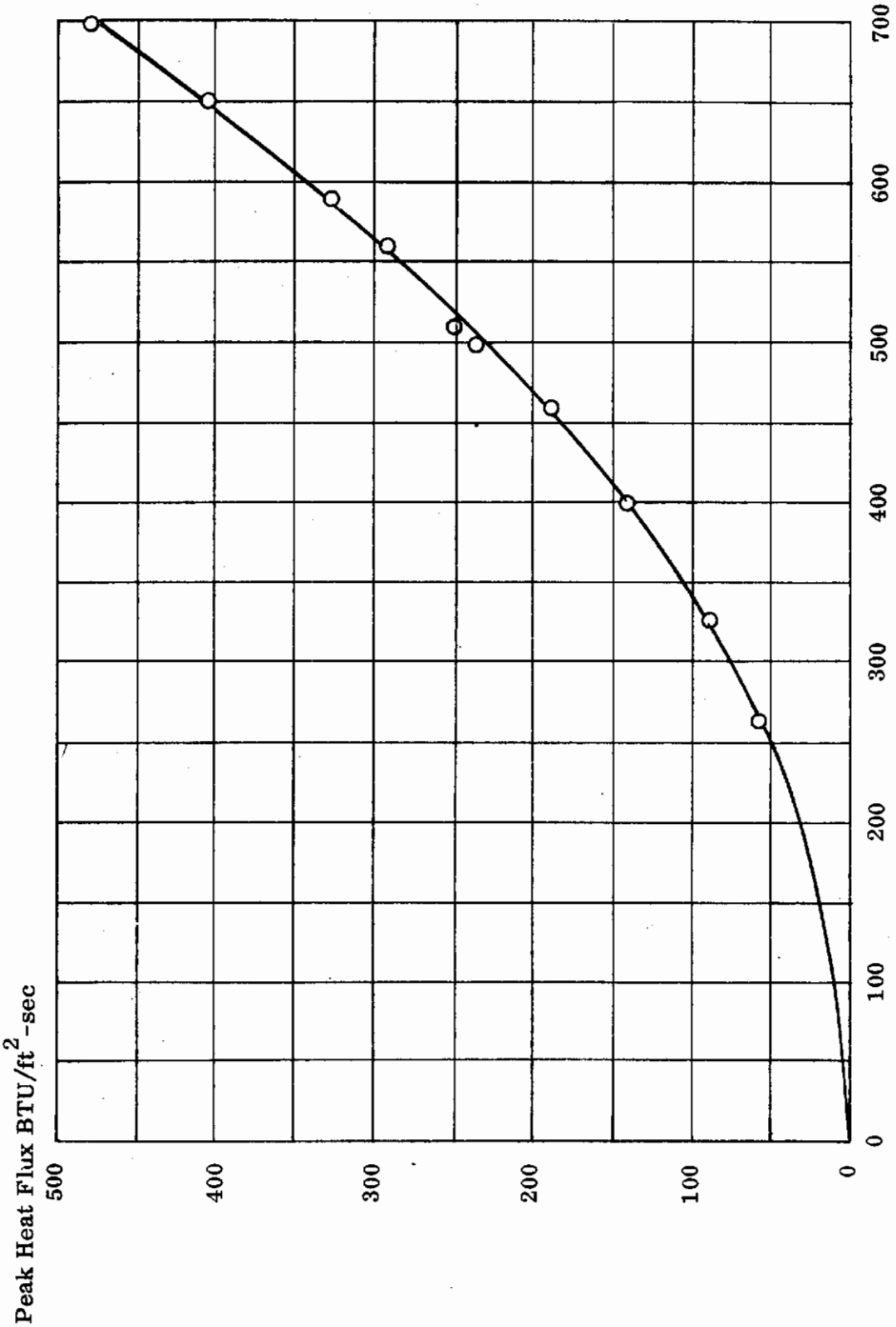

Figure 44. C Specimen Steady-State Run No. 3 Peak Heat Flux as a Function of Work-Coil Current

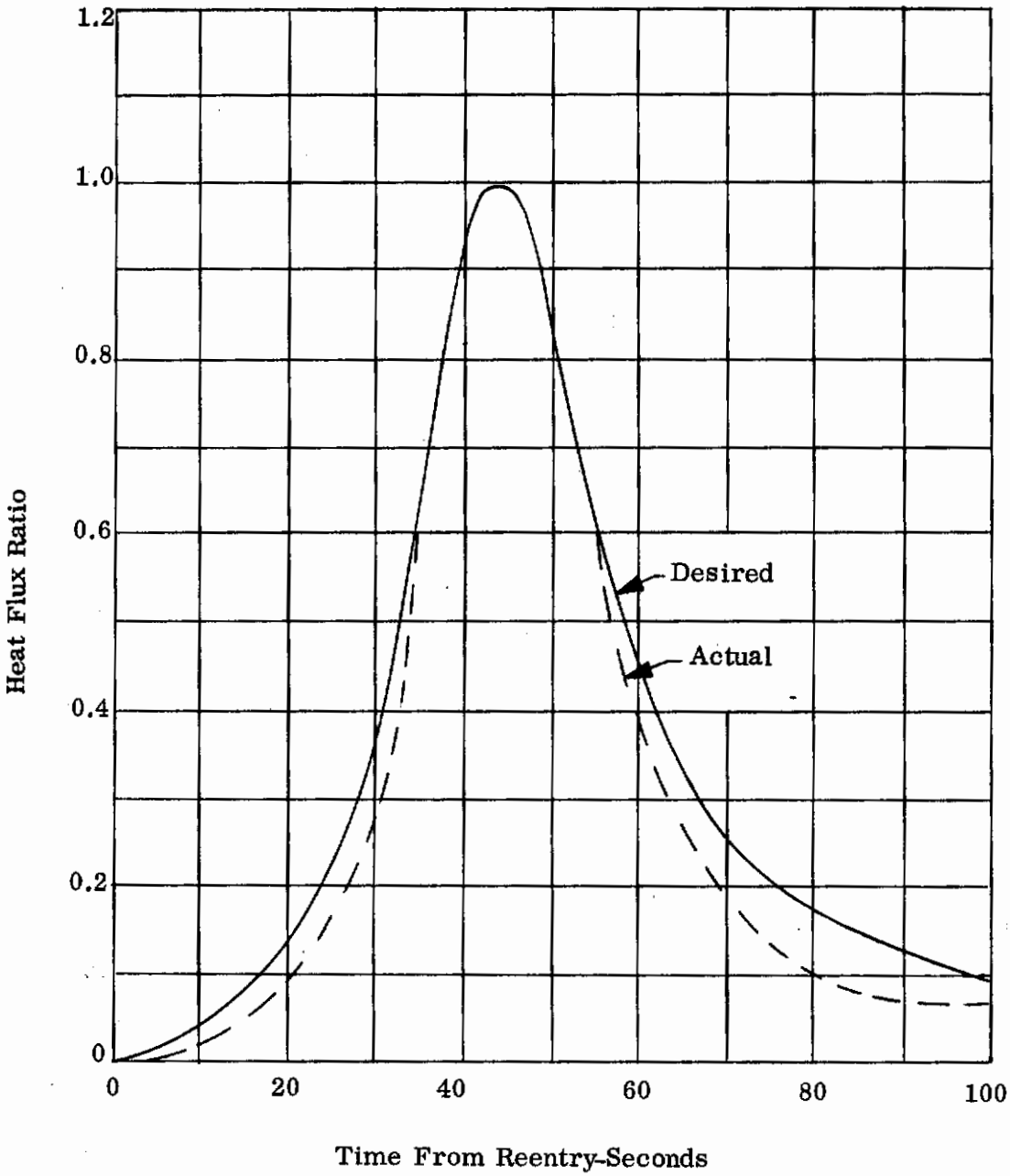

Figure 45. C Specimen Transient Heating Cycle, Comparison of Actual and Desired Variation of Heat Flux with Time

6. Effect of Work Coil to Specimen Spacing

The desired work coil to specimen spacing for the A and C specimen was 0.125 inch and was to remain constant during a test run. As is discussed in Section 4-B, this spacing could not be maintained due to the thermal growth of the test specimen during a test run. Accordingly, the work coil was set back and the specimen thermal growth would then return the test specimen to the desired spacing.

An investigation was conducted to determine the effect on the peak heat flux for a 0.125 inch spacing if the thermal growth of the test specimen was over-compensated. The work coil was set back 0.065 and 0.080 inch for the A and C specimens, respectively, to compensate for thermal growth. The results of the investigation are summarized below. The first column indicates the amount of over-compensation while the second and third columns indicate the measured percentage error in the peak heat flux determined for a 0.125 spacing for each specimen type.

Over-Compensation (in.)	A Specimen Error (%)	C Specimen Error (%)
0.010	2	6
0.020	6	13

The study showed that the effect of work-coil spacing on the peak heat flux for the A specimen was minor and for the C specimen it could be significant.

The peak heat flux is not only a function of the work-coil spacing but of the temperature of the heated surface as well, increasing as the surface temperature increases. Visual observations of the test specimen during test, indicated surface temperature which were higher than temperatures recorded by the specimen thermocouples. The work-coil spacing effect is then partly compensated in a conservative manner by using the lower temperature from the thermocouples in the determination of the peak heat flux from Figures 25 and 26.

No attempt was made to apply correction factors to the indicated peak heat fluxes during the test runs. The indicated heat fluxes may be in error at the lower levels of heat flux, but at the higher heat fluxes this error would be small.

SECTION 6

SYSTEM POTENTIAL

The purpose of this section is to show the potential of the lithium spray system and to illustrate promising applications for the system and its advantages. A discussion of areas of investigations which are required to produce a flight weight system is also presented.

A. POTENTIAL CAPABILITY

In the testing conducted, the full potential of the lithium spray system was not determined due to the instrumentation problems which have been discussed. However, when the data obtained during this program is used in conjunction with available heat transfer data for other liquids, the full potential of the lithium spray system becomes apparent.

The magnitude of the heat transfer coefficient can be determined in an approximate manner. In a paper by R. E. Lyon (Reference 7) it is shown that the temperature drop through a sodium film at the initiation of boiling was 7°F. For the A specimen, Type II, the test data showed that initiation of boiling occurred at a heat flux of 375-425 BTU/ft^2-sec. Using the lower value of heat flux and the temperature drop of sodium for the initiation of boiling, the boiling heat transfer coefficient would be 193,000 BTU/hr-ft^2°F. Even if the assumed temperature drop is in error by an order of magnitude, the boiling heat transfer coefficient is large in comparison to the heat transfer coefficients for other fluids including sodium. The heat transfer coefficient for sodium is approximately 3000 BTU/hr-ft^2°F at the onset of nucleate boiling.

In Reference 8, the ratio of the critical or burnout heat flux to the heat flux to initiate boiling for several fluids ranges from 8 to 50. Applying the lower ratio to the heat flux which initiated boiling for the A specimen, Type II, the critical heat flux for the lithium spray system could be conservatively estimated as 3000 BTU/ft^2-sec or approximately 11 x 10^6 BTU/ft^2-hr. This heat flux is equivalent to a radiation equilibrium temperature of 9700°F which is considerably beyond the temperature limitation of any structural material. It would not be surprising to find that the system concept would have an even greater capability.

B. APPLICATIONS AND ADVANTAGES

The lithium spray system could be incorporated to cool high heat intensity areas of aerospace vehicles such as nose caps, leading edges, control surfaces and rocket nozzles.

The high potential of the lithium spray system would allow for smaller radius nose caps, since the maximum temperatures of the present thermal protection

systems requires that large nose cap radii be used. The smaller radius nose caps would result in lighter weight and greater flight capabilities such as wider flight corridors and high flight maneuverability. Although the heat flux at the stagnation point is higher for a smaller radius nose, since the convective aerodynamic heating is a function of the nose radius to the minus 1/2 power, the effect on the heat flux a short distance from the stagnation point is in the opposite direction. This is illustrated below for a nose radius ratio of 2. The perimeter distance, S, aft of the stagnation point is dimensionless. The heat flux ratios shown are based upon the stagnation point heat flux of the smaller radius nose.

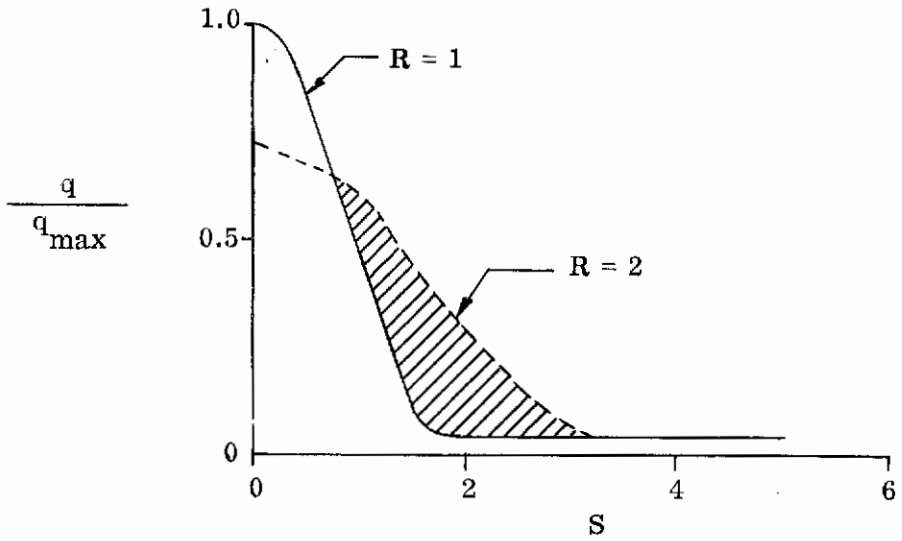

The shaded area represents the net decrease in heat flux and lower temperatures would result; therefore, structural requirements would be reduced accordingly. The same advantages listed for nose caps would also pertain to leading edges.

By use of the spray system for control surfaces, there is a distinct advantage over ablators in that the aerodynamic shape of the control surface may be maintained throughout the entire flight. The lithium spray system would only operate as required when control displacements would result in excessive temperatures. For rocket nozzles, where regenerative cooling cannot be used because of the use of solid and/or hot propellants, the lithium spray system would be ideally suited.

C. APPROACH TO FLIGHT HARDWARE

The feasibility of the lithium spray system has been demonstrated by the tests conducted, but investigations are required to obtain an optimum flight system. The types of investigations required are briefly described.

1. Spray Nozzle

The investigation of the spray nozzle should include the effect of droplet size and velocity of impact on the heat transfer coefficient and the maximum heat

flux capability. The mechanism of spray boiling requires investigation. The velocity of the exhaust vapor increases as the quality of the vapor increases due to vaporization; therefore, the exhaust vapor may impair lithium droplets from hitting the heated surface and be carried out with the exhaust vapor. There may be an optimum droplet size and velocity which will give the maximum heat transfer coefficient, the maximum heat flux capability, and provide sufficient energy for the penetration of the exhaust vapor.

The spray nozzle design studies should also determine the feasibility of varying the spray density distribution. This may also be accomplished by the use of multiple nozzles with overlapping spray distributions.

2. Material Selection

Material selection should be based upon compatibility with lithium, strength at elevated temperature, fabrication, and thermal properties. A coating for the substrate should be available. Compatibility of the material with lithium should not be under static conditions only, but with a wet mixture of lithium at high velocities, since the vaporization of lithium will result in high exhaust velocity and there may be mass transfer effects. The material should have high thermal conductivity so as to minimize the temperature drop through the wall at high heat fluxes and also to reduce thermal stresses.

3. Internal Heat Transfer Surface

The internal heat transfer surface requires study. The tests conducted indicated there is an effect on the heat transfer coefficient due to knurling. Different methods of increasing the surface area should be investigated. The resulting structure will probably be a thin wall and will require stiffening. Optimization studies should be conducted, since stiffeners may be used to increase the heat transfer surface as well as for structural requirements.

4. Experimental Determination of Burnout

The experimental determination of burnout is required. The spray boiling mechanism may preclude the establishment of a film boiling regime. The increase in exhaust velocity due to vaporization as the heat flux is increased may shear the vapor bubbles as they are formed. There may be an increase in the heat transfer coefficient at the higher heat flux levels due to this effect.

For increased efficiency of the system, heat transfer data for wet lithium mixtures are required. Because of the nature of the spray system, it is unlikely that all the lithium would be evaporized at the point of contact. Overall system optimization would undoubtedly require the transfer of heat to a vapor-liquid mixture downstream of the region of maximum heating intensity.

5. Flight Weight Accessories

Optimization studies of the lithium spray system components leading to flight weight hardware are required. Some of these accessories are a positive expulsion lithium storage tank with heaters, temperature controller, line heaters, and the pressurization system.

6. System Demonstration

Based upon the results from the previously discussed studies, a prototype model of the complete system could be fabricated and tested, both in the laboratory and during free-flight reentry. Such testing would provide designers with the complete confidence required for extensive utilization of the concept.

SECTION 7

CONCLUSIONS AND RECOMMENDATIONS

A. CONCLUSIONS

The following conclusions may be drawn from the work conducted during the program:

(1) The tests conducted demonstrated the feasibility of the lithium spray system for structural cooling.

(2) A heat flux of 600 BTU/ft^2-sec was accommodated which is equivalent to a radiation equilibrium temperature of about 5800°F.

(3) The maximum potential of the system could not be determined experimentally due to instrumentation problems but is estimated at 3000 BTU/ft^2-sec or higher.

(4) The A specimen testing indicates that increasing the internal surface area by knurling increases the effective heat transfer coefficient.

(5) The cemented thermocouple technique does not have the accuracy required to obtain temperature data suitable for heat transfer coefficient determinations.

(6) Inductive heating provides a method for high heat flux simulation. The heat flux intensity and distribution are determined by the survey coil technique and the power input to the conductive heating work coil. The simulation for the transient heating cycle was very good.

(7) Many applications could benefit from the lithium spray system such as nose caps, leading edges, control surfaces and rocket nozzles.

(8) The physical appearance of the internal surfaces of the test specimen A, exhaust lines after test, indicated the compatibility of lithium with columbium and Haynes 25.

(9) The test specimen oxidation protective coating afforded adequate protection for the static air conditions during test, but under dynamic air conditions, the extruded tin from the coating could be removed from the surface and may be deposited on unwanted areas of a vehicle.

B. RECOMMENDATIONS

As a result of the work performed and the conclusions, the following recommendations for future work are suggested to fully exploit the potential of this new cooling system concept:

(1) Conduct studies to determine optimum lithium droplet size and velocity which will give the maximum heat transfer coefficients and heat flux capability.

(2) Conduct design studies of spray nozzle to determine the feasibility of varying the spray density pattern.

(3) Conduct material compatibility tests with lithium under static and dynamic conditions.

(4) Conduct studies to determine methods for increasing the internal heat transfer surface area.

(5) Determine experimentally the burnout heat flux for the lithium spray system.

(6) Determine heat transfer coefficients for lithium vapor-liquid mixtures of various qualities.

(7) Conduct optimization studies of the lithium spray system components for flight weight hardware.

(8) Evaluate flight weight systems under laboratory and free-flight conditions.

(9) Establish a high temperature instrumentation program. The problem of thermocouple attachment to coated refractories and brittle materials has been evident for some time. Studies such as the one conducted have encountered this problem, but due to limited funds, the instrumentation problem could not be investigated extensively. A separate program should be established for the development of improved methods of thermocouple attachments.

APPENDIX I

CEMENTED THERMOCOUPLE INSTALLATION PROCEDURE

The following procedure was used for the thermocouple installations on the Syclor coated A and C specimens.

A. PROCEDURE

1. Surface Preparation

Prepare the test specimen surface by degreasing with acetone and wiping clean. Paint entire frontal area of the test specimen with Pyrochrome and scour using Kimwipe tissues on the wet Pyrochrome and repeat this operation again. Sufficient undercoating will adhere to the surface for an initial undercoating.

To prevent oxidation of the uncoated interior surfaces of the specimens during curing of the Pyrochrome with the propane torch, seal the specimen exhaust line and connect vacuum pump to the specimen inlet line, evacuate specimen and leave vacuum pump in operation during the curing cycle. The torch flame is held approximately 1-1/2 inches from the surface and heat is applied until the free tin in the coating is extruded and forms small spheres. After the entire surface has been heated, this is done in strips,1/2 inch wide and 2 inches long, the specimen is allowed to cool and the extruded tin is removed by brushing and/or filing as necessary.

The surface is rescoured with Pyrochrome and cured with the propane torch. A second brushing reveals small areas where the Pyrochrome has not adhered and these areas are avoided during thermocouple installation.

2. Thermocouple Installation

The chromel-alumel wire used for these specimens is Thermoelectric Co., Inc., Type GG-28-CT which has double fiberglass insulation; i.e., the individual wires are fiberglass insulated plus a fiberglass overbraid for the pair. Cut the wire to the desired lengths and remove insulation from wire as needed from the thermocouple location on the specimen to the point of departure of wire from the specimen. Add four fish spline insulator beads to each lead and weld the thermocouple bead with the discharge welder. After welding, remove excess wire from the bead and shape bead area into a dipole form about 5/16 inch wide.

After layout of thermocouple locations on the specimen surface, the thermocouples are formed to the contour of the surface to which they are mounted. Form one thermocouple and paint a fresh layer of Pyrochrome along path of thermocouple leads, leaving the bead location unpainted. Place thermocouple in position on

the specimen surface and secure in two places with short lengths of masking tape. Adjust the thermocouple bead to the desired location and secure with a spring loaded knife edge to the surface. Apply a coating of Pyrochrome to all exposed wire areas and fish spline insulators. Air dry and complete removal of moisture with heat lamp which will require 15 to 30 minutes depending upon coating thickness. Remove tape and knife edge and dress away excess cement from knife edge and tape edge areas. Check the bead to see that it has not lifted away from intimate contact with the surface.

Using a 4:1 volume mixture of Pyrochrome and alumina powder, coat the bead area and the previously taped areas, air dry, and complete drying with heat lamp. (The alumina mixture serves to keep the pyrochrome from running under high temperature conditions.) Apply the torch, as in initial steps, heating in short sections until cement is cured. This occurs at about 700 °F and is evidenced by a change from green to a brownish color returing to green again upon cooling. This procedure is repeated for each thermocouple. Figure 46 shows a typical installation.

C. EQUIPMENT

Pyrochrome (Preferred Utilities Co., New York, N. Y.)

Alumina Powder No. 607 (Whittaker Clark & Daniels, Inc., 260 W. Broadway, New York, N. Y.)

Unitek Weldmatic Discharge Welder Model 1015B or Equivalent

Vacuum Pump with Hoses and Adaptors

Propane Torch

Heat Lamp

Miscellaneous Acid Brushes, Kimwipes, "C" Clamps, Masking Tape.

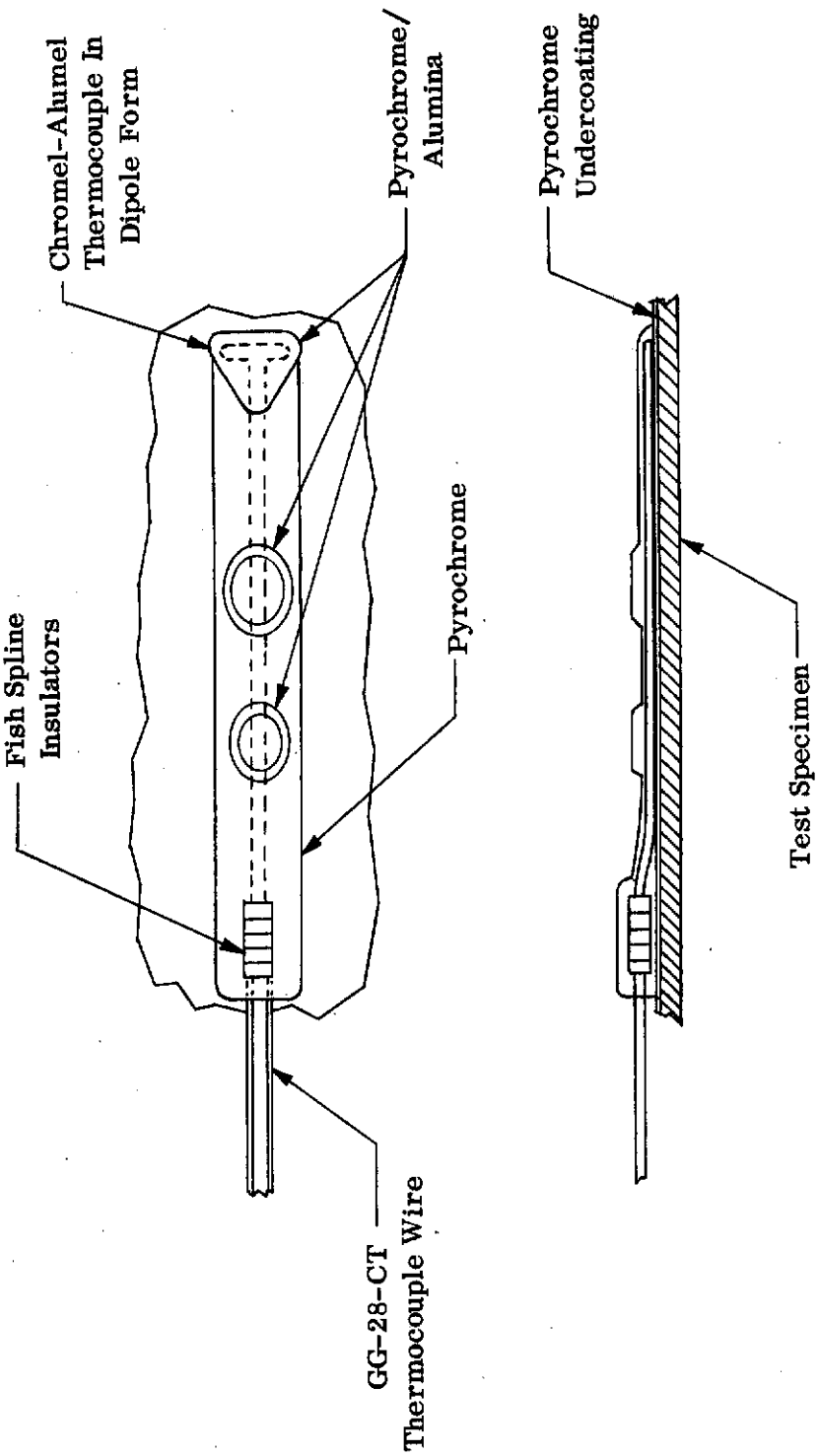

Figure 46. Typical Test Specimen Thermocouple Installation

APPENDIX II

THE LITHIUM SUPPLY TANK FAILURE

During the pretest checkout of the lithium loop, two failures of the supply tank occurred. This Appendix will present the reasons for material selection, fabrication history of the tank and possible causes of the failures.

A. MATERIAL SELECTION

The A and C test specimens were fabricated in a columbium alloy but due to size and cost considerations, it was advisable to fabricate the loop from stainless steel and superalloys. The maximum operating temperature of the supply tank was to be 2000°F; therefore, one of the few materials which has usable strength and does not require an oxidation protective coating is Haynes 25. After consultation with Oak Ridge, Pratt & Whitney and the Haynes Company, Haynes 25 was selected for the tank based upon compatibility with lithium and usable strength.

B. FABRICATION

The supply tank was fabricated from an 18-inch long section of 14-inch standard weight pipe with two 14-inch weld caps as heads. In the top head there was a 3/4-inch schedule 10 pipe projecting into the tank for the liquid level device, and a 1/2-inch schedule 40 nozzle for cover gas and vacuum. There were two schedule 40 nozzles in the bottom head for the supply line and discharge line. A thermocouple well in the lower tank head, projected horizontally into the tank, was welded close to the junction of the cylindrical shell and tank head.

The heads and shell were joined by tungsten-inert gas shielded d-c arc welding. The nozzles and thermocouple well were welded to the tank by the same process. The root and final welds were all dye checked. All welds which were below the liquid lithium level were X-rayed and the complete tank was mass spectrometer inspected.

After the two failures, as discussed in Section 4-A, the fabrication history of the tank heads were investigated. The vendor tried to form the first two heads cold and was unsuccessful. The second two were pressed hot and were satisfactory. The two heads that failed were processed as follows: first pressed cold to form the major radius; 15-minute salt bath at 2200°F; water quenched; second press to form knuckle radius. These tank heads failed in the straight section. The two heads that passed were processed as follows: first press cold; 15-minute salt bath at 2200°F; second press 2000°F; vapor degreased; pickled and then machined. Only visual inspection was made to determine if cracks were present.

C. POSSIBLE CAUSES OF FAILURES

The possible causes for the tank failure are given below, but without proper metallurgical examination with photomicrographs these reasons must be considered as postulations:

(1) Due to the thermowell weld and the tank head weld to the shell being close together, the zone became sensitized. There was no post-heat treatment of the tank after fabrication. There were other areas of the tank which should have also been sensitized, but no failures occurred. These areas were dye checked and no cracks were evident.

(2) There may have been high residual stresses in the tank head due to forming and welding. These residual stresses in combination with the pressure and thermal stresses may have caused failure.

(3) The grinding operation during the first repair, may have left additional residual stresses.

(4) Stress corrosion may have occurred. High residual stresses were probably present due to forming and welding.

D. CONCLUSION

It was concluded that it would be difficult to repair the tank with any degree of confidence. After repair, the tank would have to be properly heat treated to retain ductility. For sections greater than 0.250 inch thick, and where the tank heads and shell are 0.375 inch thick, it is recommended that water quench be used. The tank would be difficult to quench, due to the requirement of providing spray nozzles inside of the tank.

The maximum operating temperature of the supply tank had been 2000°F, but changes in the test program later reduced this temperature to 1500°F. At this temperature, 316 stainless steel could be used. A replacement tank was fabricated in 316 stainless steel and performed satisfactorily during the complete test program.

APPENDIX III

TEST DATA

This appendix contains tabulated data from the various test runs on the A and C specimens. Galvanometers numbers 1 through 12 were connected to a switching device, enabling each of these galvanometers to accommodate two thermocouples when required. Test specimen thermocouple number 18 was used for the automatic cutoff meter of the induction heating system and temperature data was not recorded. Visual observations of the test specimens during tests are indicated in tabulated data for the lithium loop.

The test specimen thermocouple data is tabulated in Tables 2 through 9. The locations of the test specimen thermocouples are shown in Figures 14 and 17. The lithium loop test data is listed in Tables 10 through 17. The locations of the lithium loop thermocouples are shown in Figure 19.

TABLE 2

A SPECIMEN, TYPE I,

TEMPERATURE DATA RUN NO. 1

Temperature In °F

Test Point Number		1	2	3	4	5	6	7	8
Galvanometer Number	Thermocouple Number	(264)*	(325)	(400)	(460)	(485)	(485)	(520)	(560)
1	2	-	-	-	-	-	-	-	-
	12	1100	1320	1645	1690	1690	1690	N. R.	
2	3	1150	1405	1690	1760	1795	1795	1840	1850
	13	1115	1490	1670	1735	1750	1735	N. R.	1830
3	4	1170	1680	1760	1780	1800	1780	1810	1830
	1	955	1075	1415	1490	-	1490	N. R.	-
4	5	1220	1525	1670	1680	1690	1680	1700	1700
	21	1030	1160	1400	1555	1575	1555	N. R.	-
5	6	1010	1120	1380	1580	1735	1690	1840	1860
	22	880	1000	1220	1415	1450	1435	N. R.	1620
6	7	865	900	990	1075	-	1120	1360	1620
	24	1000	1050	1270	1400	1460	1450	N. R.	1650
7	8	1020	1190	1450	1535	1575	1560	1650	1690
	Outlet	980	1095	1300	1450	1520	1510	N. R.	-
8	9	805	850	980	1120	1320	1190	1680	1760
	Inlet	720	720	730	725	725	730	N. R.	745
9	10	840	880	950	1020	1135	1100	1340	1620
10	11	590	830	850	980	1125	1060	1510	1760
11	19	880	920	920	1020	-	1120	1405	1600
12	20	820	840	920	1020	1170	1060	1545	1690
13	15	580	630	710	810	900	860	1060	1155
14	16	680	750	-	1095	1150	-	1170	1180
15	17	550	630	635	810	925	920	955	990
16	14	605	960	1240	1245	1230	1210	1210	1220
17	23	925	1050	1220	1415	1500	1450	1555	1640

* Work-Coil Current In Amperes

N. R. - Not Recorded

TABLE 3

A SPECIMEN, TYPE I,

TEMPERATURE DATA RUN NO. 2

Temperature In °F

Test Point Number		1	2	3	4	5	6
Galvanometer Number	Thermocouple Number	(264)*	(325)	(400)	(460)	(500)	(500)
1	2	1140	1225	1600	1660	-	-
	12	1095	1270	1690	1735	1750	1735
2	3	1115	1280	1575	1680	1750	1735
	13	1075	1380	1640	1840	2000	2200
3	4	1180	1645	1770	1805	1820	1820
	1	-	-	-	-	-	-
4	5	1135	1260	1640	1648	-	-
	21	1020	1080	1340	1530	1590	1580
5	6	1010	1050	1270	1470	1660	1630
	22	870	965	1255		1450	1460
6	7	890	890	1000	1105	1210	1210
	24	970	1030	1220	1360	1460	1470
7	8	1050	1045	1290	1470	1560	1320
	Outlet	980	1075	1240	1405	1535	1525
8	9		840	970	1120	1255	1245
	Inlet	735	720	720	720	720	720
9	10	860	850	925	990	1080	1060
10	11	-	-	-	-	-	-
11	19	-	-	-	-	-	-
12	20	840	820	900	1000	1095	1080
13	15	-	-	-	-	-	-
14	16	655	710	1080	1500	-	-
15	17	570	600	740	990	1135	990
16	14	-	-	-	-	-	-
17	23	925	990	1210	1360	1470	1460

*Work-Coil Current In Amperes

TABLE 4
A SPECIMEN, TYPE II,
TEMPERATURE DATA RUN NO. 1

Temperature in °F

Test Point No.		1	2	3	4	5	6	7	8	9	10	11
Galvanometer No.	Thermocouple No.	(264)*	(325)	(400)	(460)	(500)	(500)	(520)	(560)	(600)	(600)	(650)
1	2	900	1040	1330	1460	1510	1510	1560	1570	1570	1520	1580
	12	1135	1330	1540	1600	1610	1610	1620	1630	1630	1620	N.R.
2	3	1240	1430	1560	1580	1590	1590	1590	1610	1610	1610	1610
	13	1420	1580	1630	1650	1655	1655	1655	1670	1680	1670	N.R.
3	4	1470	1620	1660	1680	1680	1680	1680	1685	1700	1690	1700
	1	-	-	-	-	-	-	-	-	-	-	-
4	5	1000	1010	1190	1320	1440	1450	1590	1630	1630	1620	1630
	21	980	-	1240	1330	1380	1400	1500	1546	1550	1540	N.R.
5	6	880	960	-	1150	1240	1250	1330	1540	1720	1740	1830
	22	-	900	-	1040	1050	1050	1070	1330	-	-	N.R.
6	7	980	1080	1280	1400	1490	1490	1580	1720	1770	1750	1800
	24	-	910	1040	1160	1250	1250	1330	1460	1500	1490	N.R.
7	8	-	980	1130	1170	1240	1250	1310	1540	1700	1650	1830
	Outlet	920	960	1120	1250	1330	1330	1420	1510	1570	1540	N.R.
8	9	800	830	940	1030	1070	1050	1160	1710	1800	1770	1800
	Inlet	730	730	730	740	740	740	740	740	750	750	N.R.
9	10	980	800	850	900	950	960	1040	1610	1780	1740	1750
10	11	-	-	-	-	-	-	-	-	-	-	N.R.
11	19	840	860	950	1010	1085	1100	1190	1760	1875	1840	1850
	23	-	930	1100	1220	1310	1330	1390	1460	1490	1490	N.R.
12	20	820	830	870	920	970	970	1030	1450	1700	1760	1770

TABLE 4 (CONT)

Temperature in ° F

Test Point No.		1	2	3	4	5	6	7	8	9	10	11
Galvanometer No.	Thermocouple No.	(264)*	(325)	(400)	(460)	(500)	(500)	(520)	(560)	(600)	(600)	(650)
No.	No.	(264)*	(325)	(400)	(460)	(500)	(500)	(520)	(560)	(600)	(600)	(650)
13	15	585	-	720	780	840	820	870	1050	1140	1120	1145
14	16	-	-	-	-	-	-	-	-	-	-	-
15	17	520	540	630	700	750	740	840	1040	1050	1040	1050
16	14	630	710	800	870	940	900	960	1105	1160	1150	1190

*Work-Coil Current In Amperes

N.R.-Not Recorded

TABLE 5

A SPECIMEN, TYPE II,

TEMPERATURE DATA RUN NO. 2

Temperature In °F

Test Point Number		1	2	3	4	5
Galvanometer Number	Thermocouple Number	(264)*	(325)	(400)	(460)	(520)
1	2	1040	1140	1380	1470	1480
	12	870	1250	1480	1500	N.R.
2	3	1160	1320	1480	1500	-
	13	1140	1310	1500	1520	N.R.
3	4	1100	1230	1440	1500	-
	1	-	-	-		N.R.
4	5	965	1020	1180	1380	-
	21	925	1000	1160	1340	N.R.
5	6	900	940	1050	1220	-
	22	790	970	1130	1130	N.R.
6	7	980	1050	1250	1440	1660
	24	900	960	1100	1130	N.R.
7	8	900	940	1020	1175	1480
	Outlet	925	980	1110	1250	N.R.
8	9	-	-	-	1250	1820
	Inlet	760	750	750	750	N.R.
9	10	880	870	1000	1170	-
10	11	-	-	1040	1210	1550
11	19	940	940	1080	1220	1650
	23	-	960	1085	1220	N.R.
12	20	-	910	1000	1160	1630
13	15	610	590	-	730	970
14	16	620	620	690	765	1000
15	17	550	570	650	765	940
16	14	640	650	720	840	1030

*Work-Coil Current In Amperes

N.R. - Not Recorded

TABLE 6

A SPECIMEN, TYPE II,

TEMPERATURE DATA RUN NO. 3

Temperature In °F

Test Point Number		1	2	3	4	5	6
Galvanometer Number	Thermocouple Number	(264)*	(325)	(400)	(460)	(500)	(520)
1	2	1010	1120	1250	1415	1440	1440
	12	1140	1290	1460	1470	1480	1490
2	3	1110	1380	1480	1500	1500	1510
	13	1200	1415	1510	1510	1520	1525
3	4	1170	1330	1490	1510	1510	1520
	1	-	-	-	-	-	-
4	5	940	990	1160	1340	1480	1500
	21	900	970	1130	1290	1400	1385
5	6	-	-	1075	1200	1360	1540
	22	890	1000	1080	1080	1150	-
6	7	-	-	-	-	-	-
	24	880	950	1060	1170	1270	1310
7	8	860	900	1020	1140	1280	1380
	Outlet	925	970	1105	1220	1310	1350
8	9	880	925	1075	1180	1590	1630
	Inlet	-	765	750	750	745	745
9	10	900	950	1100	1200	1540	1630
10	11	-	-	-	-	-	-
11	19	-	-	-	-	-	-
	23	-	935	-	-	-	-
12	20	-	-	-	-	-	-
13	15	-	605	680	760	805	840
14	16	-	610	680	760	-	950
15	17	530	565	660	730	915	950
16	14	610	650	730	820	850	950

*Work-Coil Current In Amperes

TABLE 7
C SPECIMEN STEADY-STATE TEST
TEMPERATURE DATA RUN NO. 1

Temperature in °F

Test Point No.		1	2	3	4	5	6	7	8	9	10	11	12
Galvanometer No.	Thermocouple No.	(264)*	(325)	(400)	(460)	(500)	(520)	(560)	(590)	(650)	(700)	(750)	(775)
1	5	-	820	960	-	1030	1110	1140	1215	1500	1545	1575	1575
	1	-	840	-	980	-	1030	-	1120	-	-	1500	-
2	7	765	775	820	860	880	880	900	920	960	1130	-	1375
	2	-	-	895	-	-	-	1085	1130	1330	-	1480	-
3	10	890	915	990	1030	1095	1170	1185	1320	1650	1645	1795	1770
4	17	950	1000	1130	1245	1320	1395	1490	1580	1830	1820	1860	1885
	4	820	-	-	935	-	-	-	1095	-	1280	-	-
5	19	730	775	840	915	935	990	1020	1065	1120	1350	1450	-
	21	-	-	-	990	1040	1075	1130	1160	-	-	-	-
6	20	-	880	940	990	1020	-	-	1130	1190	1280	1330	1360
	Inlet	790	-	775	770	765	775	775	765	-	770	765	-
7	22	830	850	900	960	980	1010	1050	1085	1120	1315	1370	-
	Oulet	-	-	-	925	-	-	-	1095	-	-	-	-
8	6	800	-	970	-	1050	1125	1150	1235	1380	1525	1535	1530
	3	-	-	860	900	925	960	990	1020	1075	1250	1340	-
9	8	840	860	925	980	1010	1055	1095	1130	1150	1300	1350	1400
10	9	880	925	1020	1130	1170	1225	1340	1375	1190	1475	1515	1480
11	11	-	840	870	860	850	860	905	950	990	1210	1250	1295
12	12	-	905	1010	1075	1085	1150	1245	1300	1280	1360	1400	-

* Work-Coil Current in Amperes

TABLE 7 (CONT)

Temperature in °F

Test Point No.		1	2	3	4	5	6	7	8	9	10	11	12
Galvanometer No.	Thermocouple No.	(264)*	(325)	(400)	(460)	(500)	(520)	(560)	(590)	(650)	(700)	(750)	(775)
13	13	-	540	560	580	595	595	615	640	760	725	735	760
14	14	575	590	630	670	690	700	730	785	830	840	915	1000
15	15	470	470	490	500	520	540	550	560	590	625	670	690
16	16	605	630	680	730	765	790	850	860	840	990	1020	1080
17	**Current	0.72	1.00	1.62	2.12	2.42	2.72	3.16	3.52	4.33	5.08	5.72	6.08

*Work-Coil Current in Amperes

**Galvanometer Deflection in Inches

TABLE 8
C SPECIMEN STEADY-STATE TEST
TEMPERATURE DATA RUN NO. 3

Temperature in °F

Test Point No.		1	2	3	4	5	6	7	8	9	10
Galvanometer No.	Thermocouple No.	(264)*	(325)	(400)	(460)	(500)	(520)	(560)	(590)	(650)	(700)
1	5	870	930	1020	1135	1185	1250	1320	1400	1520	1970
	1	-	-	-	-	-	1120	1220	1290	1405	1480
2	7	-	840	-	1020	1000	1035	-	-	1270	1320
	2	-	-	-	-	-	1080	1180	1235	1370	1430
3	10	910	970	1135	1275	1360	1440	1490	1570	1660	1720
4	17	780	810	-	-	-	1050	1110	-	1200	1380
	4	-	-	-	930	-	-	-	-	1180	-
5	19	725	790	850	930	965	1000	1080	-	1260	1360
	21	-	-	-	-	-	1090	1145	1200	1315	1390
6	20	840	860	-	-	-	1065	1145	1150	1220	1285
	Inlet	755	755	735	745	755	745	-	755	750	755
7	22	815	-	930	1005	1050	1095	1170	1200	1330	1450
	Outlet	875	875	930	-	1010	-	-	1140	-	-
8	6	840	885	975	1080	1135	1190	1285	1360	1450	1525
	3	-	-	-	960	1010	-	-	1155	1275	-
9	8	-	-	840	940	-	1010	1045	1120	1163	1235
10	9	-	-	920	985	-	1080	1135	1180	1345	1500
11	11	700	725	785	860	900	950	1000	1060	1125	1295
12	12	-	825	800	940	-	1025	1070	1125	1235	1305
13	13	-	985	515	560	570	595	615	650	650	705

TABLE 8 (CONT)

Temperature in °F

Test Point No.		1	2	3	4	5	6	7	8	9	10
Galvanometer No.	Thermocouple No.	(264)*	(325)	(400)	(460)	(500)	(520)	(560)	(590)	(650)	(700)
14	14	-	570	610	655	690	710	755	-	860	950
15	15	435	450	475	500	1010	530	545	570	610	695
16	16	570	580	630	680	695	740	775	790	920	1065
17	**Current	0.72	1.00	1.62	2.12	2.45	2.75	3.20	3.52	4.35	5.05

*Work-Coil Current in Amperes

**Galvanometer Deflection in Inches

TABLE 9
C SPECIMEN TRANSIENT HEATING
TEMPERATURE DATA CYCLE NO. 1

Temperature in °F

Time-Seconds		5	15	25	35	45	55	65	75	85	95
Galvanometer No.	Thermocouple No.										
1	5	-	790	840	1080	1380	1480	1320	1120	1000	923
	1	-	-	-	-	-	-	-	-	-	-
2	7	-	740	740	870	1200	1090	855	790	750	740
	2	-	-	-	-	-	-	-	-	-	-
3	10	-	-	-	-	-	-	-	-	-	-
4	17	-	780	780	890	1090	1150	1010	930	880	850
	4	-	-	-	-	-	-	-	-	-	-
5	19	-	680	690	720	925	1120	1155	1035	980	910
	21	-	-	-	-	-	-	-	-	-	-
6	20	-	760	800	870	1060	1215	1130	1005	920	880
	Inlet	-	-	-	-	-	-	-	-	-	-
7	22	-	765	810	960	1360	1380	1145	960	900	840
	Outlet	-	-	-	-	-	-	-	-	-	-
8	6	-	740	780	1000	1390	1390	1225	1060	925	855
	3	-	-	-	-	-	-	-	-	-	-
9	8	-	-	740	845	985	1155	890	785	755	750
10	9	-	800	850	1080	1440	1305	1000	890	855	805
11	11	-	650	685	840	1135	1080	900	800	750	750
12	12	-	-	810	895	1260	1380	960	855	820	805
13	13	-	410	430	475	560	600	-	560	520	500

TABLE 9 (CONT)

Temperature in °F

Time-Seconds		5	15	25	35	45	55	65	75	85	95
Galvanometer No.	Thermocouple No.										
14	14	-	530	570	665	850	850	705	635	605	580
15	15	-	440	470	590	740	680	560	500	475	470
16	16	-	540	600	725	1010	880	685	616	580	570
17	*Current	0.05	0.22	0.87	3.00	4.80	2.96	1.30	0.77	0.53	0.43

*Galvanometer Deflection in Inches

TABLE 10

A SPECIMEN, TYPE I,

LITHIUM LOOP DATA RUN NO. 1

Time (Min)	Thermocouple Number 4 °F	5 °F	6 °F	7 °F	8 °F	9 °F	10 °F	11 °F	12 °F	13 °F	15 °F	Flow lb/hr	Remarks
0	680	680	670	665	575	565	480	560	370	630	700	0	93 psig on supply tank, 0.5 psia on condenser.
3	683	683	750*	665	580	580	480	560	380	630	700	60.0	Test point 1
6	690	665	695	665	610	610	480	565	525	605	700	60.0	Test point 2
9	690	665	690	660	680	650	470	570	565	638	700	60.0	Test point 3
12	690	665	685	920	750	663	465	580	625	700	720	60.0	Test point 4, Flow increased slightly at 11 min.
18	700	670	680	1183	850	670	460	600	700	780	740	60.0	Test point 5, Condenser blower on, damper closed.
23	702	675	680	1165	890	680	460	600	660	850	770	60.0	Test point 6
25	705	675	682	1230	920	690	445	600	555	850	790	64.2	Test point 7
30	700	680	690	1520	1070	680	320	525	470	810	800	62.2	Test point 8, At 22 min. flow increased rapidly and became unstable, pressure lowered to 60 psig.

* Conditions Fluctuating

TABLE 11

A SPECIMEN, TYPE I,

LITHIUM LOOP DATA RUN NO. 2

Time (Min)	Thermocouple Number 4 °F	5 °F	6 °F	7 °F	8 °F	9 °F	10 °F	11 °F	12 °F	13 °F	15 °F	Flow lb/hr	Remarks
0	660	660	680	560	560	682	532	615	385	605	700	0	82 psig on supply tank, 0.5 psia on condenser.
2	660	660	685	580	590	682	530	612	492	615	700	60.0	Test point 1
4	665	665	675	615	615	680	530	612	538	620	700	60.0	Test point 2
8	665	660	670	675	650	680	530	615	580	650	700	60.0	Test point 3, Specimen red front center.
11	668	660	670	830	685	685	530	615	602	670	710	60.0	Test point 4, Blower on, damper closed.
14	670	660	665	1070	750	690	520	620	605	702	720	60.0	Test point 5
18	675	663	665	1195	855	692	485	610	570	755	730	60.0	Test point 6, Opened damper 1/4 in.
20	680	665	665	1245	925	690	410	580	455	770	740	60.0	Heat off.

TABLE 12
A SPECIMEN, TYPE II,
LITHIUM LOOP DATA RUN NO. 1

Time (Min)	Thermocouple Number 4 °F	5 °F	6 °F	7 °F	8 °F	9 °F	10 °F	11 °F	12 °F	13 °F	15 °F	Flow lb/hr	Remarks
0	690	670	740*	683	555	620	495	580	422	638	700	0	118 psig on supply tank, 0.5 psia on condenser.
3	690	670	700*	683	555	620	495	580	422	638	700	60.0	Test point 1
6	688	670	690	700	608	620	493	580	562	625	700	60.0	Test point 2
9	690	670	690	730	632	625	492	582	585	645	700	60.0	Test point 3, 2 in. dia red on spec.
11	692	673	688	795	668	623	492	585	600	660	705	60.0	Test point 4, 3 in. dia red on spec, red down vapor line.
13	695	675	685	920	705	625	495	590	610	682	715	60.0	Test point 5, condenser blower on, damper closed.
17	700	680	680	1030	785	630	470	585	545	730	725	60.0	Test point 6
19	705	680	680	1060	808	630	450	580	538	742	730	60.9*	Test point 7, slightly red at top of spec, red orange front and down vapor line. Slight flow increase at 20 min.
21	710	680	680	1170	860	630	430	560	540	750	730	61.7*	Test point 8, flow increasing rapidly, reducing pressure to bring down.
26	718	685	670	1360	960	630	400	535	550	780	740	60.0*	Test point 9
33	720	690	660	1360	970	630	340	490	595	830	780	60.0*	Test point 10, specimen completely orange.
37	722	690	650	1463	1025	633	330	478	600	840	790	70.2*	Going to Test point 11, shut down.

* Conditions Fluctuating

TABLE 13
A SPECIMEN, TYPE II,
LITHIUM LOOP DATA RUN NO. 2

Time (Min)	Thermocouple Number 4 °F	5 °F	6 °F	7 °F	8 °F	9 °F	10 °F	11 °F	12 °F	13 °F	15 °F	Flow lb/hr	Remarks
0	700	700	675	470	520	620	440	520	390	750	700	0	115 psig on supply tank, 0.1 psia on condenser.
1	695	695	785	470	525	615	440	520	410	625	700	60.8	Test point 1
3	700	680	720	520	560	615	440	525	480	608	700	60.8	Test point 2, slightly red at center of spec.
6	700	680	700	595	600	615	440	530	530	630	700	60.8	Test point 3
10	700	680	695	705	650	620	440	535	560	660	705	60.8	Test point 4
12	700	675	690	985	710	620	445	540	600	690	715	60.8	Test point 5, flow started up. Spec. orange at front and down to vapor line. Top slightly red.

TABLE 14

A SPECIMEN, TYPE II,

LITHIUM LOOP DATA RUN NO. 3

Time (Min)	Thermocouple Number 4 °F	5 °F	6 °F	7 °F	8 °F	9 °F	10 °F	11 °F	12 °F	13 °F	15 °F	Flow lb/hr	Remarks
0	690	695	725	730	580	700	540	630	400	685	700	67.6	155 psig on supply tank, 0.5 psia on condenser.
2	690	695	725	725	600	700	540	630	490	650	700	67.6	Test point 1
4	690	690	730	750	630	700	545	635	560	675	710	67.6	Test point 2
6	695	690	720	780	665	700	545	640	545	700	715	67.6	Test point 3
8	695	685	700	830	710	705	545	640	615	720	720	67.6	Test point 4
11	695	685	700	1020	760	710	540	650	660	760	730	67.6	Test point 5, flow increased slightly.
14	695	685	685	1100	800	715	545	650	695	785	740	69.4	Test point 6
17	695	685	680	1180	870	730	545	665	740	830	780	71.0	Shut down.

TABLE 15

C SPECIMEN STEADY-STATE TEST

LITHIUM LOOP DATA RUN NO. 1

Time (Min)	Thermocouple Number 4 °F	5 °F	6 °F	7 °F	8 °F	9 °F	10 °F	11 °F	12 °F	13 °F	15 °F	Flow lb/hr	Remarks
0	718	750	710	535	610	750	570	665	365	605	700	0	137 psig on supply tank, 0.5 psia on condenser.
1	720	720	745	540	610	750	570	662	460	610	700	79.5	Test point 1, no color on spec.
3	720	715	725	580	630	750	570	665	560	650	700	79.5	Test point 2, no color on spec.
4	720	710	720	620	645	750	570	665	595	670	710	79.5	Test point 3, no color in spec.
6	720	705	710	650	660	750	570	670	610	685	715	79.5	Test point 4, slightly red at tip.
8	725	700	710	690	690	750	570	670	630	700	720	79.5	Test point 5, slightly red at tip.
12	725	700	700	730	700	750	565	670	650	720	725	79.5	Test point 6
14	725	700	700	770	730	750	565	670	665	735	725	79.5	Test point 7
16	725	700	700	800	745	750	560	670	675	750	730	79.5	Test point 8
21	725	700	700	850	770	755	560	675	700	780	740	82.8*	Test point 9, pressure reduced to 95 psig between points 9 and 10.
24	725	695	695	900	800	750	560	675	710	795	750	79.5	Test point 10, bright orange at tip, slightly orange all over.
29	715	690	690	980	815	740	555	670	735	820	770	79.5	Test point 11, pressure 87 psig.
30	715	685	680	1010	835	740	550	670	730	815	770	79.5	
31	715	685	680	1110	875	745	550	670	740	830	780	79.5	Power off.

* Conditions fluctuating

TABLE 16

C SPECIMEN STEADY-STATE TEST

LITHIUM LOOP DATA RUN NO. 3

Time (Min)	Thermocouple Number 4 °F	5 °F	6 °F	7 °F	8 °F	9 °F	10 °F	11 °F	12 °F	13 °F	15 °F	Flow lb/hr	Remarks
0	700	745	810	500	585	730	570	685	400	625	700	0	74 psig on supply tank, 0.5 psia on condenser.
2	700	700	740	530	600	735	575	690	515	635	700	49.8	Test point 1
3	700	680	720	550	610	735	575	690	550	655	700	52.0	Test point 2
4	700	675	710	570	620	735	575	690	570	670	705	52.0	Test point 3
6	700	675	700	630	640	740	580	700	610	690	705	51.5	Test point 4
7	700	675	700	675	655	740	580	700	620	695	705	52.0	Test point 5
8	705	675	695	730	670	740	585	700	625	700	705	52.0	Test point 6
9	705	675	695	790	685	745	585	700	635	710	710	52.4	Test point 7
10	710	675	695	850	700	745	585	705	640	720	710	52.8	Test point 8
12	710	675	690	885	720	750	590	720	685	760	715	55.7	Test point 9, orange all over.
13	715	680	690	980	740	750	590	720	685	760	715	61.6	Test point 10
	778	680	690	1040	775	760	590	725	690	775	720	62.5	Shut down.

TABLE 17

C SPECIMEN TRANSIENT HEATING

LITHIUM LOOP DATA

Time (Min)	Thermocouple Number 4 °F	5 °F	6 °F	7 °F	8 °F	9 °F	10 °F	11 °F	12 °F	13 °F	15 °F	First Cycle Flow lb/hr	Remarks
0	735	700		635	635	818	688	790	590	690	700	54.0	70 psig on supply tank, 0.5 psia on condenser.
100 sec	735	695		665	655	818	688	788	630	712	700	54.0	Flow peaked at 60 lb/hr.
	Second Cycle												
0	-	-	-	-	-	810	685	780	648	710	700	53.2	70 psig on supply tank, 0.5 psia on condenser.
100 sec	-	-	-	-	-	810	685	780	645	702	700	55.0	Flow peaked at 60 lb/hr.

REFERENCES

1. Detra, R.W., N.H. Kemp, and F.R. Riddell, Addendum to "Heat Transfer to Satellite Vehicles Re-entering The Atmosphere," Jet Propulsion, Vol. 27, December 1957.

2. Fay, J.A. and F.R. Riddell, "Theory of Stagnation Point Heat Transfer in Dissociated Air," Avco Research Laboratory, Research Report 1, Revised 1957.

3. Kivel, B., "Radiation From Hot Air and Stagnation Heating," AFBMD-TR59-20 Research Report 79.

4. Dickson, J.A., "Interim Report on Lithium Spray Structural Cooling," Bell Aerosystems Report No. 7149-937001.

5. Anthony, F.M. and Mistreta, A.C., "Tests of Molybdenum and Graphite Leading Edge Assemblies," WADC TR59-744, Volume VIII, January 1961.

6. Mathews, B.E., et al, " Research and Development on Induction-Heating Methods of Simulating Aerodynamic Heating," WADC-TR-59-523, Part IV, June 1962.

7. Balzhiser, R.E., et al, " Literature Survey on Liquid Metal Boiling," ASD TR-61-594.

8. McAdams, W.H., "Heat Transmission, " McGraw-Hill Book Company.

9. Weatherford, Jr., W.D., et al, "Properties of Inorganic Energy-Conversion and Heat Transfer Fluids for Space Applications," WADD TR 61-96, November 1961.

10. Anthony, F.M., et al, "Investigation of Feasibility of Utilization Available Heat-Resistant Materials for Hypersonic Leading Edge Applications," WADC TR 59-744, Volume II, November 1960.

UNCLASSIFIED
Security Classification

DOCUMENT CONTROL DATA - R&D

(Security classification of title, body of abstract and indexing annotation must be entered when the overall report is classified)

1. ORIGINATING ACTIVITY (Corporate author) Bell Aerosystems Company, P.O. Box 1, Buffalo, New York	2a. REPORT SECURITY CLASSIFICATION Unclassified 2b. GROUP

3. REPORT TITLE

Lithium Spray Structural Cooling

4. DESCRIPTIVE NOTES (Type of report and inclusive dates)

Final Report, May 1962 to October 1964

5. AUTHOR(S) (Last name, first name, initial)

Mistretta, Andrew L.

6. REPORT DATE	7a. TOTAL NO. OF PAGES	7b. NO. OF REFS
12 November 1964	120	10

8a. CONTRACT OR GRANT NO.	9a. ORIGINATOR'S REPORT NUMBER(S)
AF33(657)-8386 b. PROJECT NO. 1368 c. Task No. 136804 d.	AFFDL-TR-64-169 9b. OTHER REPORT NO(S) (Any other numbers that may be assigned this report)

10. AVAILABILITY/LIMITATION NOTICES

Qualified requesters may obtain copies of this report from DDC.
Foreign announcement and dissemination of this report by DDC is not authorized.

11. SUPPLEMENTARY NOTES	12. SPONSORING MILITARY ACTIVITY
	AF Flight Dynamics Laboratory Research and Technology Division Wright Patterson Air Force Base, Ohio

13. ABSTRACT

The objective of this program was to demonstrate the feasibility of an open cycle lithium spray absorptive cooling system for nose cap applications and to determine maximum heat flux capability of the system.

Test specimens were designed and fabricated. The experimental program which was established demonstrated the feasilibity of the lithium spray system. While subjected to a heat flux of 600 BTU/ft^2-sec, equivalent to a radiation equilibrium temperature of about 5800°F, specimen surface temperature did not exceed 2200°F. Instrumentation difficulties precluded tests at higher heat fluxes; therefore, the maximum potential of the system could not be determined experimentally. Approximate analytical estimates indicate a minimum potential capability of 3000 BTU/ft^2-sec.

For the application of the test heat fluxes, the Inductive Heating System of the University of Florida was used.

DD FORM 1 JAN 64 1473

UNCLASSIFIED
Security Classification

14. KEY WORDS	LINK A		LINK B		LINK C	
	ROLE	WT	ROLE	WT	ROLE	WT
Liquid Metal Lithium Spray						

INSTRUCTIONS

1. ORIGINATING ACTIVITY: Enter the name and address of the contractor, subcontractor, grantee, Department of Defense activity or other organization *(corporate author)* issuing the report.

2a. REPORT SECURITY CLASSIFICATION: Enter the overall security classification of the report. Indicate whether "Restricted Data" is included. Marking is to be in accordance with appropriate security regulations.

2b. GROUP: Automatic downgrading is specified in DoD Directive 5200.10 and Armed Forces Industrial Manual. Enter the group number. Also, when applicable, show that optional markings have been used for Group 3 and Group 4 as authorized.

3. REPORT TITLE: Enter the complete report title in all capital letters. Titles in all cases should be unclassified. If a meaningful title cannot be selected without classification, show title classification in all capitals in parenthesis immediately following the title.

4. DESCRIPTIVE NOTES: If appropriate, enter the type of report, e.g., interim, progress, summary, annual, or final. Give the inclusive dates when a specific reporting period is covered.

5. AUTHOR(S): Enter the name(s) of author(s) as shown on or in the report. Enter last name, first name, middle initial. If military, show rank and branch of service. The name of the principal author is an absolute minimum requirement.

6. REPORT DATE: Enter the date of the report as day, month, year; or month, year. If more than one date appears on the report, use date of publication.

7a. TOTAL NUMBER OF PAGES: The total page count should follow normal pagination procedures, i.e., enter the number of pages containing information.

7b. NUMBER OF REFERENCES: Enter the total number of references cited in the report.

8a. CONTRACT OR GRANT NUMBER: If appropriate, enter the applicable number of the contract or grant under which the report was written.

8b, 8c, & 8d. PROJECT NUMBER: Enter the appropriate military department identification, such as project number, subproject number, system numbers, task number, etc.

9a. ORIGINATOR'S REPORT NUMBER(S): Enter the official report number by which the document will be identified and controlled by the originating activity. This number must be unique to this report.

9b. OTHER REPORT NUMBER(S): If the report has been assigned any other report numbers *(either by the originator or by the sponsor)*, also enter this number(s).

10. AVAILABILITY/LIMITATION NOTICES: Enter any limitations on further dissemination of the report, other than those imposed by security classification, using standard statements such as:

(1) "Qualified requesters may obtain copies of this report from DDC."

(2) "Foreign announcement and dissemination of this report by DDC is not authorized."

(3) "U. S. Government agencies may obtain copies of this report directly from DDC. Other qualified DDC users shall request through _____."

(4) "U. S. military agencies may obtain copies of this report directly from DDC. Other qualified users shall request through _____."

(5) "All distribution of this report is controlled. Qualified DDC users shall request through _____."

If the report has been furnished to the Office of Technical Services, Department of Commerce, for sale to the public, indicate this fact and enter the price, if known.

11. SUPPLEMENTARY NOTES: Use for additional explanatory notes.

12. SPONSORING MILITARY ACTIVITY: Enter the name of the departmental project office or laboratory sponsoring *(paying for)* the research and development. Include address.

13. ABSTRACT: Enter an abstract giving a brief and factual summary of the document indicative of the report, even though it may also appear elsewhere in the body of the technical report. If additional space is required, a continuation sheet shall be attached.

It is highly desirable that the abstract of classified reports be unclassified. Each paragraph of the abstract shall end with an indication of the military security classification of the information in the paragraph, represented as *(TS)*, *(S)*, *(C)*, or *(U)*.

There is no limitation on the length of the abstract. However, the suggested length is from 150 to 225 words.

14. KEY WORDS: Key words are technically meaningful terms or short phrases that characterize a report and may be used as index entries for cataloging the report. Key words must be selected so that no security classification is required. Identifiers, such as equipment model designation, trade name, military project code name, geographic location, may be used as key words but will be followed by an indication of technical context. The assignment of links, rules, and weights is optional.